Electronic Supplementary Material (ESI) for ChemComm.

Supporting Information

Electrophilic and Nucleophilic Displacement Reactions at the Bridgehead Borons of Tris(pyridyl)borate Scorpionate Complexes

Joydeb Goura,[a†] James McQuade,[a†] Daisuke Shimoyama,[a] Roger A. Lalancette,[a] John B. Sheridan [a] and Frieder Jäkle *[a]

[a] Department of Chemistry, Rutgers University-Newark, 73 Warren Street, Newark, NJ 07102, USA.

† Equal contribution

Experimental Section

Materials and General Methods. NEt_3 and anthracene were purchased from Fisher Scientific, 2-bromopyridine from Oakwood Chemical, methanol (anhydrous) from Pharmco-AAPER, BBr_3, BCl_3 (1M in hexane), *n*-BuLi (1.6 M in hexanes), $RuCl_3 \cdot 3H_2O$, CF_3SO_3H, $LiAlH_4$, and methoxy(trimethylsilane) from Sigma-Aldrich, 3-bromopyridine from AK Scientific, and Me_3SiCl (TMSCl) from Acros. All chemicals were used as received without further purification unless noted otherwise. $[RuCl_2(dmso)_4]$[1] and the *t*-butylphenyl-tris(2-pyridyl)borate ligand[2] were synthesized according to literature procedures. Solvents were purchased from Pharmco-AAPER. Ether solvents were distilled from Na/benzophenone prior to use. Hexanes, toluene and dichloromethane were purified using a solvent purification system (Innovative Technologies; alumina/copper columns for hydrocarbon solvents). Chlorinated solvents were subsequently distilled from CaH_2 and degassed via nitrogen purging followed by several freeze-pump thaw cycles. Hydrocarbon solvents were stored over Na/K alloy prior to use. Reactions and manipulations involving reactive boron halides and ruthenium species were carried out under an atmosphere of prepurified nitrogen using either Schlenk techniques or an inert-atmosphere glove box.

The 500 MHz ^1H, 125.8 MHz $^{13}C\{^1H\}$, 470.3 MHz ^{19}F, and 160.4 MHz ^{11}B NMR spectra were recorded on Bruker 500 MHz spectrometers and the 599.7 MHz ^1H, 150.8 MHz $^{13}C\{^1H\}$ NMR and 192.4 MHz ^{11}B NMR spectra on a Varian Inova 600 spectrometry. ^{11}B NMR spectra were acquired with boron-free quartz NMR tubes on a Bruker 500 MHz spectrometer equipped with a 5mm PH SEX 500S1 11B-H/F-D probe. The ^1H NMR spectra (7.26 ($CDCl_3$), 7.16 (C_6D_6), 1.94 (CD_3CN)) and $^{13}C\{^1H\}$ NMR spectra (77.16 ($CDCl_3$), 128.22 (C_6D_6), 1.32 (CD_3CN)) were referenced internally to the solvent peaks[3] and all other NMR spectra externally to $SiMe_4$ (0 ppm). All NMR spectra were recorded at ambient temperature. All chemical shifts are given in ppm and the following abbreviations are used for signal assignments: s (singlet), d (doublet), pst (pseudo-triplet), br (broad), n.r. (not resolved), BrPy (3-bromopyridine). ESI-MS measurements were performed on an Apex-ultra 7T Hybrid FT-MS (Bruker Daltonics). MALDI-TOF (time-of-flight) MS data were obtained in reflectron +mode on a Bruker Ultraflextreme. The samples were dissolved in chloroform (ca. 1-10 mg/mL), mixed with a solution of the matrix (anthracene, 20 mg/mL) in a 1:2 (v/v) ratio, and then spotted on the wells of a sample plate. Cyclic voltammetry (CV) experiments were carried out on a CV-50W analyzer from BAS. The three-electrode system consisted of a gold disk as the working electrode, a platinum wire as the secondary electrode, and a Ag/AgCl reference electrode. The voltammograms were recorded with ca. 0.5 mM solutions of the compound in ca. 0.1 M solutions of supporting electrolyte $Bu_4N[PF_6]$ in CH_2Cl_2 and referenced by the addition of a small amount of Cp^*_2Fe. The potentials are reported relative to the $Cp_2Fe^{+/0}$ redox couple using a redox potential of –560 mV for the $Cp^*_2Fe^{+/0}$ redox couple relative to $Cp_2Fe^{+/0}$. UV−vis absorption data were acquired on an Agilent Technologies Cary 500 series UV−vis near-IR spectrophotometer. Raman spectra were collected using a confocal Raman Microscope by Wi-Tec (Alpha 3000R) with an excitation laser at 785 nm. FT-IR absorption data were acquired in ATR mode on a Thermo Nicolet IR 200 Spectrophotometer using a

SmartMIRacle accessory and a ZnSe lens. Elemental analyses were obtained from Intertek/Quantitative Technologies Inc., Whitehouse, NJ.

X-ray diffraction analysis. X-ray crystallographic data for **1** and **2-H** were collected on a Bruker SMART APEX III ULTRA CCD diffractometer using CuKα radiation (λ = 1.54178 Å) at 100 K. Data processing, Lorentz-polarization, and face-indexed numerical absorption corrections were performed using SAINT, APEX, and SADABS computer programs.[4] The crystal structures were solved by direct method using the SHELXS-2014 program[5] and refined by successive differential Fourier syntheses and full-matrix least-squares procedures using the SHELXL-2018 program.[6] Anisotropic thermal factors were applied for all atoms except for the hydrogen atoms. All H atoms were found in electron-density difference maps and treated as idealized contribution except for the B-H hydrogens of compound **2-H** which were fully refined.

Data for **2-OTf** and **3-Py** were recorded at 100 K using a Rigaku XtaLAB Synergy-S Dual Source diffractometer equipped with a PhotonJet Cu-microfocus source (λ = 1.54178 Å) and a HyPix-6000HE detector. Data reduction and processing was performed with CrysAlis^{Pro}.[7] Using the SCALE3 ABSPACK scaling algorithm, empirical and numerical (Gaussian) absorption corrections, determined by face indexing and integration were applied to the data.[8] The structure was solved by intrinsic phasing method with SHELXT and refined by full-matrix least-squares techniques against F^2 (SHELXL) in the Olex2 graphical user interface.[6] All H atoms were placed in idealized positions and refined using a riding model. Structural data have been deposited with the Cambridge Structure Database as supplementary publications CCDC 2117577-2117580.

DFT calculations were performed with the Gaussian16 suite of programs.[9] The input files were generated from the X-ray data as far as available or in Chem3D. Geometries were then optimized in Gaussian16 at the B3LYP/LanL2DZ [Ru, Br] + 6-311G++(d,p) [C, H, N, B, O, S, F, Cl] level. Frequency calculations were performed to confirm the presence of local minima (only positive frequencies). Vertical excitations were calculated by TD-DFT methods at the same level of theory.

Caution! BBr_3 and BCl_3 are toxic and corrosive and should be handled appropriately with great care. Fluorinated grease was used for ground glass joints in reactions involving boron halides.

Synthesis of Bis(*t*-butylphenyl-tris(2-pyridyl)borate) Ruthenium(II) (1). Under the protection of nitrogen, $[RuCl_2(dmso)_4]$ (0.292 g, 0.60 mmol) and *t*-butylphenyltris(pyrid-2-yl)borate free acid (0.457 g, 1.20 mmol) were suspended in degassed methanol (50 mL) and triethylamine (0.68 mL, 4.9 mmol) was added. The mixture was kept stirring at 80 °C for 72 h. A yellow precipitate formed, which was collected by filtration of the hot suspension and washed with cold methanol (2 x 5 mL) and diethyl ether (2 x 3 mL). The yellow solid was dried under high vacuum at RT for 5 h. Yield: 0.28 g (54 %). The product was isolated as a yellow powdery solid. Single crystals for X-ray diffraction were obtained by slow evaporation of a solution in toluene and n-decane. ^{1}H NMR (500 MHz, $CDCl_3$) δ = 8.06 (d, J = 7.5 Hz, 4H, Ph-H2,6), 7.63 (d, J = 8.0 Hz, 6H, pyridyl-H3), 7.58 (d, J = 8.0 Hz, 4H, Ph-H3,5), 7.30 (pst, J = 7.5 Hz, 6H, pyridyl-H4), 7.09 (d, J = 5.5 Hz, 6H, pyridyl-H6), 6.51 (pst, J = 6.2 Hz, 6H, pyridyl-H5), 1.51 (s, 18H, *t*-Bu).

^{1}H NMR (599.7 MHz, C_6D_6) δ = 8.51 (d, J = 7.8 Hz, 4H, Ph-H2,6), 8.06 (d, J = 7.8 Hz, 6H, pyridyl-H3), 7.78 (d, J = 8.2 Hz, 4H, Ph-H3,5), 7.16 (overlapped, 6H, pyridyl-H6), 6.94 (pst, J = 7.8 Hz, 6H, pyridyl-H4), 5.99 (pst, J = 6.3 Hz, 6H, pyridyl-H5), 1.54 (s, 18H, *t*-Bu). ^{13}C{^{1}H} NMR (125.8 MHz, $CDCl_3$) δ = 183.5 (q, $^{1}J(^{11}B, ^{13}C)$ = 49 Hz, pyridyl-C2), 155.0 (pyridyl-C6), 147.3 (*t*Ph-C4), 136.7 (Ph-C2,6), 131.7 (pyridyl-C4), 127.8 (pyridyl-C3), 124.4 (Ph-C3,5), 120.6 (pyridyl-C5), 34.6 ($C(CH_3)_3$), 31.9 ($C(CH_3)_3$), Ph-C1 (not observed). ^{13}C{^{1}H} NMR (150.8 MHz, C_6D_6) δ = 182 (n.r., pyridyl-C2), 155.5 (pyridyl-C6), 147.5 (*t*Ph-C4), 137.3 (Ph-C2,6), 132.0 (pyridyl-C4), 128.5 (pyridyl-C3), 125.0 (Ph-C3,5), 120.8 (pyridyl-C5), 34.7 ($C(CH_3)_3$), 32.0 ($C(CH_3)_3$), Ph-C1 (not observed). ^{11}B NMR (160.4 MHz, $CDCl_3$) δ = -6.8 ($w_{1/2}$ = 45 Hz). High-res ESI-MS (DCM/acetonitrile, pos. mode): m/z = 858.3342 ($[M]^+$, calcd for $^{12}C_{50}{}^{1}H_{50}{}^{11}B_2{}^{14}N_6{}^{101}Ru$ 858.3348). IR (ATR) with tentative assignments based on comparison with computational data *ν* (cm^{-1}): 2963 (m, C-H stretching), 1587 (w, Py C=C stretch), 1453 (s, Py C-H bending), 1416 (m, C-H bending), 1361 (w, C_{Ar}-C_{tBu} stretch), 1259 (w, Py ring stretch), 1217 (w, Py C-B stretch), 1113 (m, Ar ring breathing), 1066 (w, Ph ring breathing) 1015 (s, Py ring breathing), 822 (m, Ph C-H out-of-plane bending), 759 (s, Py B-C stretching), 747 (s, Py B-C stretch), 638 (m, Py ring stretching), 574 (w, Ph ring puckering).

Synthesis of Bis(bromotris(pyrid-2-yl)borate) Ruthenium(II) (2-Br). In a glove box, to a solution of **1** (80 mg, 93 μmol) in 40 mL of dry CH_2Cl_2 was slowly added a solution of BBr_3 (26 μL, 0.27 mmol) in 10 mL of CH_2Cl_2 and the mixture was kept stirring 12 h at room temperature in a teflon-stoppered Schlenk tube. Methoxy(trimethyl)silane (80 μL, 0.58 mmol) was then added neat and the reaction was kept stirring overnight. A yellow precipitate was collected by filtration, washed first with CH_2Cl_2 and then hexanes, and dried under high vacuum at RT for 5 h. Yield for **2-Br**: 39 mg (56 %). An alternative synthesis using hydrobromic acid was also discovered. In a glovebox, to a solution of **1** (42 mg, 48 μmol) in 10 mL dry, degassed dry CH_2Cl_2 was added 22 μL degassed aqueous hydrobromic acid (48% in water, 8.77 M, 193 μmol). The solution was stirred at room temperature overnight, taken to dryness under vacuum. The solid was then stirred overnight with 2 mL degassed water, the solvent was decanted and the solid washed with 2 x 2 mL water. The solid was then stirred with 10 mL pentane overnight, the solvent was decanted, and the solid dried for 8 hours at 50 °C. Yield for **2-Br**: 15.6 mg (43%). ^{1}H NMR (500 MHz, $CDCl_3$) δ = 8.62 (d, J = 7.5 Hz, 6H, pyridyl-H3), 7.52 (pst, J = 7.7 Hz, 6H, pyridyl-H4), 6.92 (br, 6H, pyridyl-H6), 6.62 (pst, J = 6.0 Hz, 6H, pyridyl-H5). ^{1}H NMR (599.7 MHz, C_6D_6) δ = 9.04 (d, J = 7.8 Hz, 6H, pyridyl-H3), 7.01 (pst, J = 6.6 Hz, 6H, pyridyl-H4), 6.84 (d, J = 5.4 Hz, 6H, pyridyl-H6), 5.99 (pst, J = 6.6 Hz, 6H, pyridyl-H5). ^{13}C NMR data could not be obtained due to low solubility. ^{11}B NMR (160.4 MHz, C_6D_6) δ = –0.2 ($w_{1/2}$ = 500 Hz). ^{11}B NMR (160.4 MHz, $CDCl_3$) δ = 0.0 ($w_{1/2}$ = 520 Hz). MALDI-TOF MS (anthracene, pos. mode): m/z = 751.9639 ($[M]^+$, calcd for $^{12}C_{30}{}^{1}H_{24}{}^{11}B_2{}^{79}Br{}^{81}Br{}^{14}N_6{}^{101}Ru$ 751.9654). IR (ATR) with tentative assignments based on comparison with computational data *ν* (cm^{-1}): 3068 (w, C-H stretching), 1591 (m, Py C=C stretch), 1454 (s, Py C-H bending), 1420 (m, Py C-H bending), 1265 (w, Py ring stretching), 1221 (w, Py C-B stretch), 1155 (m, Py ring stretch), 1063 (w, Py ring breathing), 1021 (m, Py ring breathing),

850 (w, Py ring breathing), 792 (s, C-H out-of-plane bending), 754 (s, B-Br stretch), 670 (s, B-Br stretch), 650 (m, Py ring deformation), 627 (m, Py ring stretching), 546 (w, Py ring puckering).

Synthesis of Bis(chlorotris(pyrid-2-yl)borate) Ruthenium(II) (2-Cl). A solution of **1** (73 mg, 85 μmol) in 60 mL of dry CH_2Cl_2 in a teflon-stoppered Schlenk tube was cooled to 0°C in an ice-bath. Pre-cooled BCl_3 solution (11 mL, 1M in hexane, 11 mmol) was injected, the tube sealed and inverted, and the mixture was kept stirring for 96 hours while slowly returning to room temperature. Methoxy(trimethyl)silane (4.5 mL, 33 mmol) was then added neat and the reaction mixture was kept stirring for 24 h. A yellow precipitate formed, which was collected by filtration, washed first with CH_2Cl_2 and then hexanes, and dried under high vacuum at 80 °C for 24 h. Yield for **2-Cl**: 50.2 mg (89 %). ^{1}H NMR (500 MHz, $CDCl_3$) δ = 8.39 (d, J = 7.5 Hz, 6H, pyridyl-H3), 7.53 (pst, J = 7.5 Hz, 6H, pyridyl-H4), 6.94 (br, 6H, pyridyl-H6), 6.63 (pst, J = 5.7 Hz, 6H, pyridyl-H5). ^{1}H NMR (599.7 MHz, C_6D_6) δ = 8.80 (d, J = 7.8 Hz, 6H, pyridyl-H3), 7.05 (pst, J = 7.2 Hz, 6H, pyridyl-H4), 6.89 (d, J = 5.4 Hz, 6H, pyridyl-H6), 6.02 (pst, J = 6.6 Hz, 6H, pyridyl-H5). ^{13}C NMR data could not be obtained due to low solubility. ^{11}B NMR (160.4 MHz, $CDCl_3$) δ = -0.7 ($w_{1/2}$ = 440 Hz). High-res ESI-MS (DCM/MeOH, pos. mode): m/z = 662.0669 ($[M]^+$, 100%, calcd for $^{12}C_{30}{}^{1}H_{24}{}^{11}B_2{}^{35}Cl_2{}^{14}N_6{}^{101}Ru$ 662.0677). IR (ATR) with tentative assignments based on comparison with computational data *ν* (cm^{-1}): 2922 (w, C-H stretch), 2851 (w, C-H stretch), 1712 (w, Py C=C stretch) 1551 (w, C=C stretch), 1541 (w, C=C stretch), 1454 (s, C-H bending), 1418 (m, C-H bending), 1261 (s, Py ring deformation), 1222 (w, B-C stretch), 1157 (s, B-C stretch), 1108 (w, C-H bending), 1063 (m, Py ring breathing), 1019 (s, Py ring breathing), 849 (s, Py ring breathing/B-C stretch), 822 (s, B-Cl stretch), 770 (s, C-H out-of-plane bending), 753 (s, C-H out-of-plane bending), 675 (s, Py ring deformation), 650 (s, Py ring deformation), 630 (m, Py ring deformation), 598 (w, Py ring puckering), 558 (Py ring puckering).

Synthesis of Bis((trifluoromethylsulfonyl)tris(pyrid-2-yl)borate) Ruthenium(II) (2-OTf). In a glove box, to a solution of **1** (47 mg, 54 μmol) in 2 mL of deoxygenated CD_2Cl_2 was slowly added a solution of deoxygenated CF_3SO_3H (12.5 μL, 0.14 mmol) in 0.25 mL of CD_2Cl_2 and the mixture was stirred for 8 hours at room temperature. Degassed water (13 μL, 0.72 mmol) was then added and the mixture was stirred overnight, resulting in the formation of a bright yellow precipitate. The reaction mixture was brought to dryness, extracted with 1 mL water for 5 hours and washed with a further 1 mL water to remove any traces of acid. The product was then stirred overnight with 10 mL hexanes, the hexanes was decanted, the solvent removed, and the residue dried under high vacuum at 50 °C for 24 hours. Single crystals of **2-OTf** for XRD analysis were obtained by slow evaporation of a solution in CH_2Cl_2 Yield: 26 mg (47%). ^{1}H NMR (500 MHz, $CDCl_3$) δ = 8.06 (d, J = 8.0 Hz, 6H, pyridyl-H3), 7.52 (pst, J = 7.5 Hz, 6H, pyridyl-H4), 6.88 (d, J = 5.5 Hz, 6H, pyridyl-H6), 6.61 (pst, J = 6.3 Hz, 6H, pyridyl-H5). ^{1}H NMR (500 MHz, C_6D_6) δ 8.52 (d, *J* = 8.0 Hz, 6H, pyridyl-H3), 6.99 (pst, *J* = 7.3 Hz, 6H, pyridyl-H5), 6.67 (d, *J* = 5.5 Hz, 6H, pyridyl-H6), 5.99 (pst, *J* = 6.5 Hz, 6H, pyridyl-H4). ^{13}C{^{1}H} NMR (125.8 MHz, $CDCl_3$) δ = 173.7 (br, pyridyl-C2), 154.7 (pyridyl-C6), 134.3 (pyridyl-C4), 125.1 (pyridyl-C3), 122.7 (pyridyl-C5), 119.7 (q, ^{1}J(C,F) = 317 Hz, CF_3). ^{11}B NMR (160.4 MHz, $CDCl_3$) δ = +5.9 ($w_{1/2}$ = 1000 Hz). ^{19}F NMR (470.3 MHz, $CDCl_3$) δ = -76.2 (s). High-res MALDI-TOF MS (anthracene, pos. mode):

m/z = 890.0372 ([M]$^+$, 100%, calcd for $^{12}C_{32}{}^{1}H_{24}{}^{11}B_2{}^{14}N_6{}^{16}O_6{}^{19}F_6{}^{32}S_2{}^{101}Ru$ 890.0345), 741.0924 ([M-OTf]$^+$, 20%). High-res ESI-MS (DCM/MeOH, pos. mode): m/z = 773.1065 ([M–OTf+HOMe]$^+$, 100%, calcd for Ru(Tpyb-OTf)(Tpyb-HOMe), $^{12}C_{32}{}^{1}H_{28}{}^{11}B_2{}^{19}F_3{}^{14}N_6{}^{16}O_4{}^{32}S_1{}^{101}Ru$ 773.1074). IR (ATR) with tentative assignments based on comparison with computational data *v* (cm^{-1}): 2961 (w, C-H stretching), 2924 (w, C-H stretching), 2850 (w, C-H stretching), 1464 (m, C-H bending), 1421 (s, C-H bending) 1360 (s, C-N stretch), 1261 (m, ring deformation), 1205 (w, B-O/C-S stretch), 1183 (s, C-H bending/C-F stretch), 1108 (b, C-H bending/S=O stretch/C-F stretch), 1065 (w, ring bending), 1013 (s, B-O stretch), 817 (sh, B-O stretch), 798 (s, C-H bending), 767 (w, C-H bending), 754 (s, ring stretching), 685 (w, ring stretching), 650 (m, ring breathing), 639 (m, ring stretching), 619 (s, S=O bending), 580 (m, S=O bending).

Synthesis of Bis(hydridotris(pyrid-2-yl)borate) Ruthenium(II) (2-H). In a 100 mL Schlenk flask compound **2-Br** (95 mg, 126 μmol) was suspended in 30 mL of anhydrous THF. $LiAlH_4$ (48 mg, 1.26 mmol, 10 equiv) was added and the reaction mixture was heated to 80 ºC for 3 d upon which a greenish yellow solution formed. As ^{1}H NMR analysis of the mixture revealed incomplete conversion, another portion of $LiAlH_4$ (48 mg, 1.26 mmol, 10 equiv) was added and the mixture continued to heat to 80 ºC for 2 d. ^{1}H and ^{11}B NMR analysis of the mixture indicated essentially quantitative conversion to the product. The mixture was filtered to remove salts and unreacted $LiAlH_4$, poured into an aqueous sodium bicarbonate solution, and extracted several times with diethyl ether. After rotary evaporation of the solvents, the yellow-orange crude product was subject to column chromatography on silica gel with a mixture of toluene and pentane (1:1) containing 1% of NEt_3 as the eluent. The product was obtained as a light-yellow solid upon rotary evaporation, washed with pentane and dried under high vacuum. Yield for **2-H**: 57 mg (76%). Single crystals for X-ray diffraction were obtained by slow evaporation of a solution in a mixture of benzene and *n*-octane. ^{1}H NMR (599.7 MHz, C_6D_6) δ = 8.14 (d, J = 7.2 Hz, 6H, pyridyl-H3), 7.12 (d, J = 5.4 Hz, 6H, pyridyl-H6), 7.04 (dpst, J = 7.2 Hz, 1.2 Hz, 6H, pyridyl-H4), 6.06 (dpst, J = 6.6 Hz, 1.8 Hz, 6H, pyridyl-H5), 4.71 (br q, $^1J(^{11}B, ^1H)$ = 89 Hz, 2H, B-H). $^{13}C\{^1H\}$ NMR (150.8 MHz, C_6D_6) δ = 184 (q, $^1J(^{11}B, ^{13}C)$ = 38 Hz, pyridyl-C2), 154.8 (pyridyl-C6), 132.4 (pyridyl-C4), 128.7 (pyridyl-C3), 120.8 (pyridyl-C5), Ph-C1 (not observed). ^{11}B NMR (160.4 MHz, C_6D_6) δ = -6.7 (d, $^1J(^{11}B, ^1H)$ = 89 Hz, B-H). High-res ESI-MS (DCM/acetonitrile, pos. mode): m/z = 594.1435 ([M]$^+$, calcd for $^{12}C_{30}{}^{1}H_{26}{}^{11}B_2{}^{14}N_6{}^{101}Ru$ 594.1461). IR (ATR) with tentative assignments based on comparison with computational data *v* (cm^{-1}): 3061 (w, C-H stretch), 2313 (m, B-H stretch), 1588 (w, C=C stretch), 1550 (w, C=C stretch), 1450 (s, C-H bending), 1417 (m, C-H bending), 1264 (w, Py ring deformation), 1216 (w, Py ring deformation), 1150 (m, Py ring stretch), 1016 (s, B-H wagging/Py ring breathing), 765 (s, C-H out-of-plane bending), 747 (s, C-H out-of-plane bending), 649 (m, Py ring deformation), 604 (m, Py ring puckering).

Synthesis of Bis((3-bromopyridyl)tris(pyrid-2-yl)borate) Ruthenium(II) Triflate (3-Py). In a glovebox, **2-OTf** (11.8 mg, 13.0 μmol) was weighed in a tared 20 mL scintillation vial. Dried, degassed 3-bromopyridine (1 mL, 10.3 mmol) was added, forming a bright yellow solution, and the vial sealed. The vial was then removed from the glovebox and heated to 150 °C overnight. The next day, the orange solution was allowed to cool to room temperature and the formation of light-

orange crystals was observed. The residue was dried under high vacuum at room temperature for 1 h, and then at 50 °C under high vacuum for a further 6 h to remove excess 3-bromopyridine. The product was extracted with toluene overnight, taken up in a mixture of DCM and toluene (1:1), and then precipitated by storing the solution at -20 °C overnight. The product was isolated as a yellow powdery solid. Single crystals for X-ray diffraction were obtained by slow evaporation of a solution in a mixture of CH_2Cl_2 and acetronitrile. Yield for [**3-Py**](**OTf**)$_2$: 11.4 mg (71%). ^{1}H NMR (500 MHz, CD_3CN) δ 9.51 (s, 1H s, 2H, BrPy-H2), 9.45 (d, *J* = 5.8 Hz, 2H d, J = 5.5 Hz, 2H, BrPy-H6), 8.90 (d, *J* = 8.3 Hz, 2H, BrPy-H4), 8.23 (dd, *J* = 8.3, 5.9 Hz, 2H, BrPy-H5), 7.63 (td, *J* = 7.8, 1.4 Hz, 6H, pyridyl-H4), 7.13 (d, *J* = 7.8 Hz, 6H, pyridyl-H3), 7.10 (d, *J* = 5.3 Hz, 6H, pyridyl-H6), 6.81 (td, *J* = 7.2, 5.8, 1.3 Hz, 6H, pyridyl-H5). ^{13}C{^{1}H} NMR (126 MHz, $CDCl_3$) δ 156.7, 150.6, 148.7, 148.5, 135.5, 130.2, 126.2, 124.1, 123.9, Ph-C1 (not observed). ^{11}B NMR (160.4 MHz, CD_3CN) δ = 0.8 ($w_{1/2}$ = 380 Hz). ^{19}F NMR (470.3 MHz, $CDCl_3$) δ –74.04 High-res ESI-MS (DCM/acetonitrile, pos. mode): m/z = 1056.9892 ([M–OTf]$^+$, calcd for $^{12}C_{41}{}^1H_{32}{}^{11}B_2{}^{79}Br^{81}Br{}^{19}F_3{}^{14}N_8{}^6O_3{}^{101}Ru_1{}^{32}S_1$ 1056.9866). IR (ATR) with tentative assignments based on comparison with computational data *v* (cm^{-1}): 2962 (m, C-H stretching) 2919 (w C-H stretching), 2850 (w, C-H stretching), 1613 (m, ring deformation,) 1462 (m, C-H bending). 1262 (s, Py ring deformation), 1146 (m, C-H bending), 1108 (w, C-H bending), 1027 (s, B-N stretch), 837 (w, ring breathing), 799 (s, C-H out-of-plane bending), 750 (m, ring deformation), 726 (m, ring puckering), 704 (w, ring deformation), 686 (w, ring deformation), 633 (s, ring stretching), 567 (w, ring puckering)

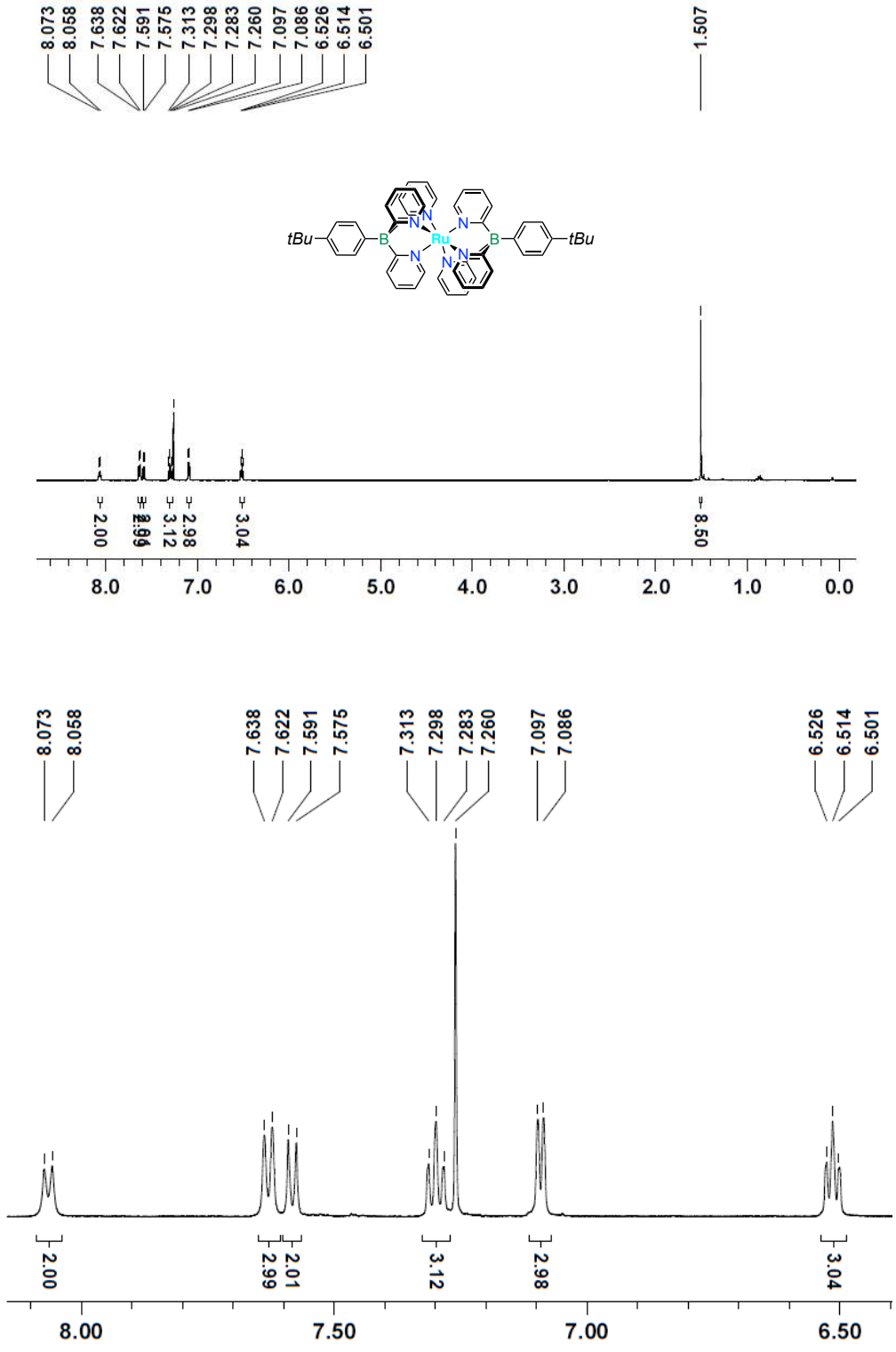

Figure S1. ^{1}H NMR spectrum of complex **1** in $CDCl_3$ and expansion.

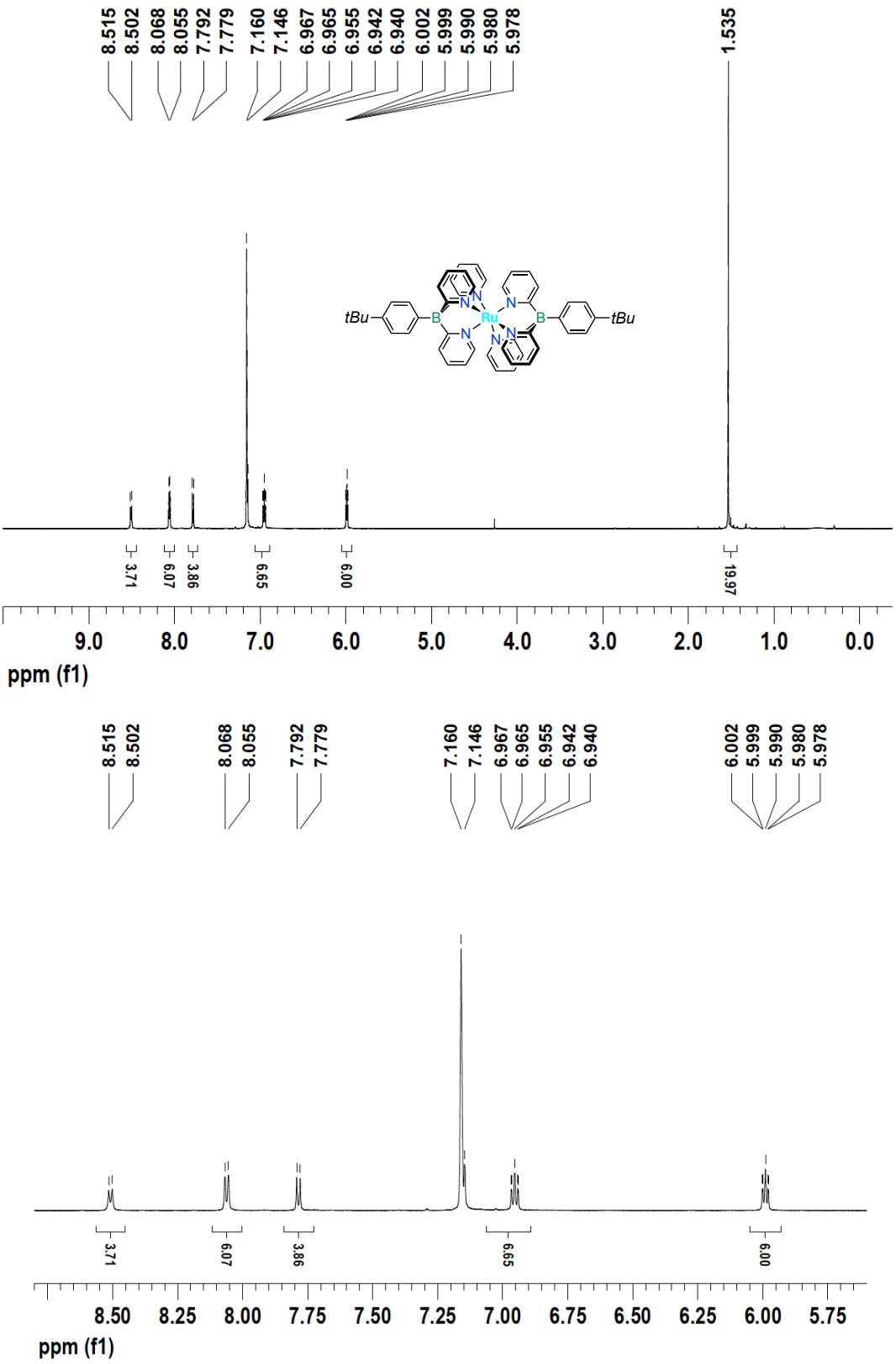

Figure S2. ^{1}H NMR spectrum of complex **1** in C_6D_6 and expansion.

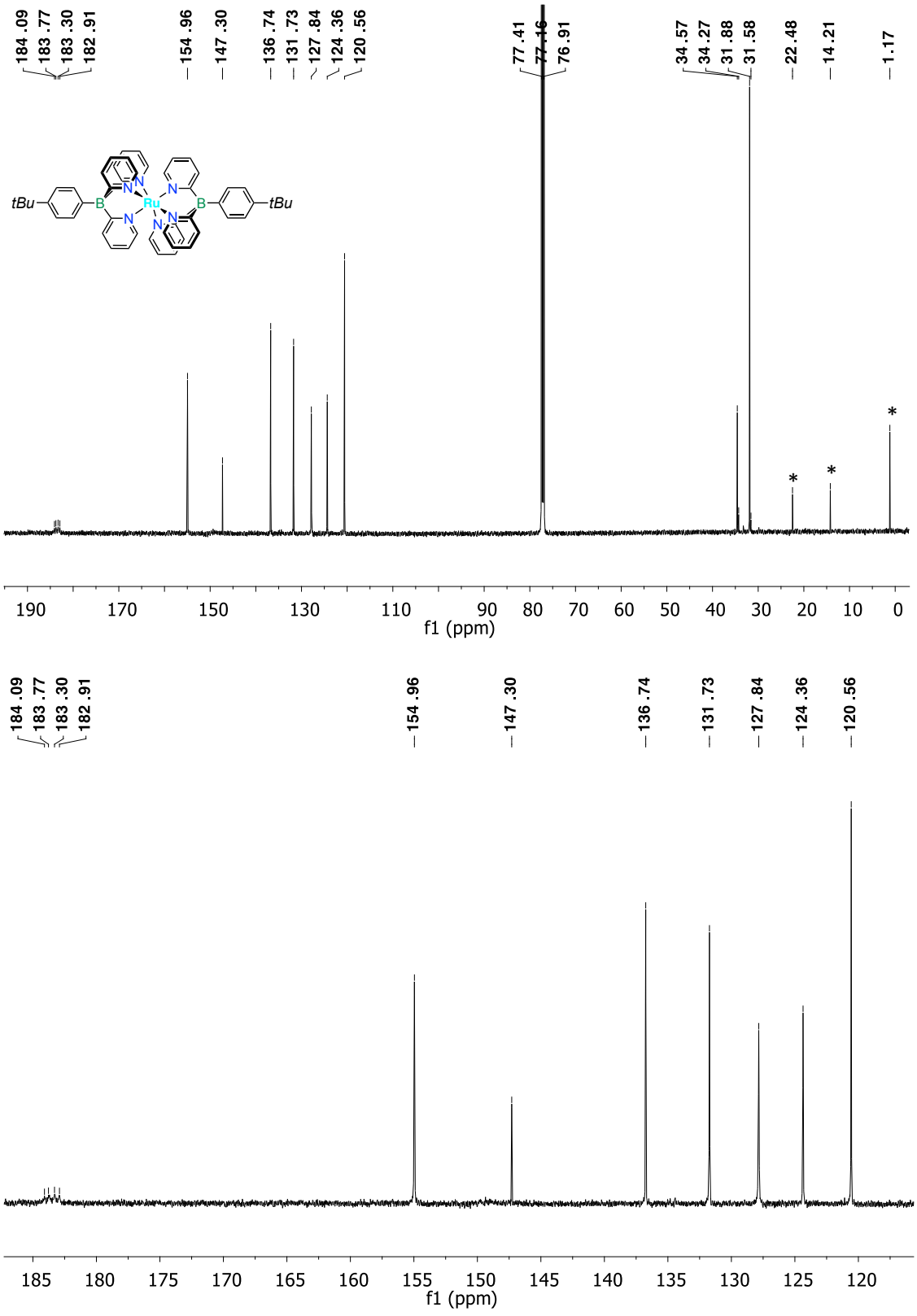

Figure S3. $^{13}C\{^{1}H\}$ NMR spectrum of complex **1** in $CDCl_3$ and expansion. * = hexanes

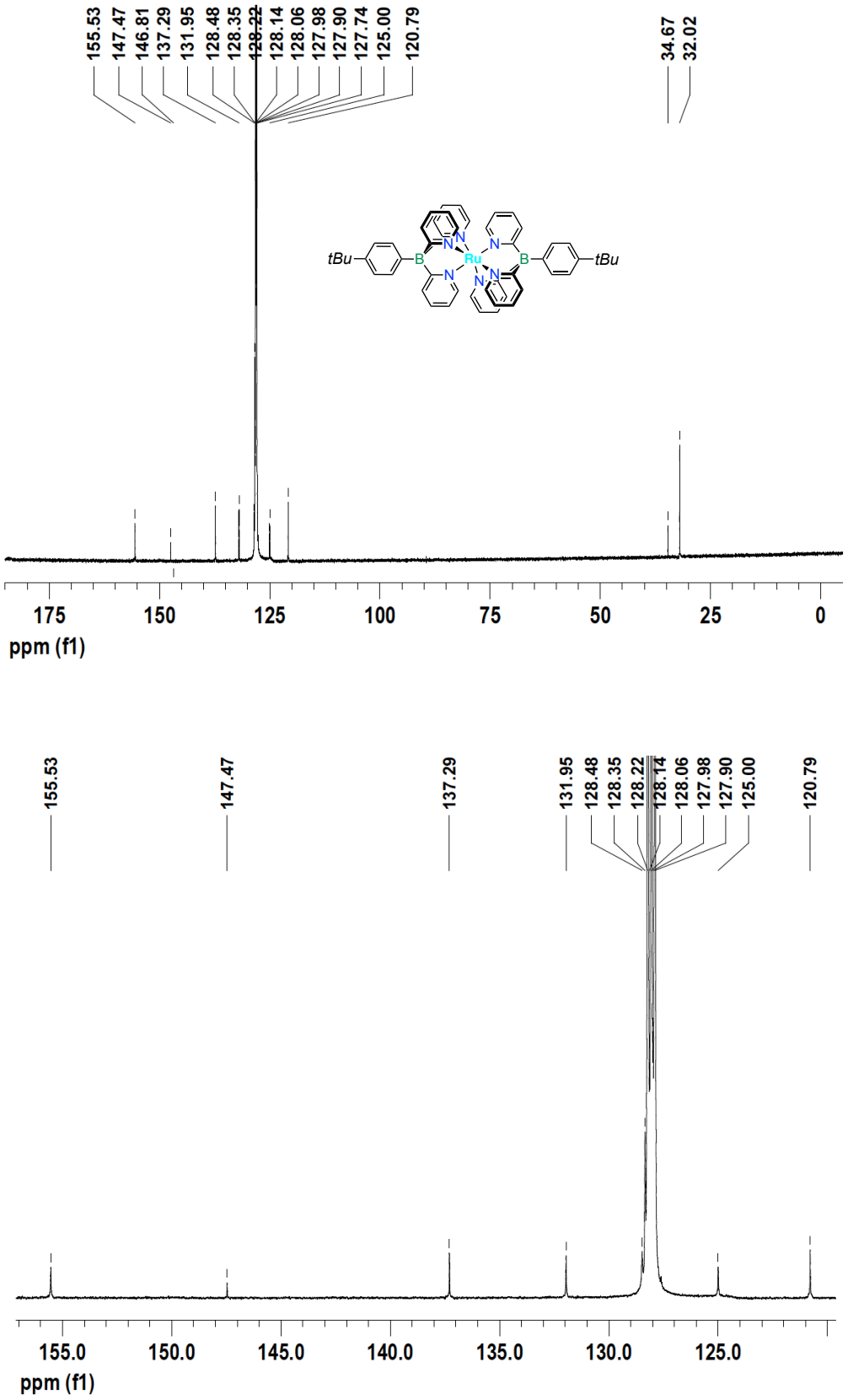

Figure S4. $^{13}C\{^{1}H\}$ NMR spectrum of complex **1** in C_6D_6 and expansion.

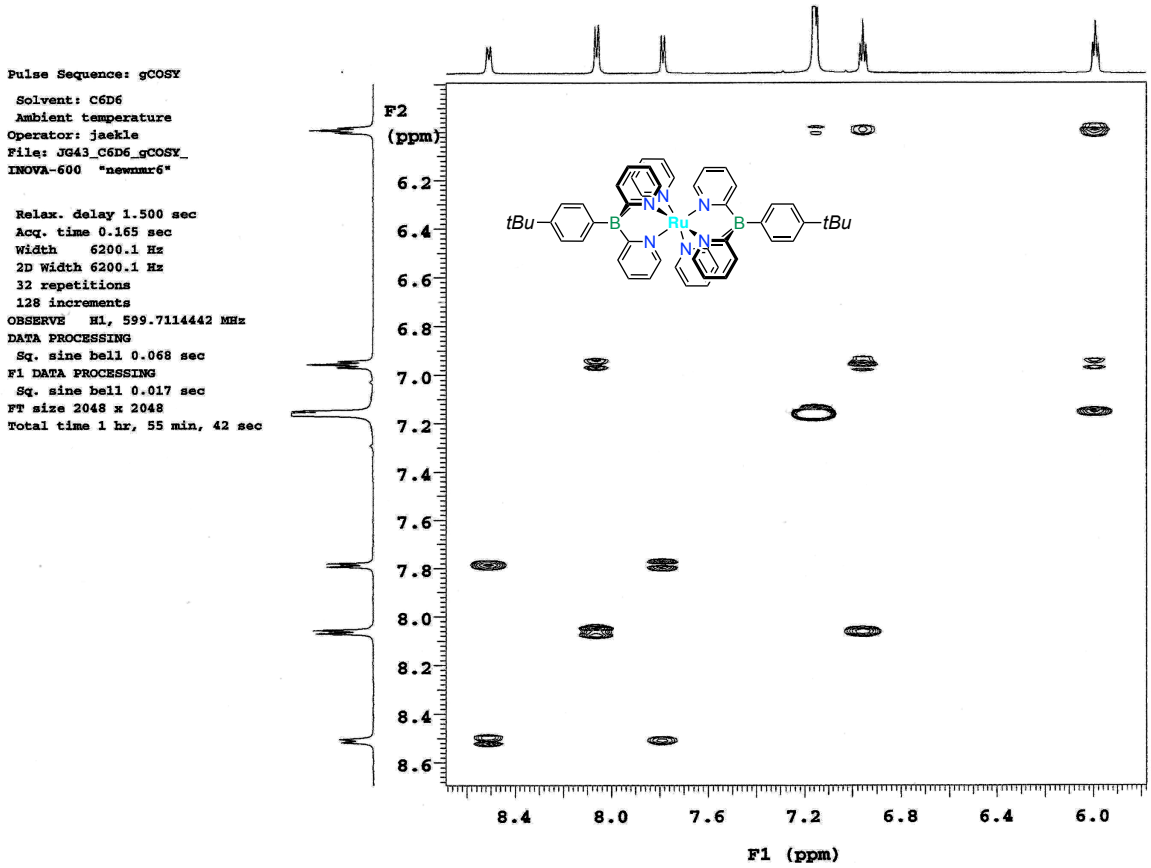

Figure S5. H,H-COSY NMR data of complex **1** in C_6D_6 (aromatic region).

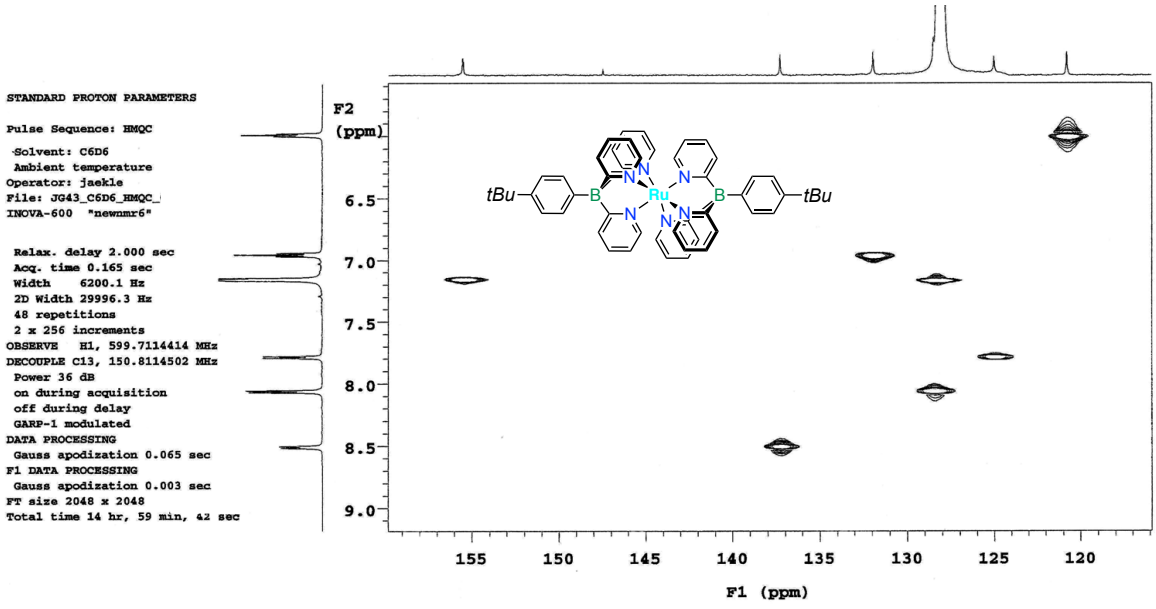

Figure S6. HMQC NMR data of complex **1** in C_6D_6 (aromatic region).

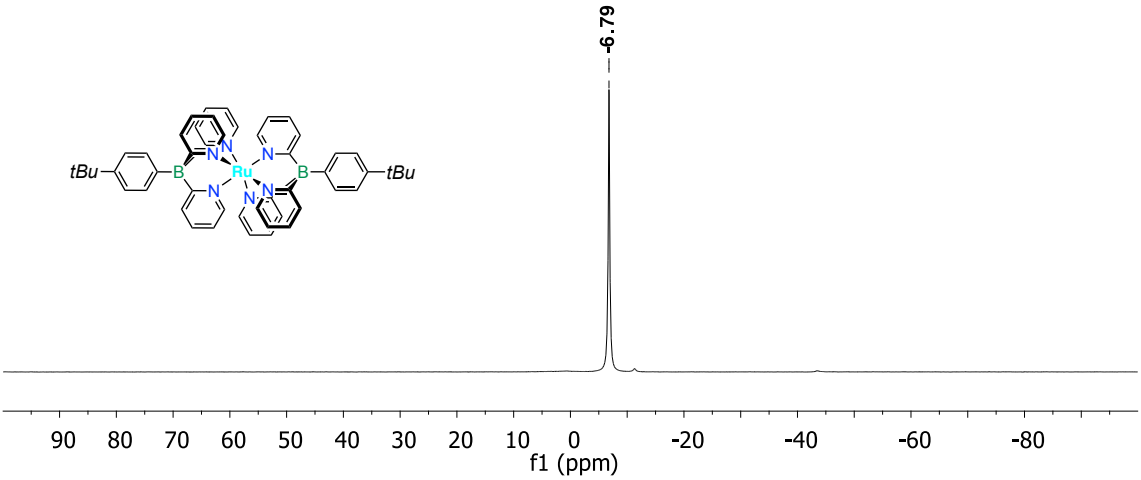

Figure S7. ^{11}B NMR spectrum of complex **1** in $CDCl_3$.

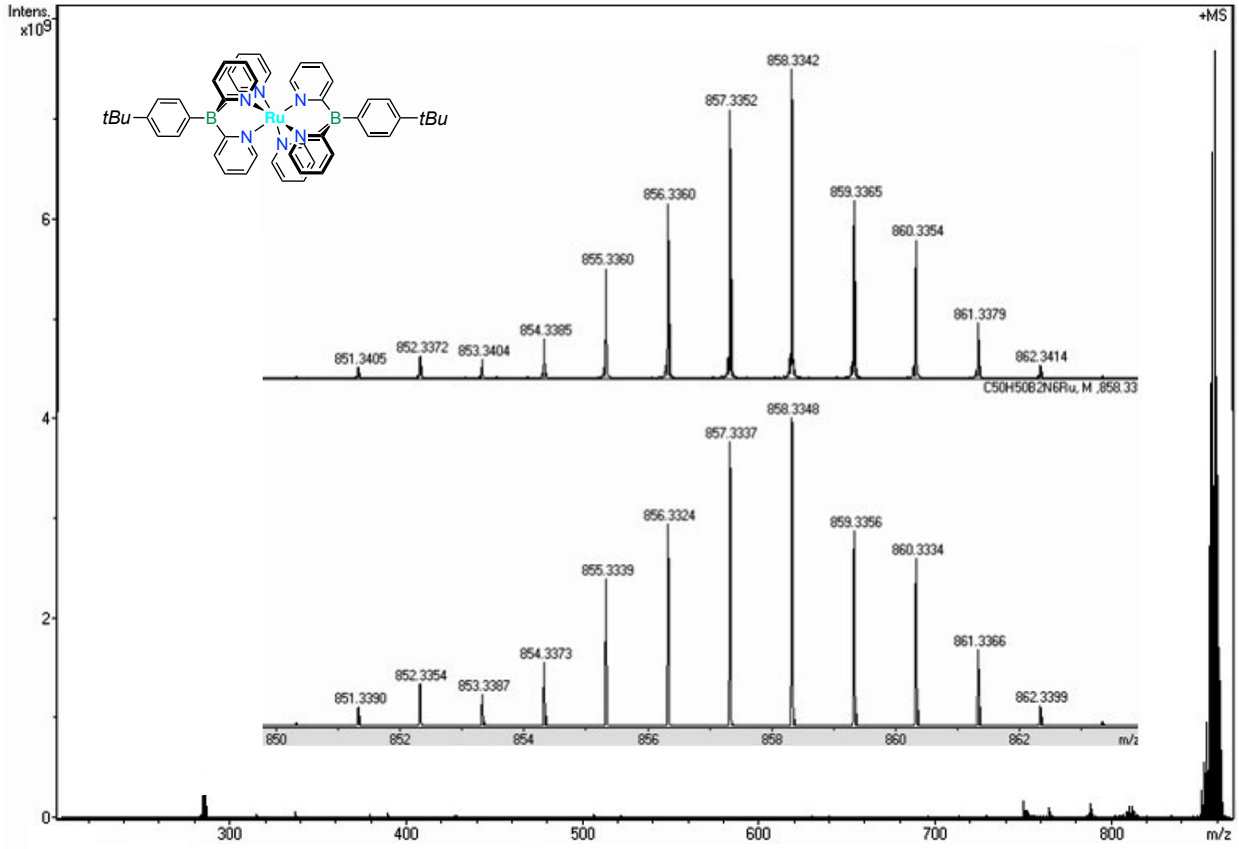

Figure S8. ESI-MS data of complex **1** (DCM/acetonitrile).

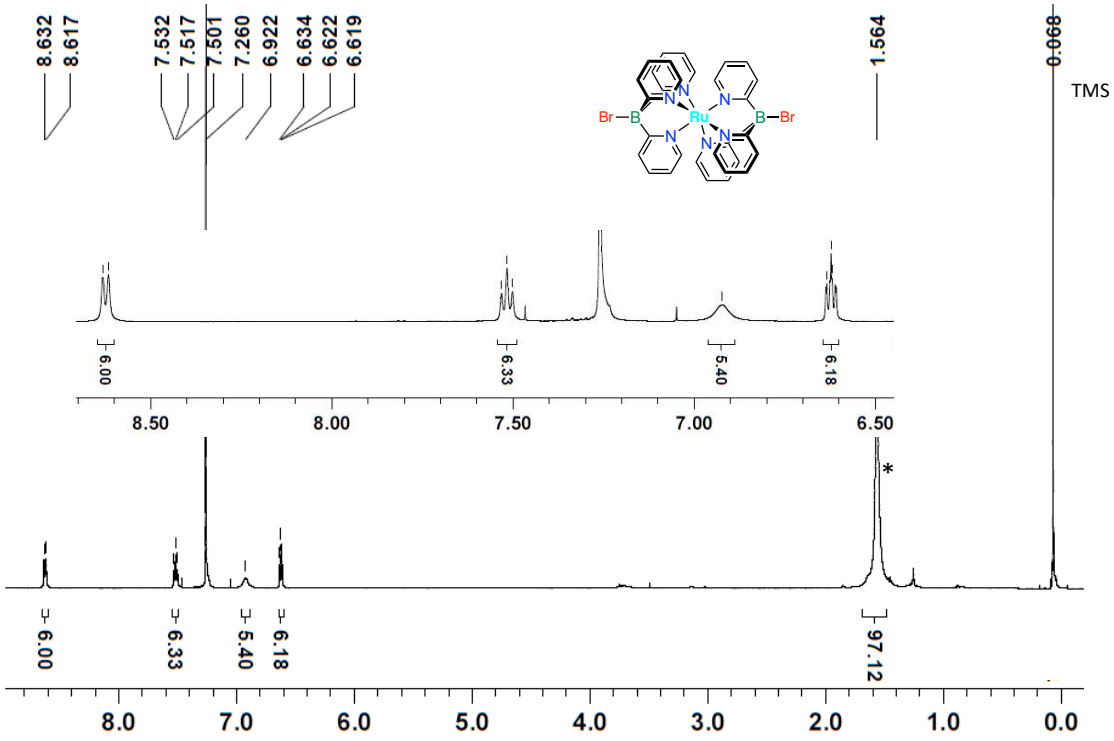

Figure S9. ^{1}H NMR spectrum of complex **2-Br** in $CDCl_3$ and expansion (* H_2O).

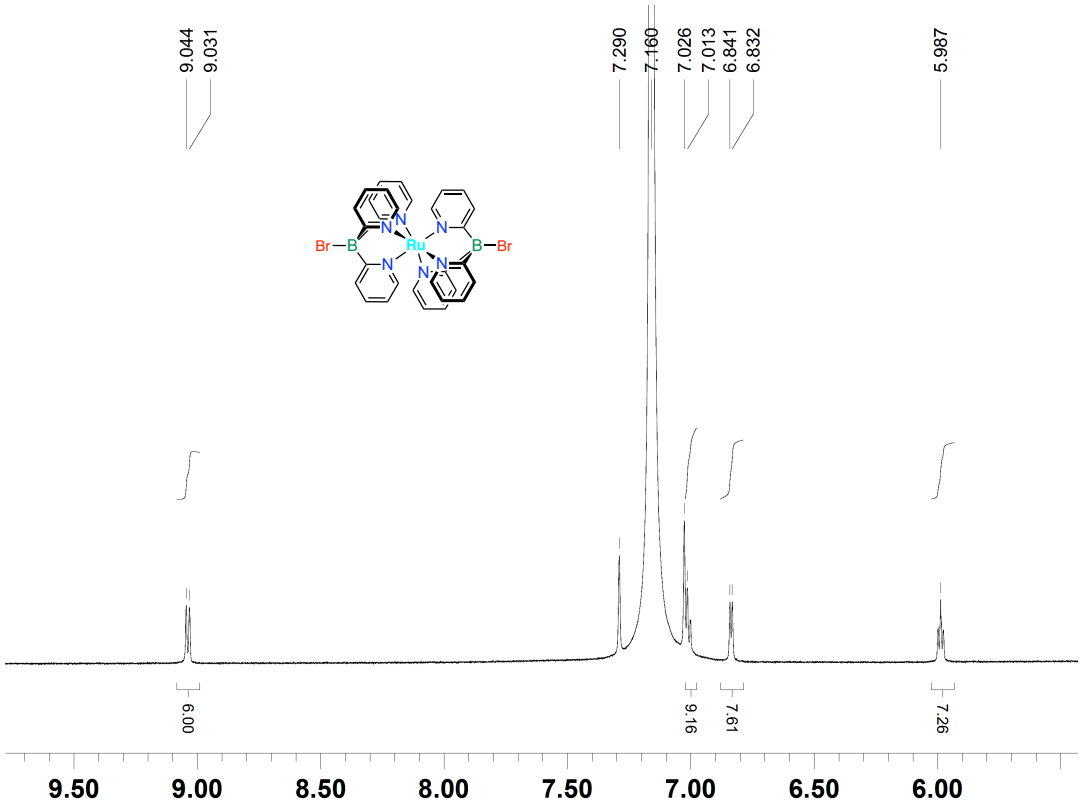

Figure S10. ^{1}H NMR spectrum of complex **2-Br** in C_6D_6.

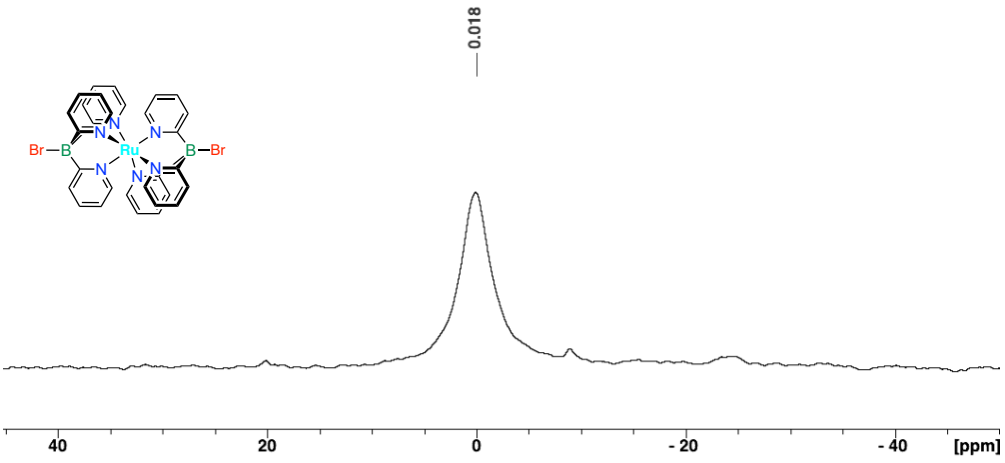

Figure S11. ^{11}B NMR spectrum of complex **2-Br** in $CDCl_3$.

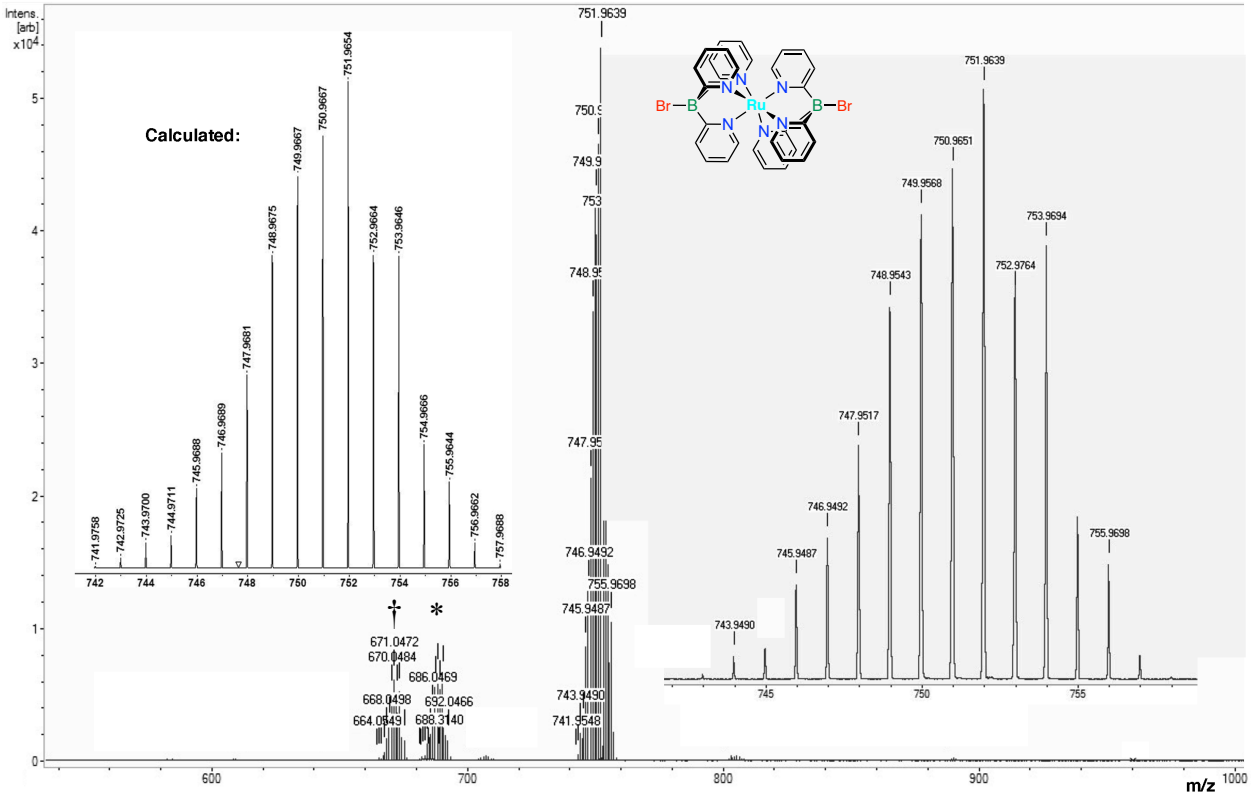

Figure S12. MALDI-TOF MS data of complex **2-Br** (anthracene, positive mode, from $CHCl_3$).

* = [Ru(Tpyb-Br)(Tpyb-OH)], † = fragment

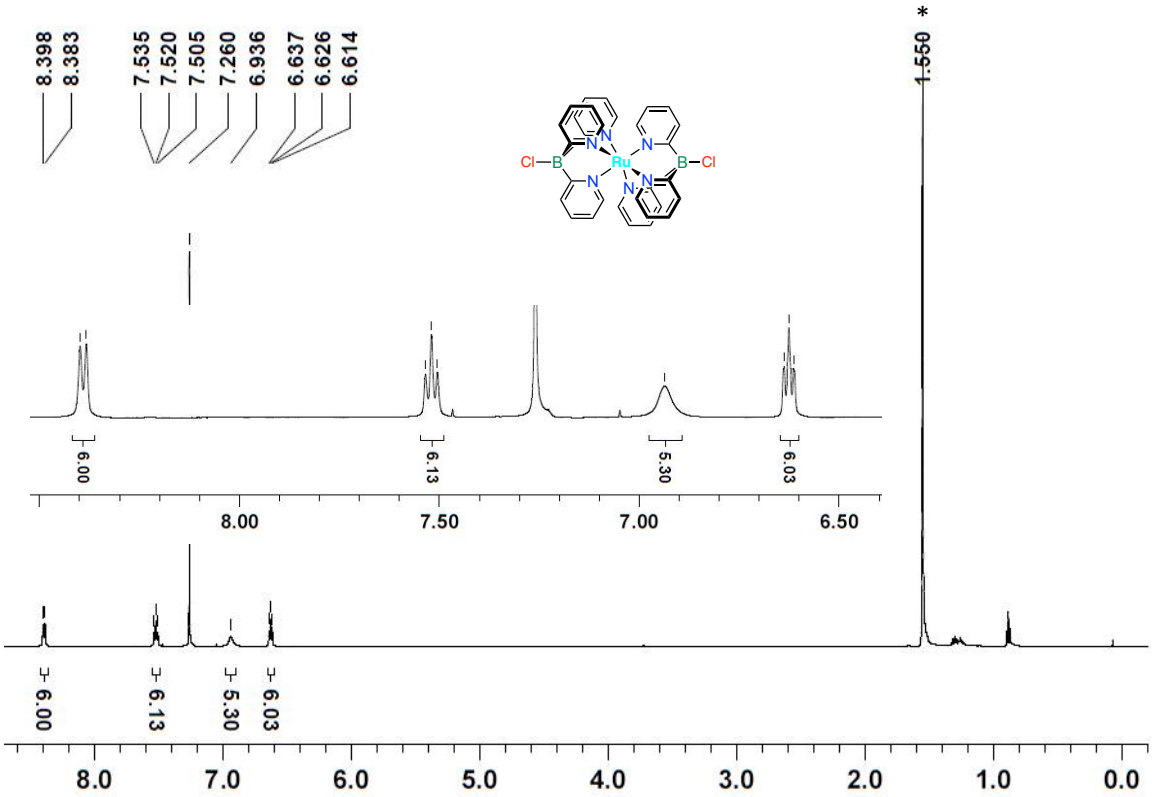

Figure S13. ^{1}H NMR spectrum of complex **2-Cl** in $CDCl_3$ and expansion (* H_2O).

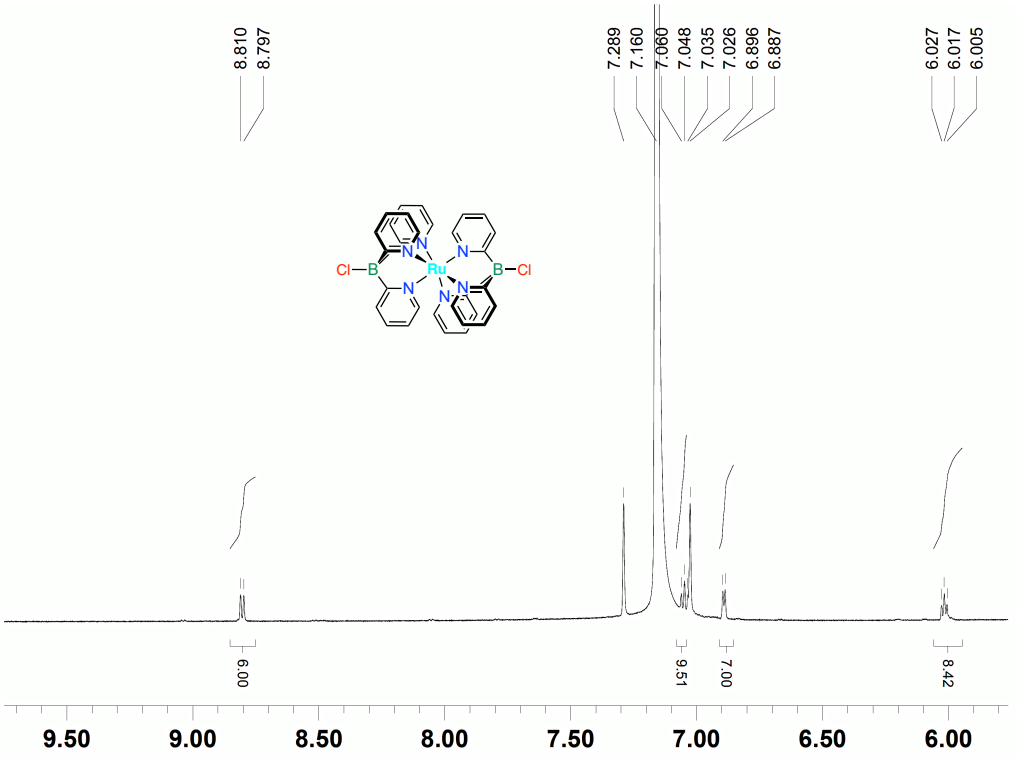

Figure S14. ^{1}H NMR spectrum of complex **2-Cl** in C_6D_6.

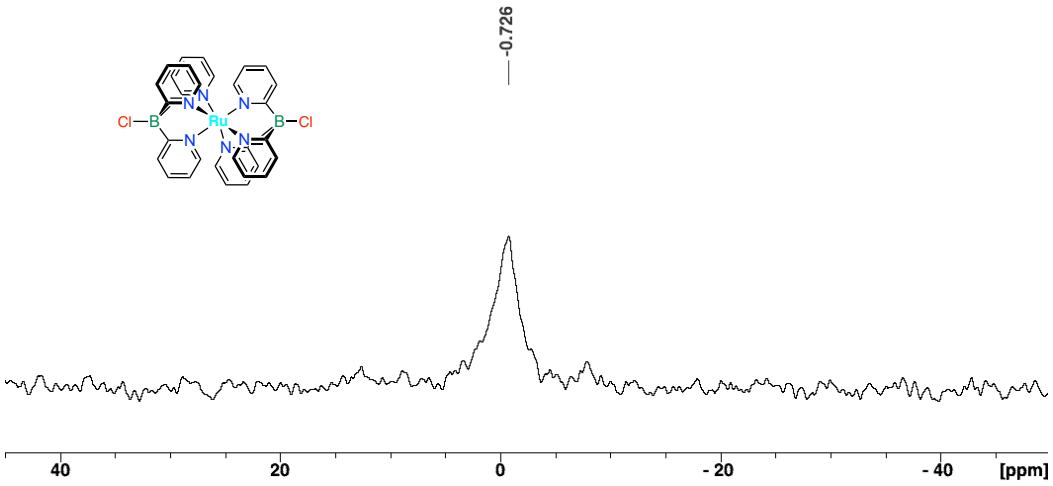

Figure S15. ^{11}B NMR spectrum of complex **2-Cl** in $CDCl_3$.

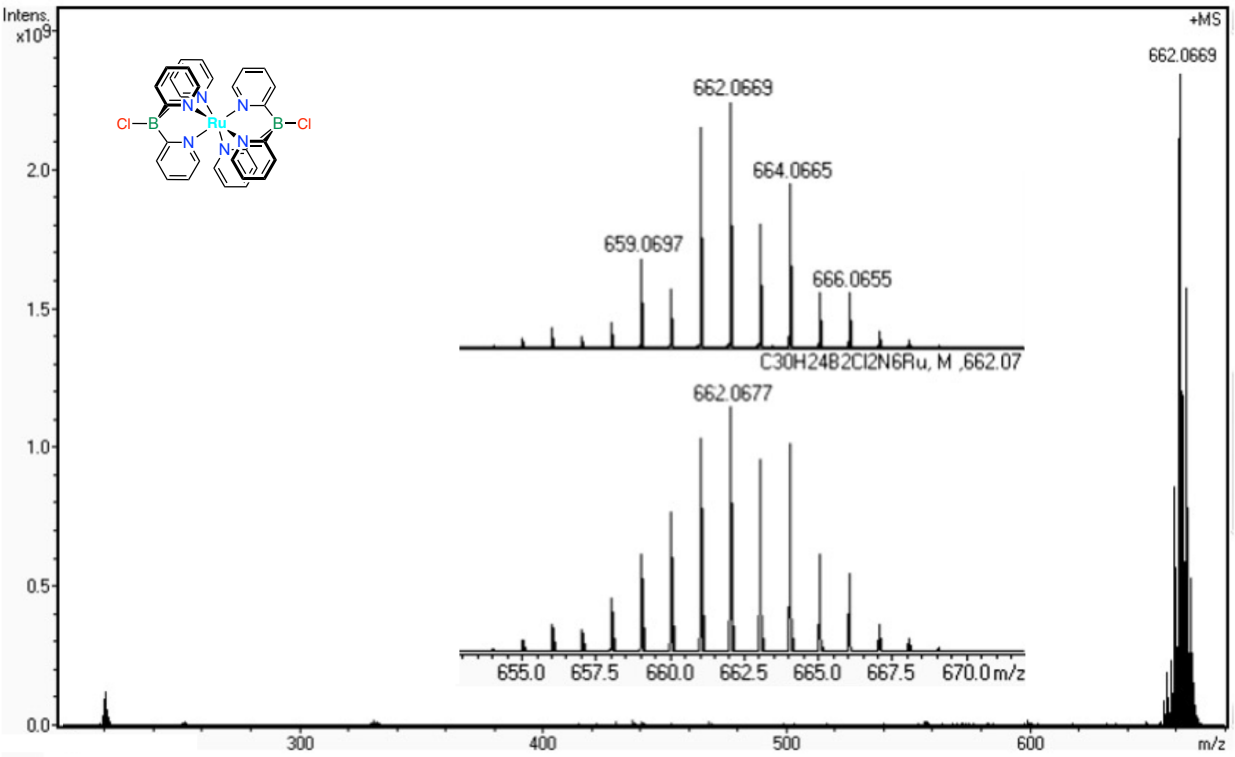

Figure S16. ESI-MS data of complex **2-Cl** (DCM).

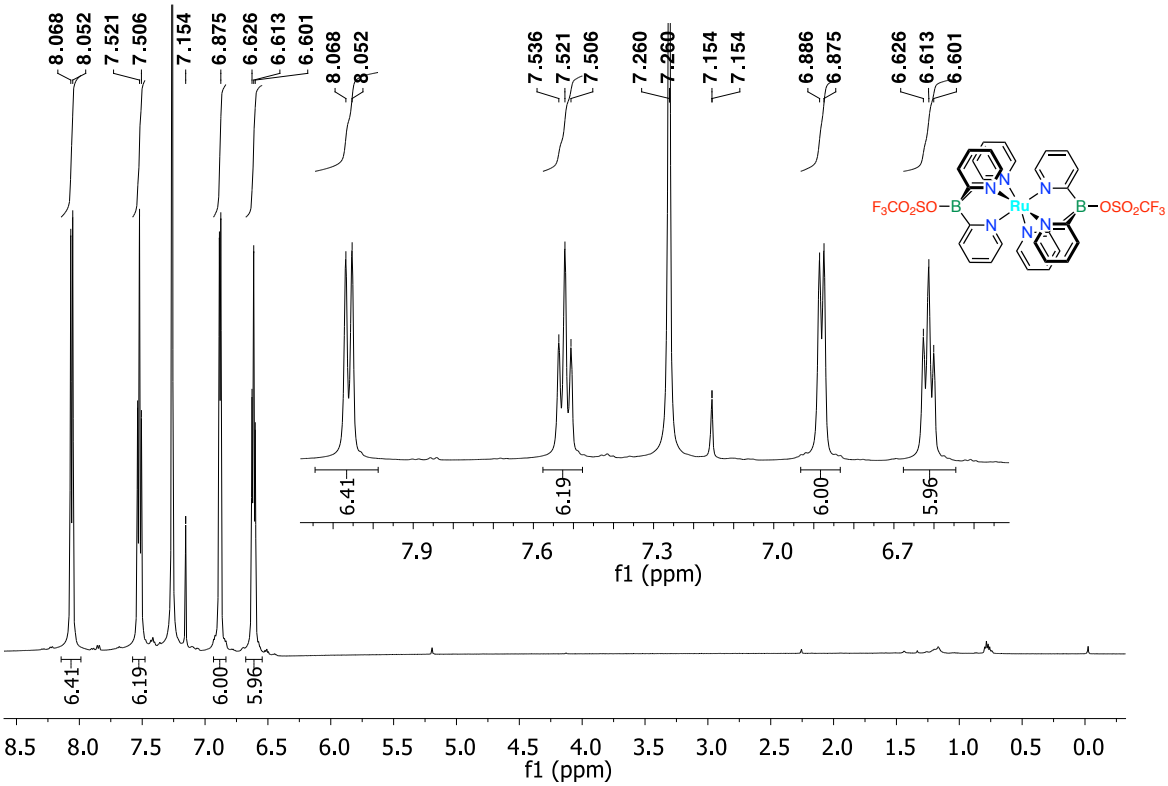

Figure S17. ^{1}H NMR spectrum of **2-OTf** in $CDCl_3$ and expansion.

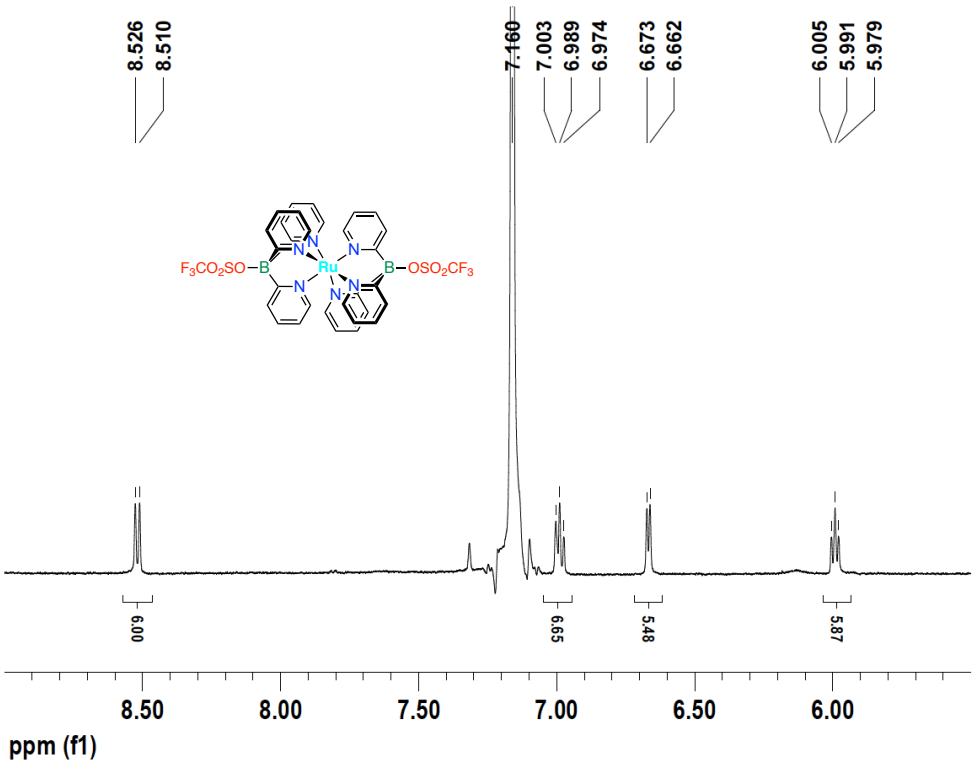

Figure S18. ^{1}H NMR spectrum of **2-OTf** in C_6D_6 (expansion)

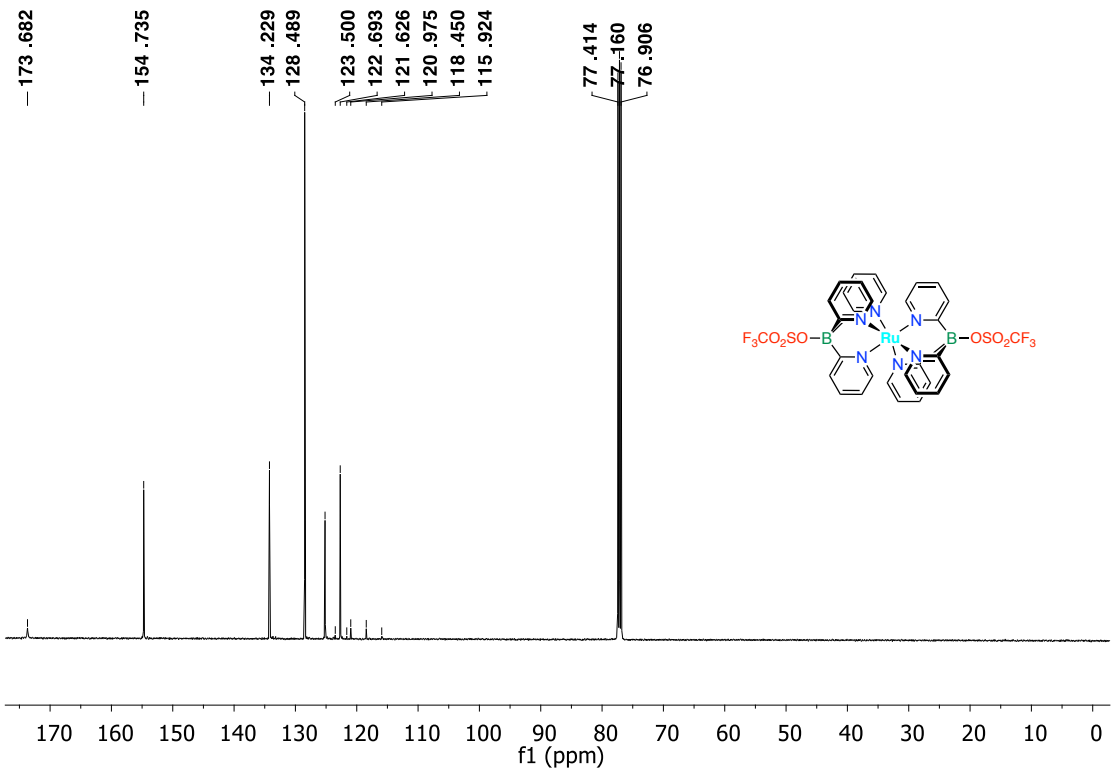

Figure S19. $^{13}C\{^{1}H\}$ NMR spectrum of complex **2-OTf** in $CDCl_3$.

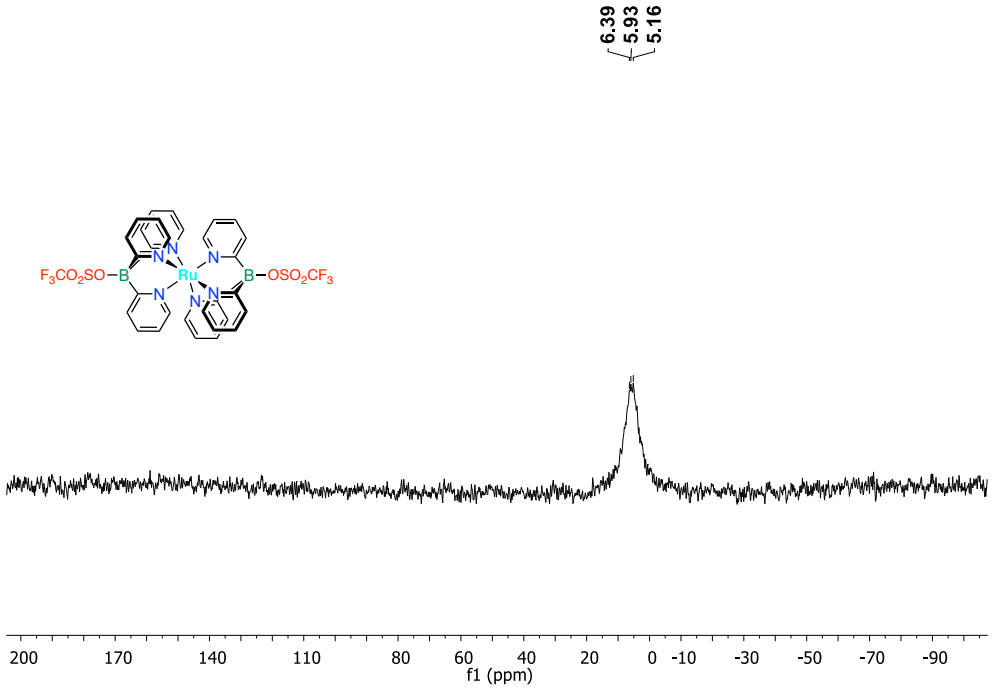

Figure S20. ^{11}B NMR spectrum of complex **2-OTf** in $CDCl_3$.

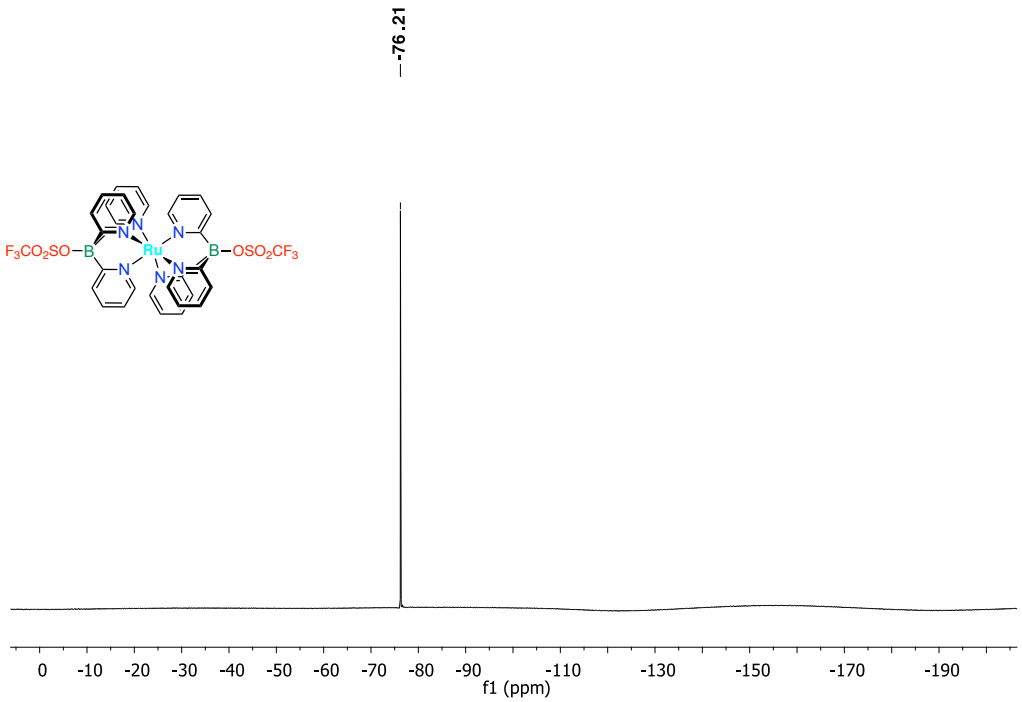

Figure S21. ^{19}F NMR spectrum of complex **2-OTf** in $CDCl_3$

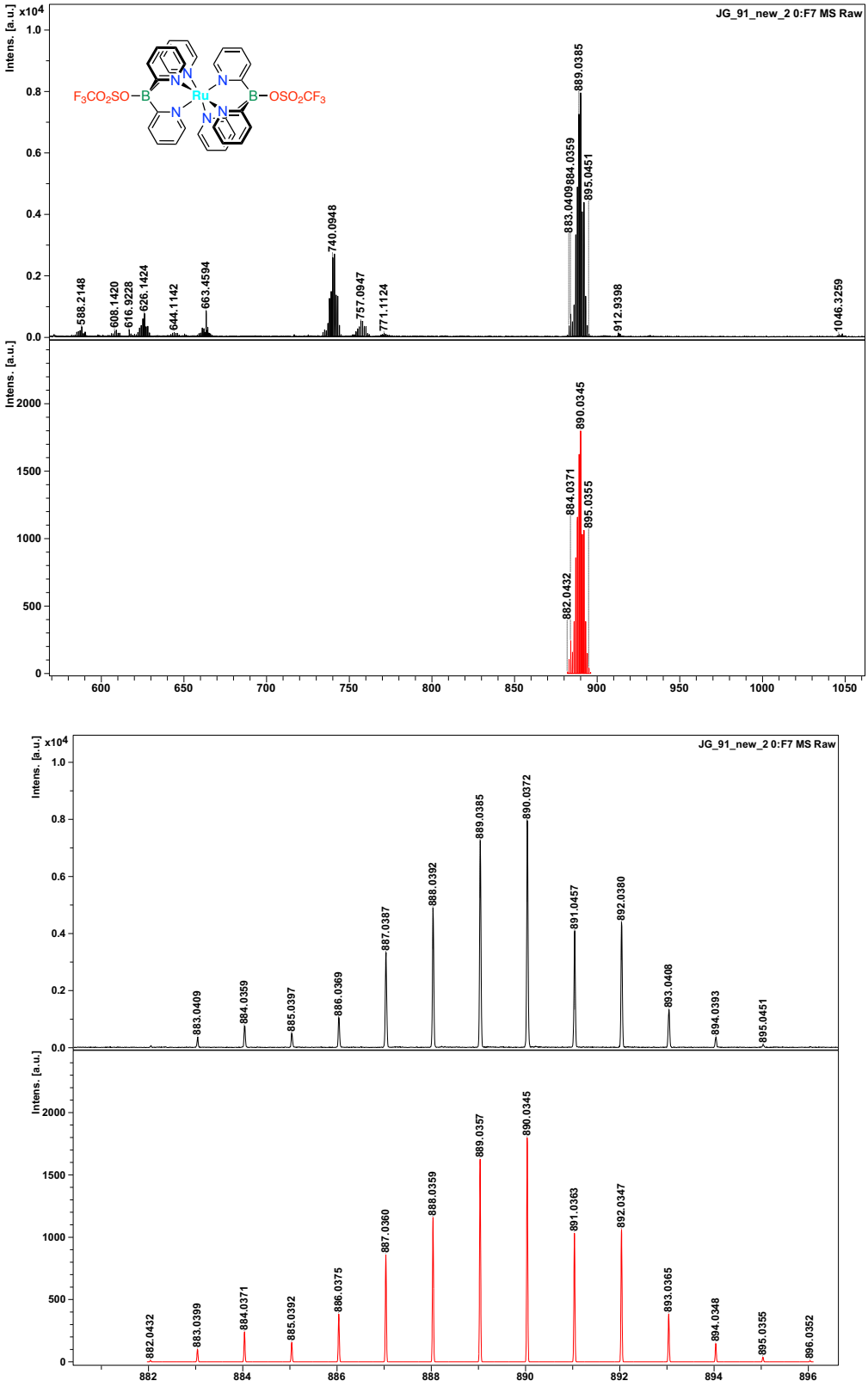

Figure S22. MALDI-TOF MS data of complex **2-OTf** (anthracene, positive mode, from $CHCl_3$).

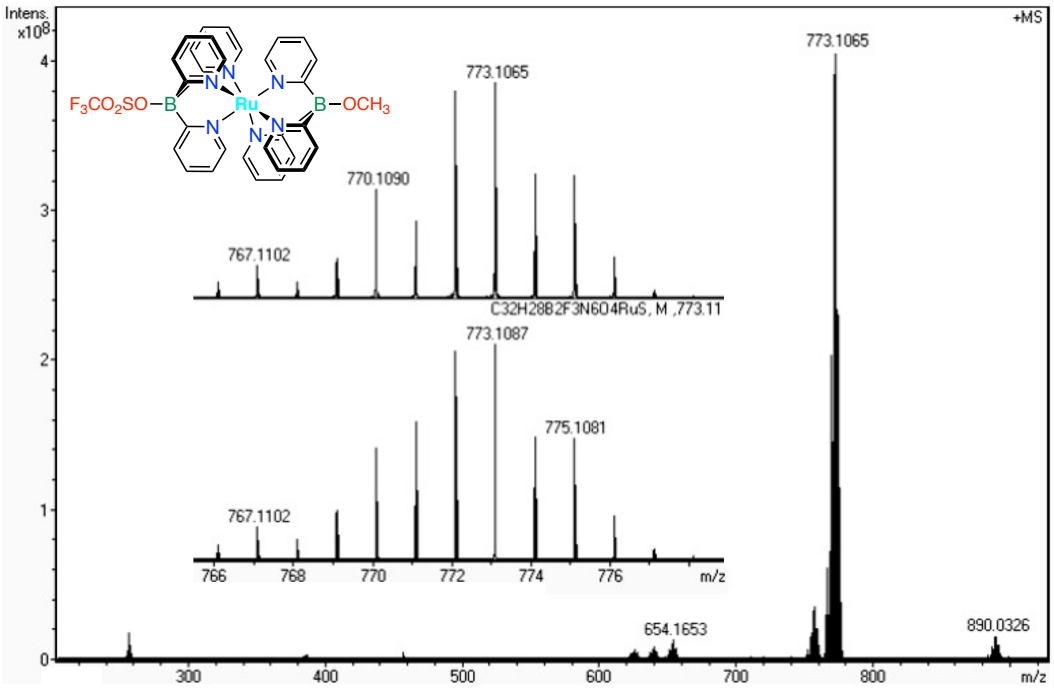

Figure S23. ESI-MS data from DCM/MeOH showing formation of [Ru(Tpyb-OTf)(Tpyb-OMe)]

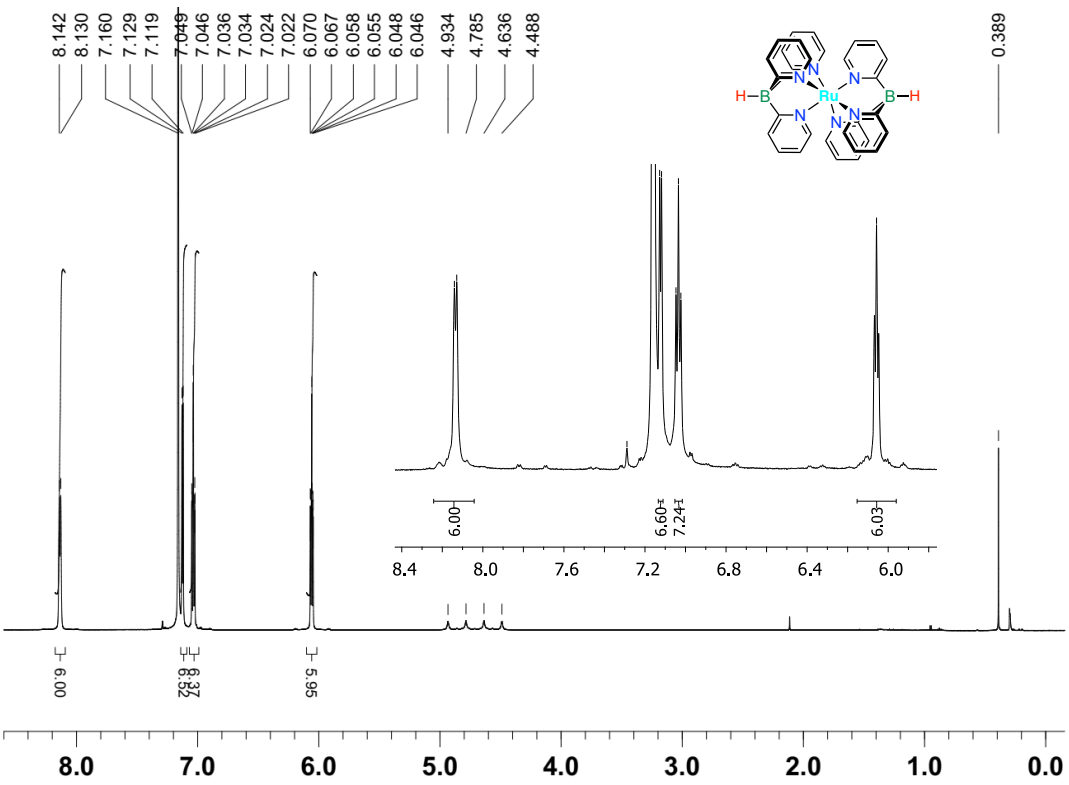

Figure S24. ^{1}H NMR spectrum of complex **2-H** in C_6D_6 and expansion

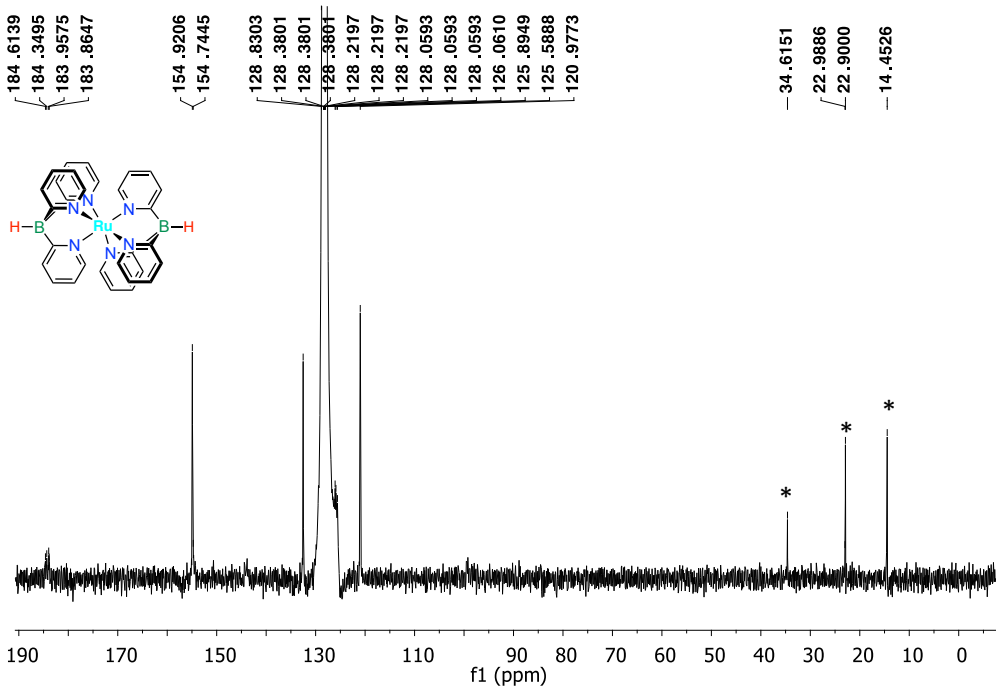

Figure S25. $^{13}C\{^{1}H\}$ NMR spectrum of complex **2-H** in C_6D_6 (* pentane)

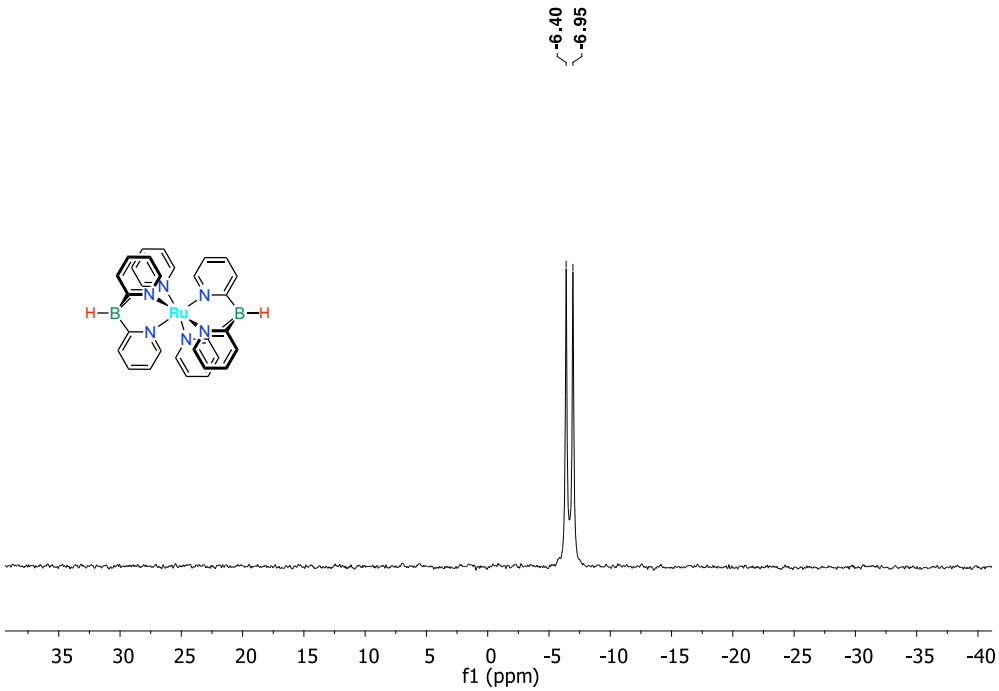

Figure S26. ^{11}B NMR spectrum of complex **2-H** in C_6D_6.

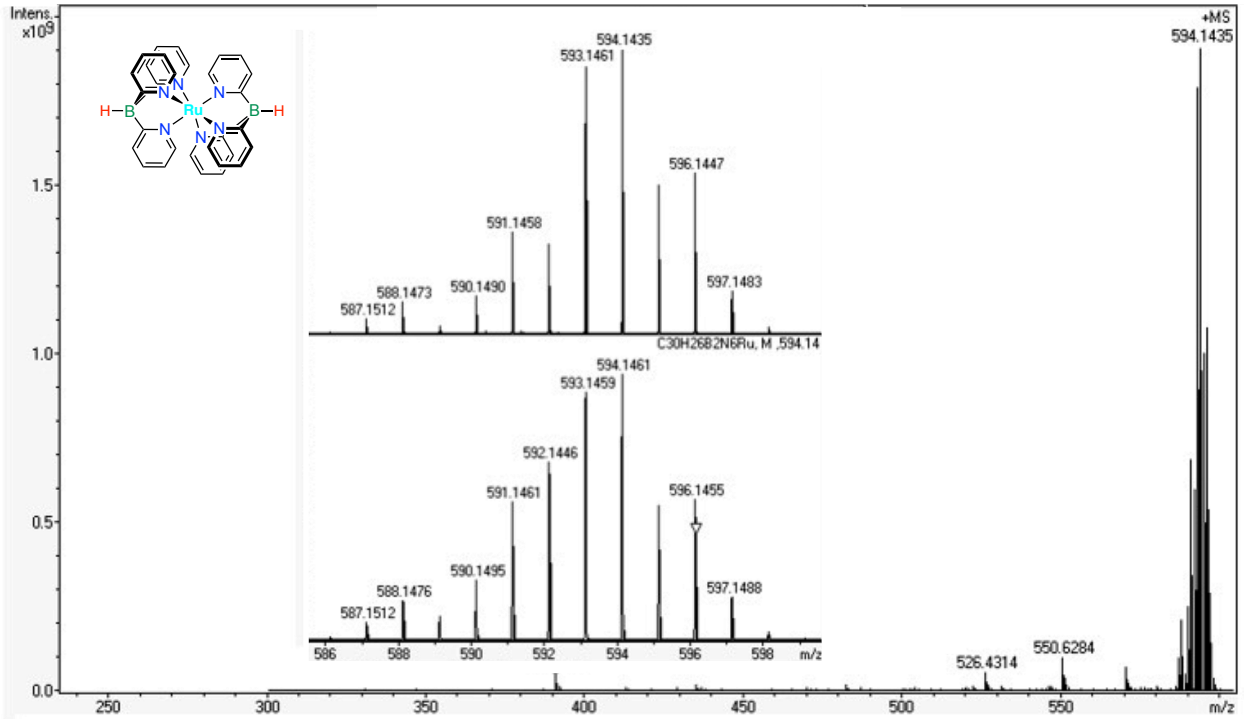

Figure S27. ESI-MS data of complex **2-H** (DCM/acetonitrile).

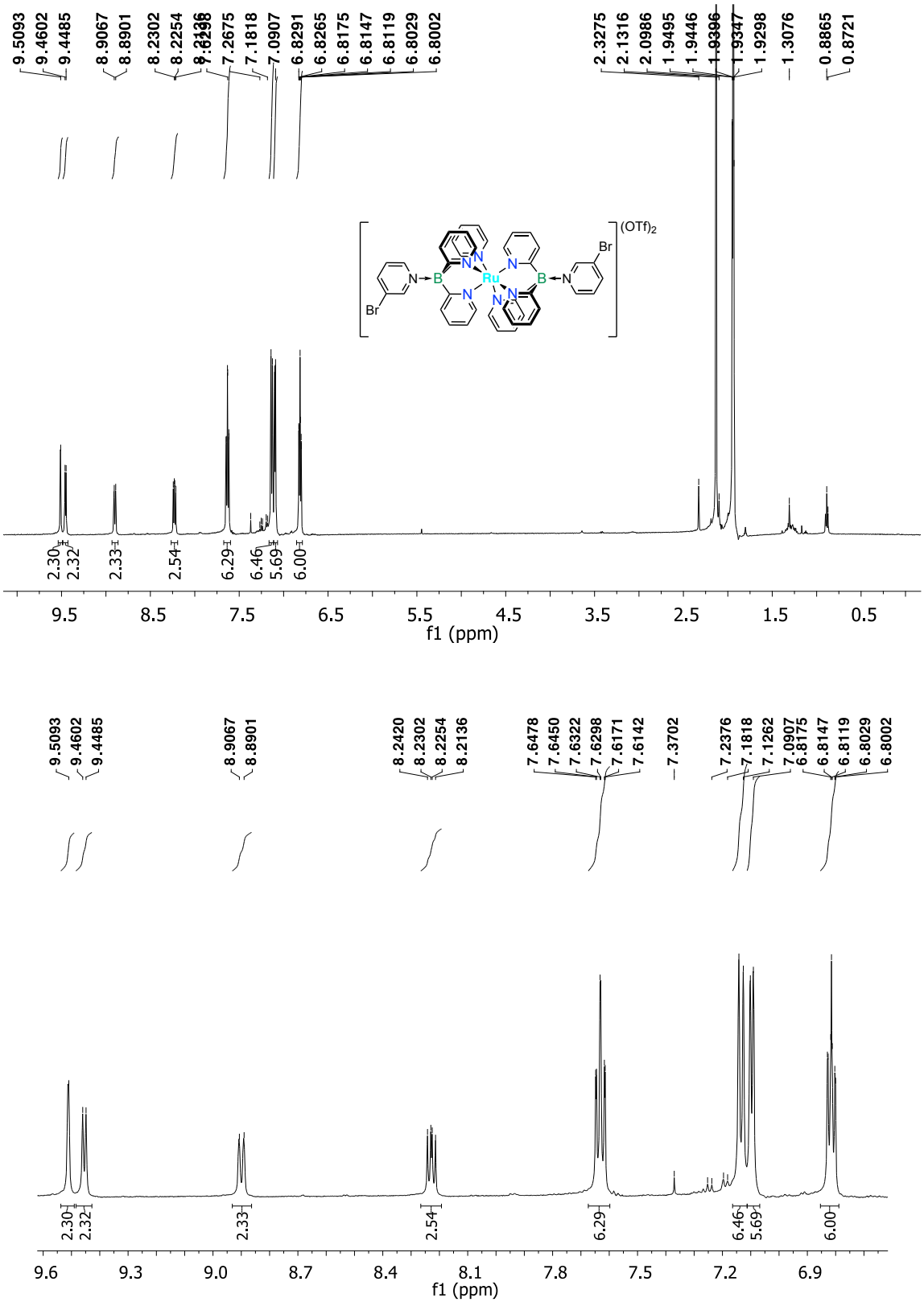

Figure S28. ^{1}H NMR spectrum of [**3-Py**](OTf)$_2$ in CD_3CN and expansion.

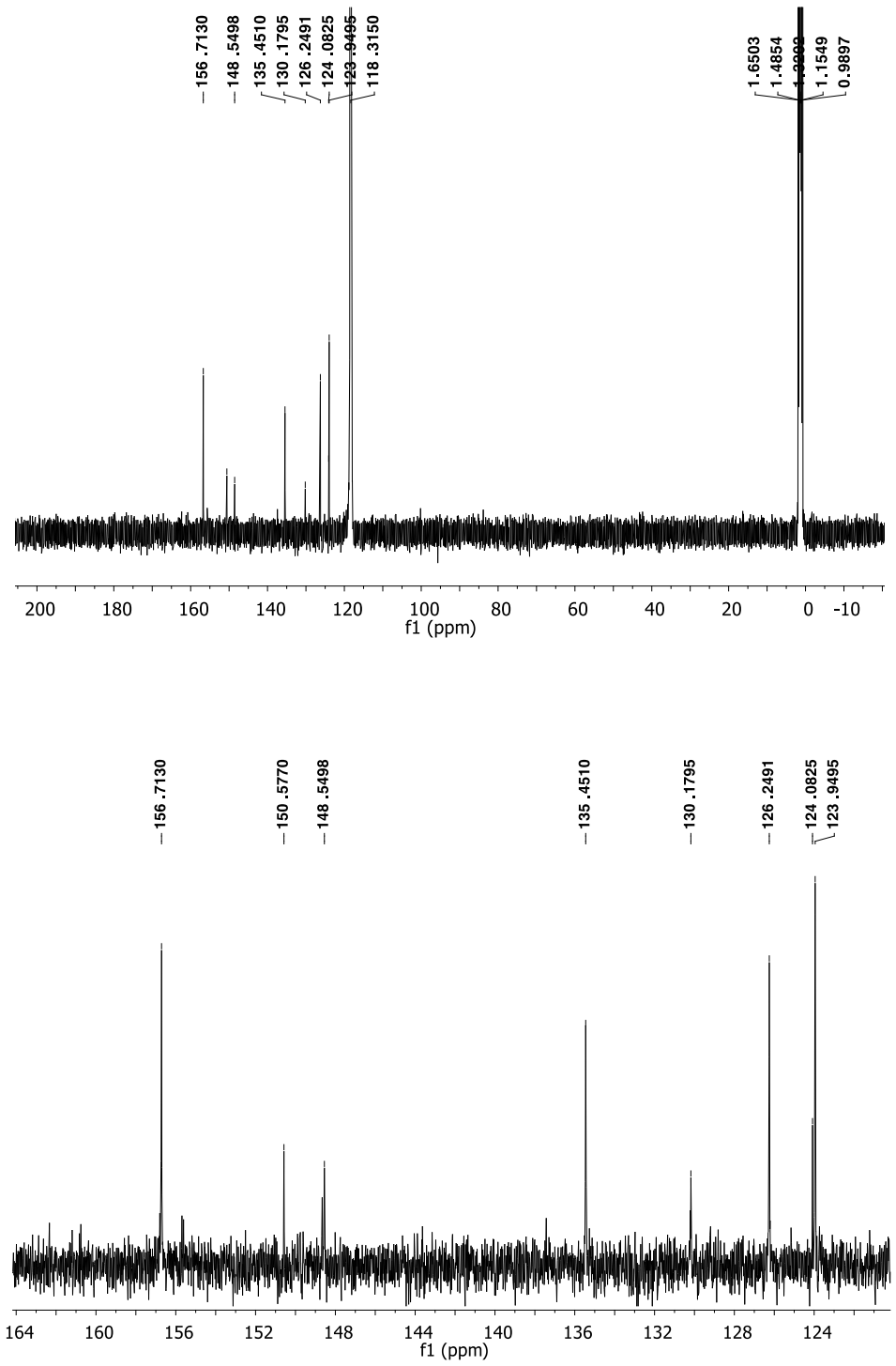

Figure S29. Expansion of the $^{13}C\{^{1}H\}$ NMR spectrum of complex [**3-Py**](OTf)$_2$ in CD_3CN and expansion.

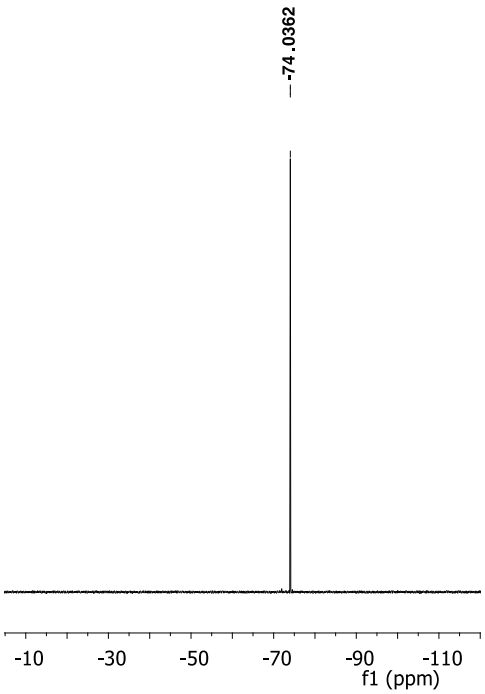

Figure S30. ^{19}F NMR spectrum of complex [**3-Py**](OTf)$_2$ in CD_3CN.

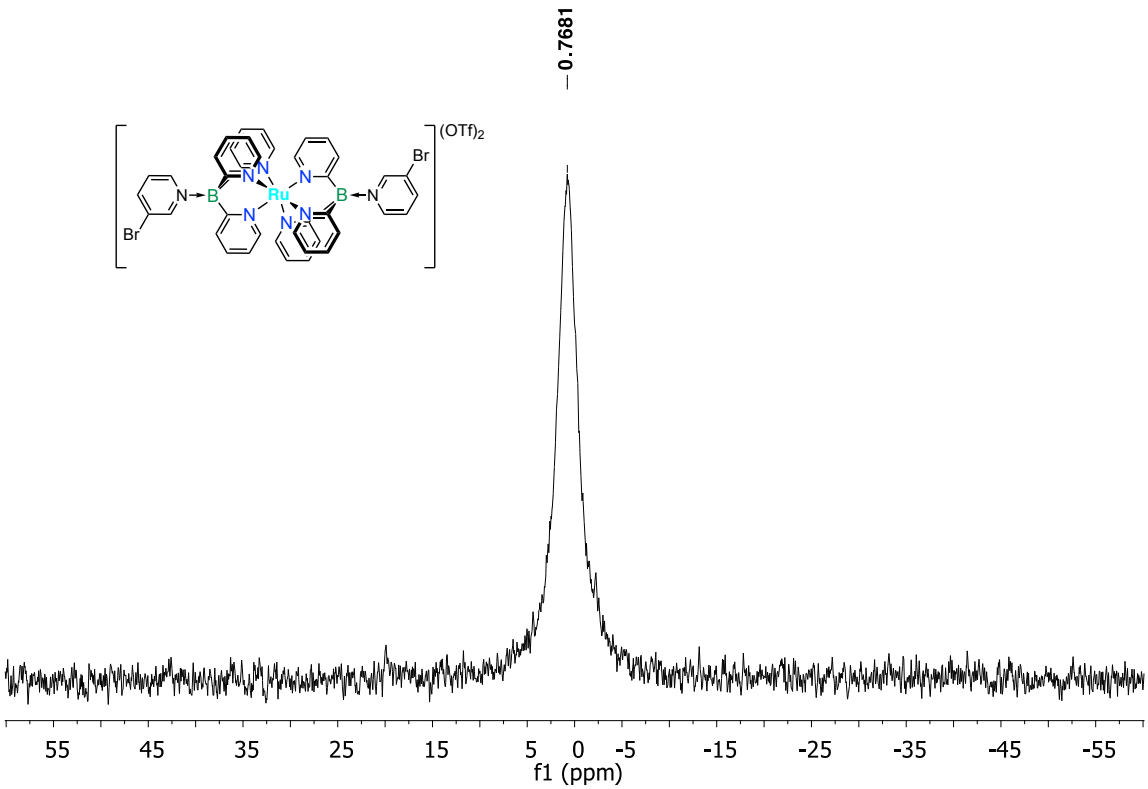

Figure S31. ^{11}B NMR spectrum of complex [**3-Py**](OTf)$_2$ in CD_3CN.

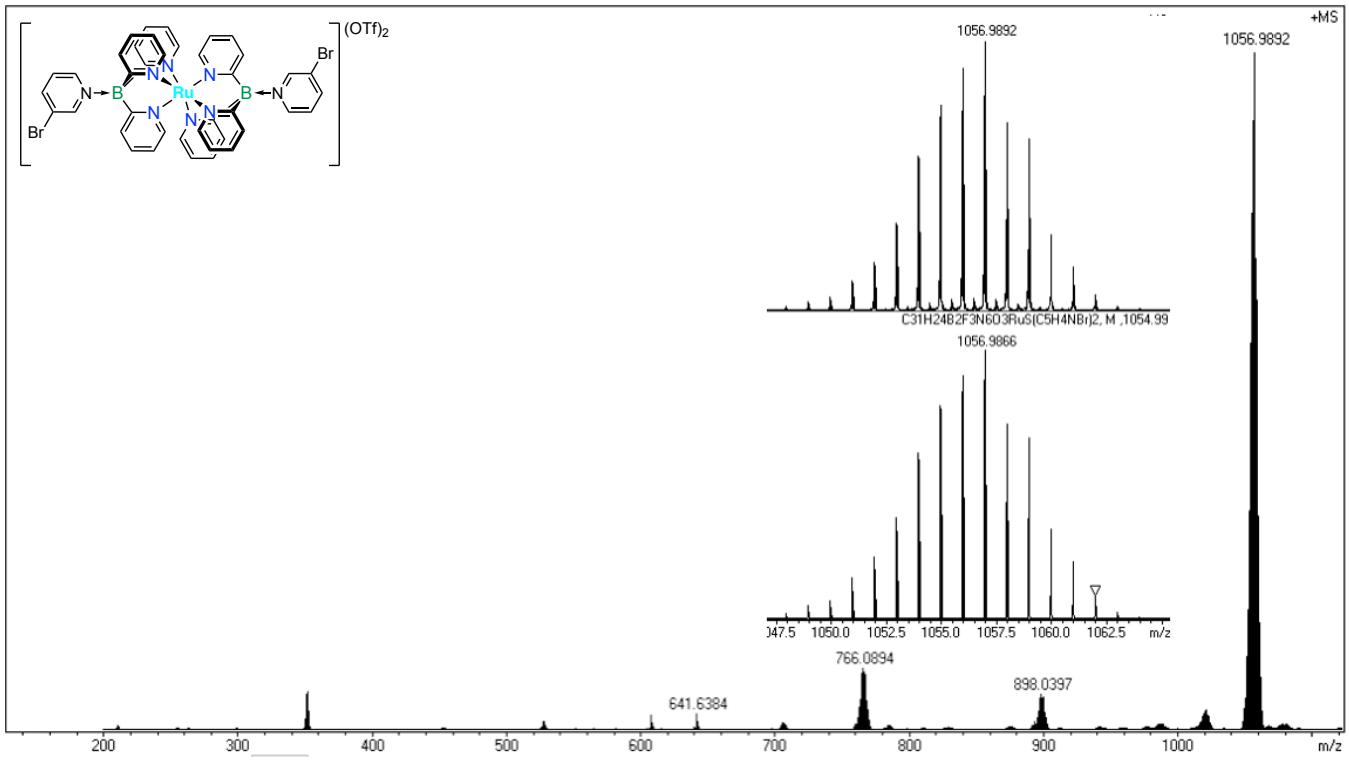

Figure S32. ESI-MS data of complex [**3-Py**](OTf)$_2$ (acetonitrile) showing [M–OTf]$^+$ peak.

Attempted Mono-Substitution of 1 with One Equivalent of Triflic Acid

In a glove box, to a solution of **1** (31 mg, 36 µmol) in 2 mL of deoxygenated CD_2Cl_2 was slowly added a solution of deoxygenated CF_3SO_3H (5.4 mg, 36 µmol) in 0.5 mL of CD_2Cl_2. An 0.5 mL aliquot was then transferred to a quartz J Young NMR tube and the reaction monitored by ^{1}H and ^{11}B NMR overnight. The aliquot was then transferred back to the reaction mixture, degassed water (20 µL, 1.1 mmol) was added, and the mixture was stirred overnight, resulting in the formation of a bright yellow precipitate. The reaction mixture was brought to dryness, washed with 3 x 2 mL degassed water and 3 x 2 mL pentane, the solvent removed, and the residue dried under high vacuum at 80 °C for 24 hours. A mixture of the starting material, mono-substituted and bis-triflate-substituted product was obtained.

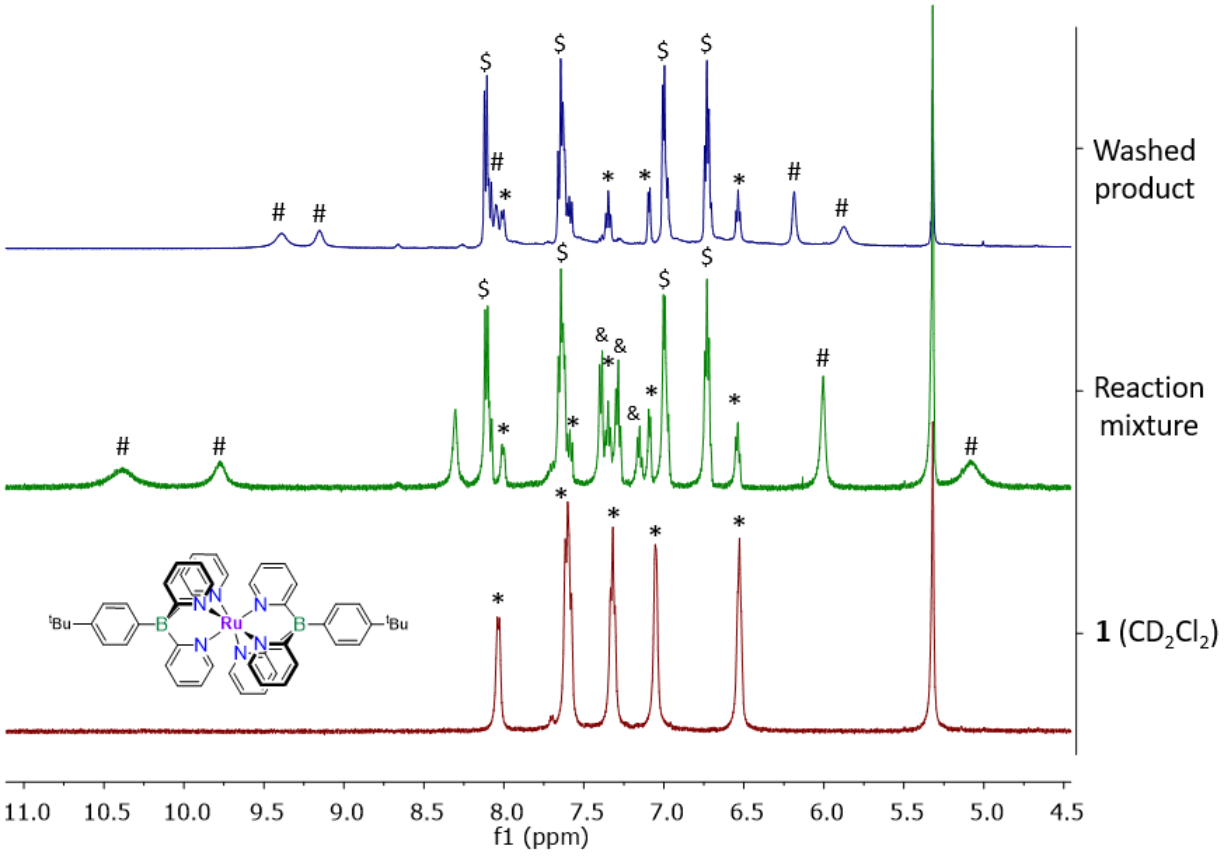

Figure S33a: ^{1}H NMR spectra for the reaction of **1** with one equiv of triflic acid in CD_2Cl_2. Bottom: Complex **1** before addition of triflic acid. Middle: Reaction mixture after overnight reaction with triflic acid. Top: Product mixture after washing with H_2O and pentane, and drying under high vacuum for 24 hours at 80 °C. A mixture of partially oxidized starting material **1**, mono-substituted and bis-triflate-substituted product **2-OTf** is observed. * = complex **1**. # = partially oxidized **1**. & = *tert*-butyl benzene. $ = **2-OTf**.

The more electron-rich precursor **1** underwent partial oxidation under the reaction conditions.

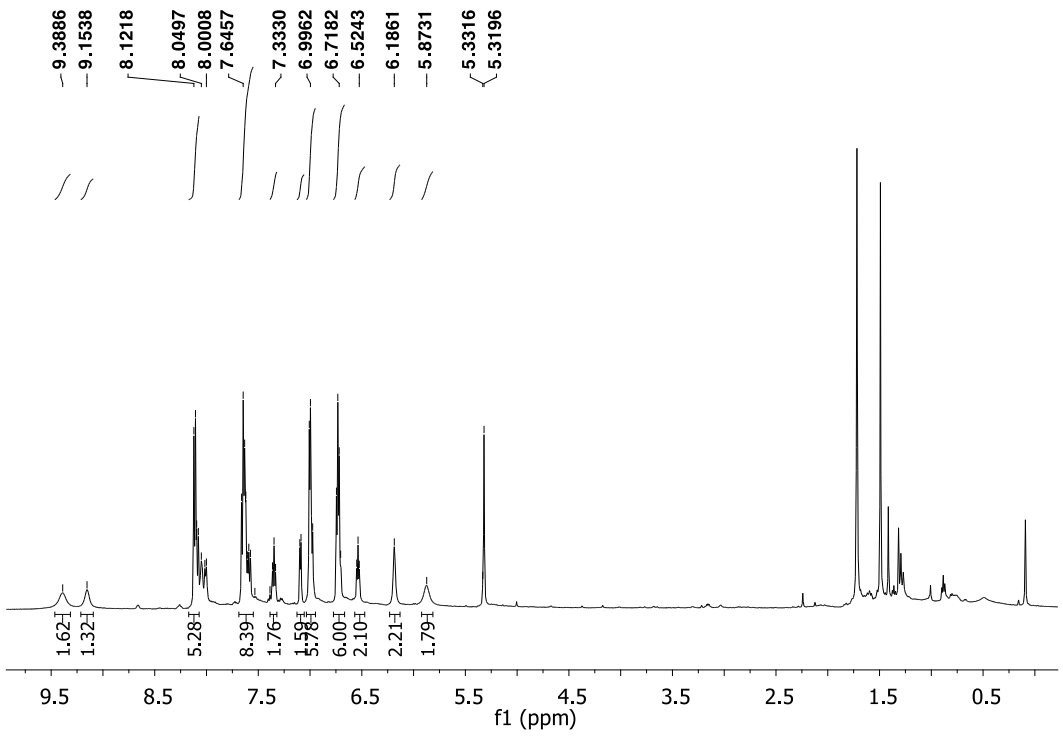

Figure S33b: ^{1}H NMR spectrum for the reaction of **1** with one equiv of triflic acid in CD_2Cl_2.

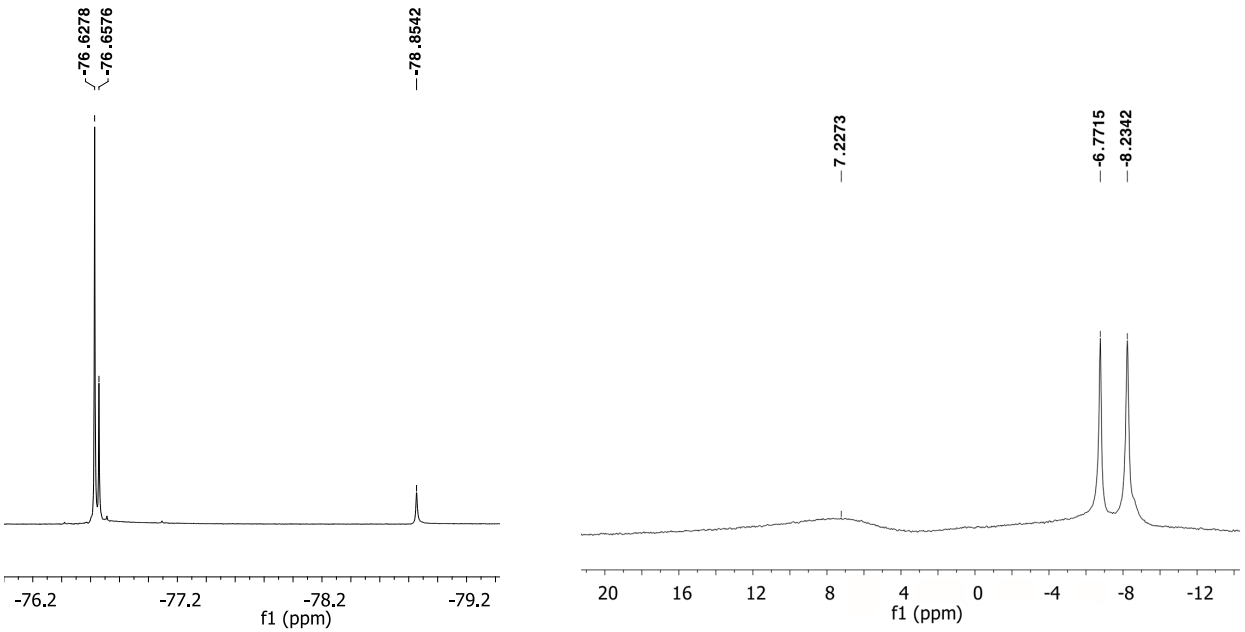

Figure S33c: ^{19}F NMR (left) and ^{11}B NMR (right) spectra for the reaction of **1** with one equiv of triflic acid in CD_2Cl_2. The signal at -6.77 ppm in the ^{11}B NMR spectrum is assigned to the precursor **1**, the signal at -8.23 ppm to the B-Ph in the mono-substituted product, and the signal at 7.23 ppm to the mono- and disubstituted B-OTf)

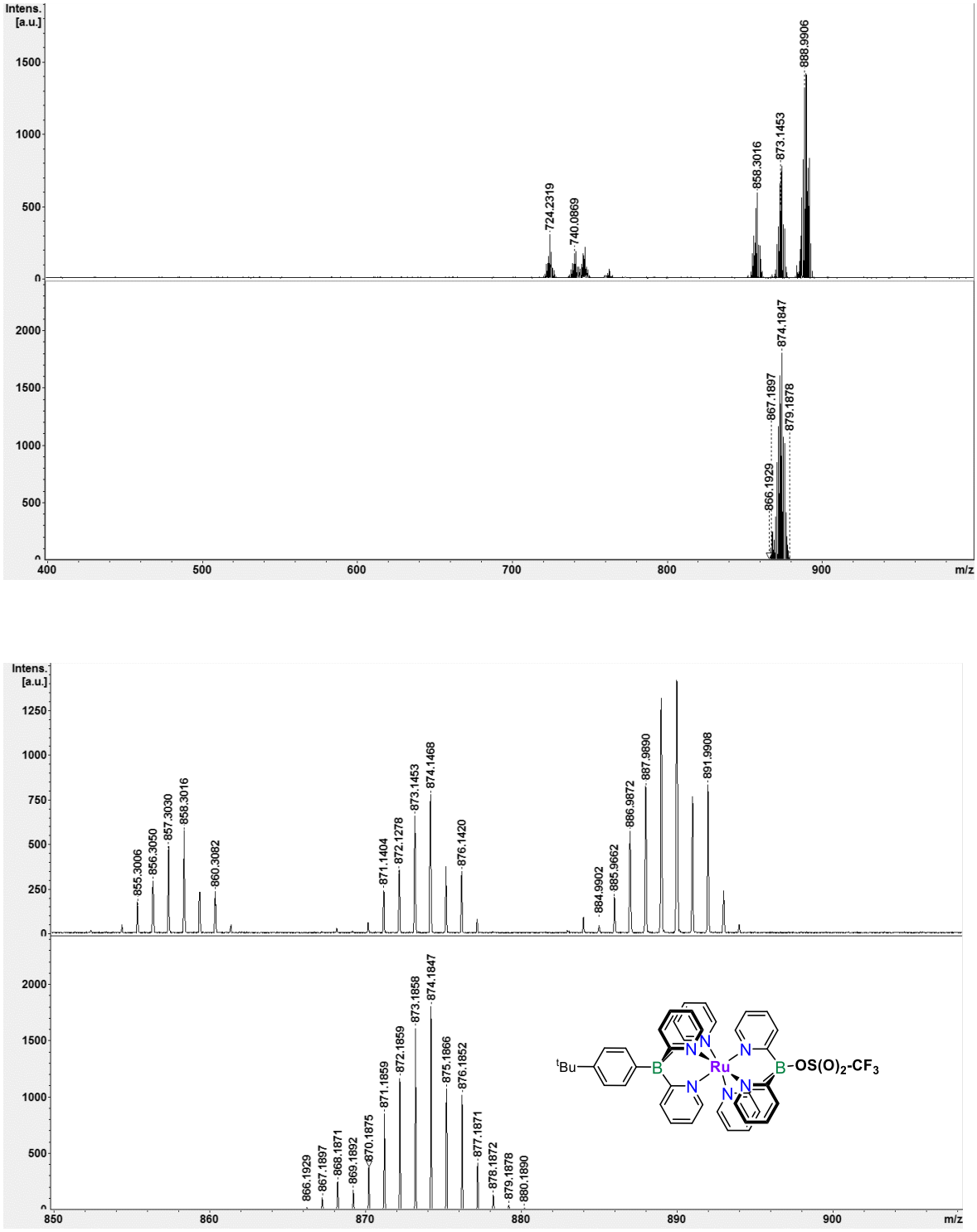

Figure S34: MALDI-TOF MS data for the products from reaction of **1** with one equiv of triflic acid in CD_2Cl_2 (anthracene, positive mode, from CD_2Cl_2). A mixture of the starting material **1**, mono-substituted and bis-triflate-substituted product **2-OTf** is observed.

Attempted Mono-Substitution of 1 with One Equivalent of BBr_3

In a glove box, to a solution of **1** (20 mg, 23 μmol) in 1 mL of deoxygenated CD_2Cl_2 was slowly added a solution of deoxygenated BBr_3 (5.2 mg, 21 μmol) in 0.5 mL of CD_2Cl_2. The reaction mixture was stirred overnight resulting in a brown solution with a dark green precipitate. The composition was investigated by MALDI-TOF mass spectroscopy. The mixture was then filtered through a short silica plug to remove oxidized components and the byproduct ($tBuPhBBr_2$) and an ^{11}B NMR spectrum was acquired.

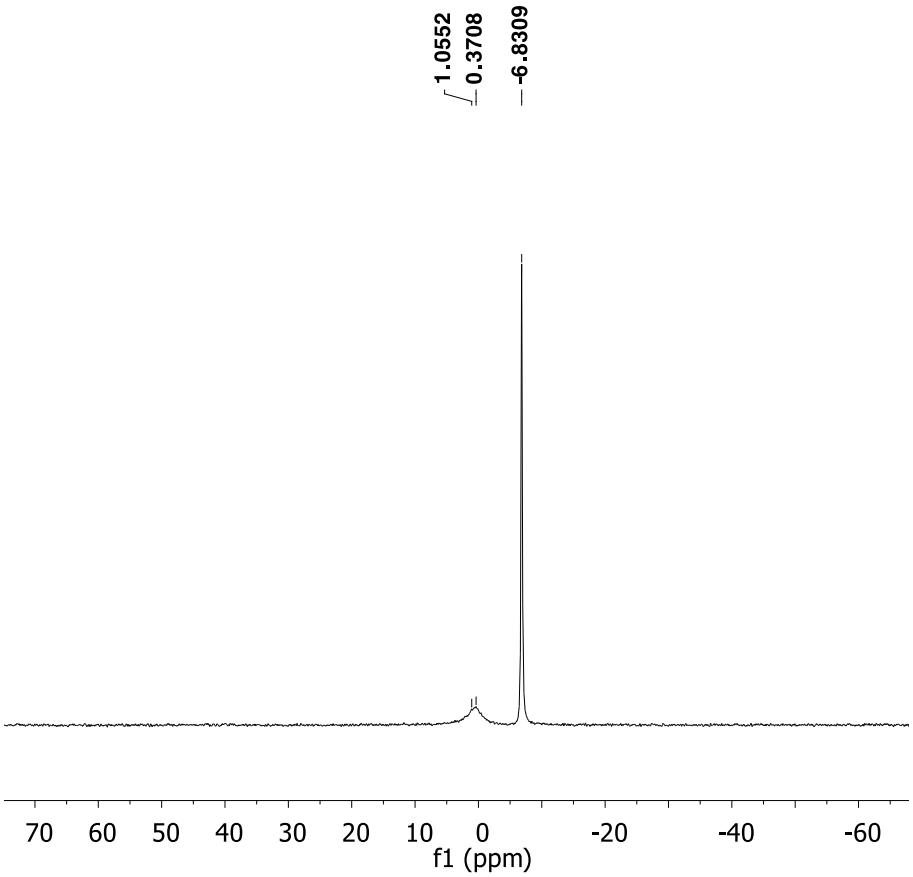

Figure S35: ^{11}B NMR spectrum for the reaction of **1** with one equiv of BBr_3 in CD_2Cl_2, before (left) and after (right) filtration through silica. The signal at 0.37 ppm in the ^{11}B NMR spectrum is assigned to B-Br units and the signal at -6.83 ppm to the B-Ph units. The signals for **1** and the B-Br unit of the mono-substituted product, and the signals for **2-Br** and the B-Br unit of the mono-substituted compound could not be distinguished.

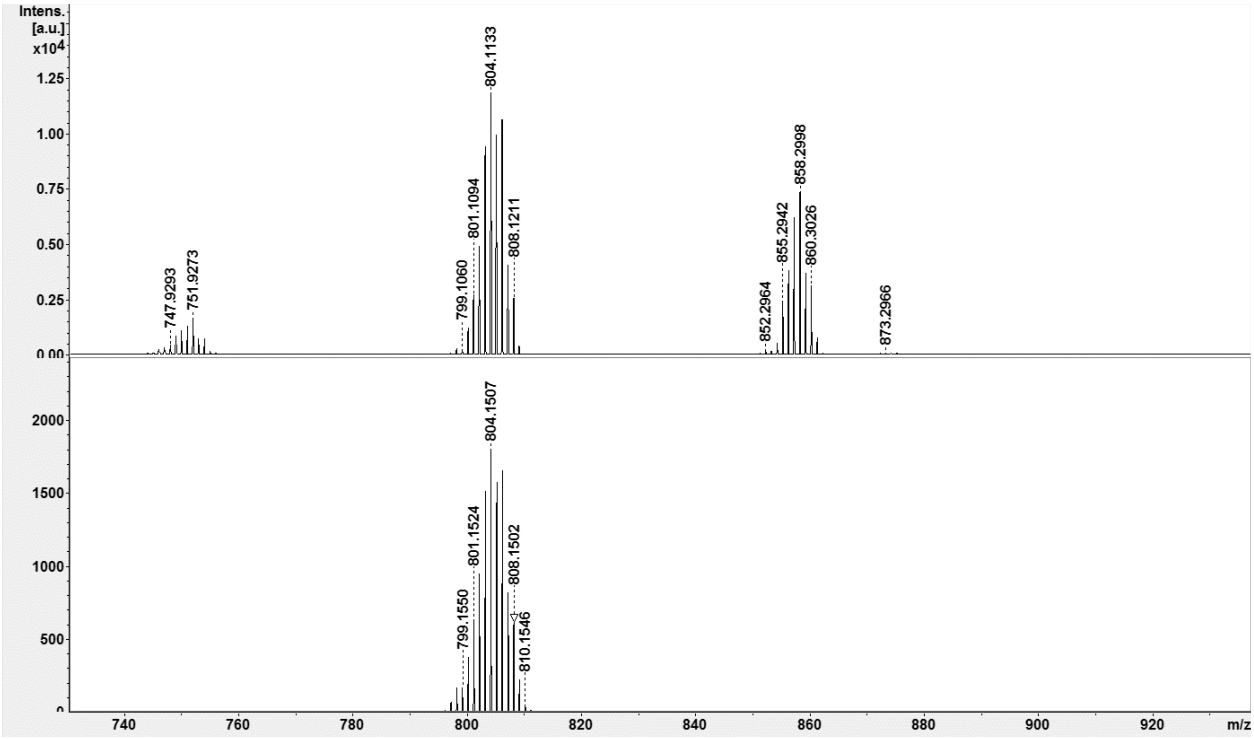

Figure S36: MALDI-TOF MS data for the products from reaction of **1** with one equiv of BBr_3 in CD_2Cl_2 (anthracene, positive mode, from CD_2Cl_2). A mixture of the starting material **1**, mono-substituted and bis-Br-substituted product **2-Br** is observed.

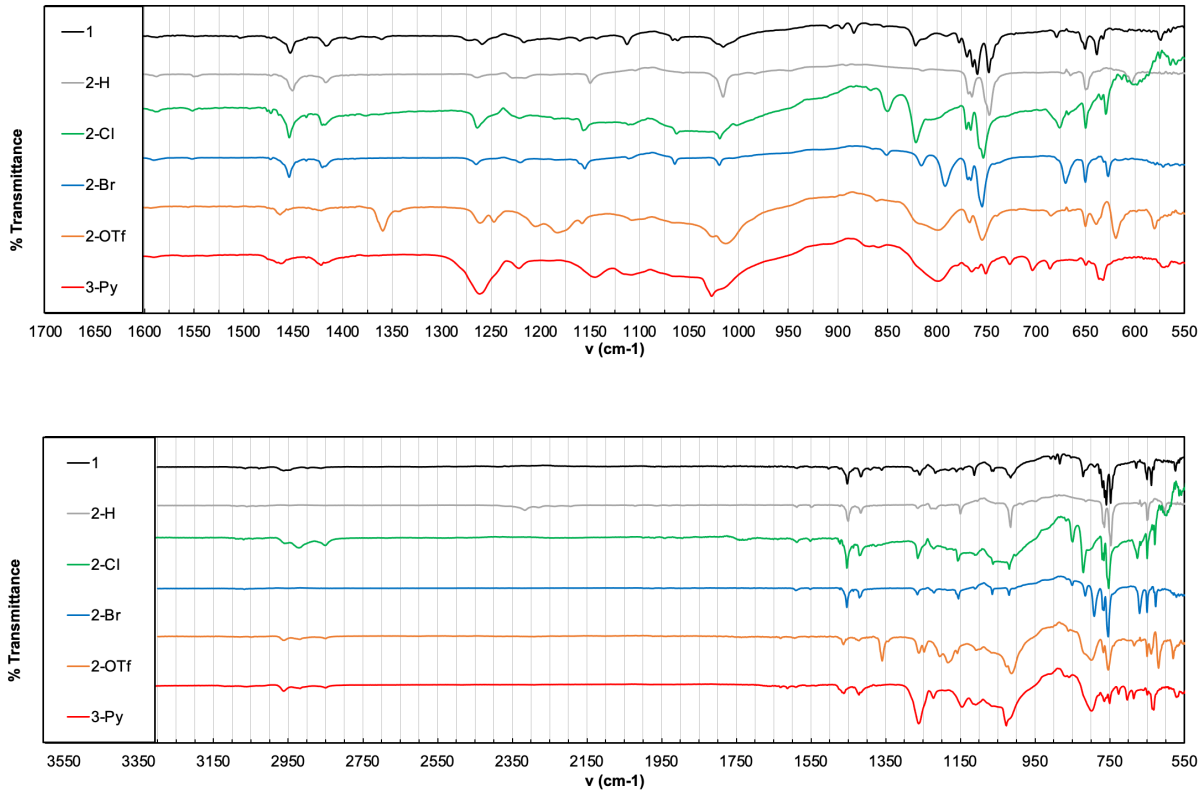

Figure S37. Comparison of ATR-IR spectra and expansions

Table S1. Summary of computed IR-active modes (cm^{-1}).

	1	**2-H**	**2-Cl**	**2-Br**	**2-OTf**	**3-Py**
B-X stretch	890	2423	818	784 (coupled with Py ring deformation)	937	1094
Py C-H stretch	3166	3190	3169	3191	3192	3214
Py C-H bending	1450	1485	1489	1453	1195 (coupled with C-F scissoring)	1456
Py C-H out-of-plane bending	775	766	772	773	771	781
Py ring stretch	651	661	690	675	662	695
Py ring breathing	1030	1031	1034	1034	1082	1085

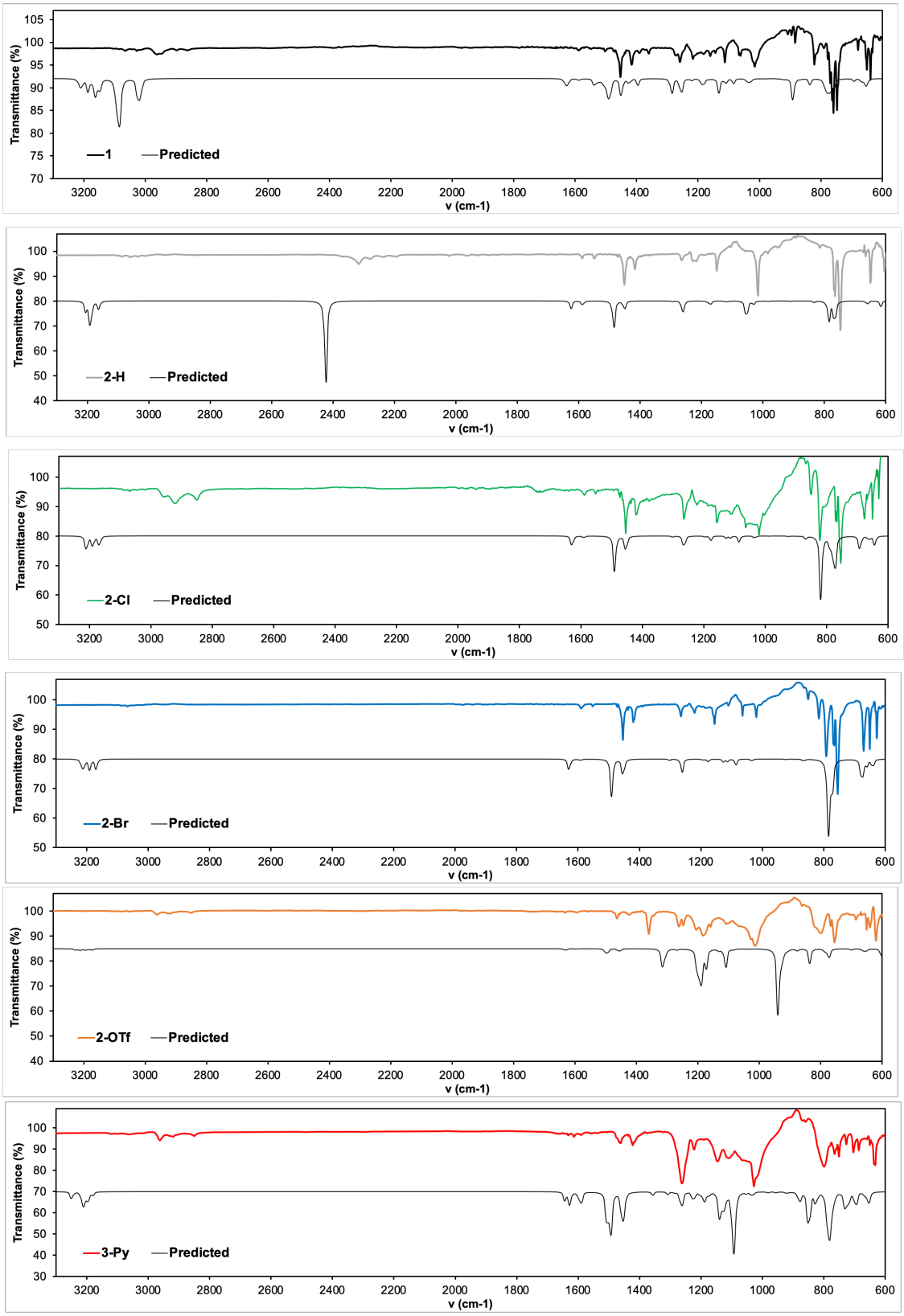

Figure S38a. Comparison of computed ATR-IR spectra with experimental data

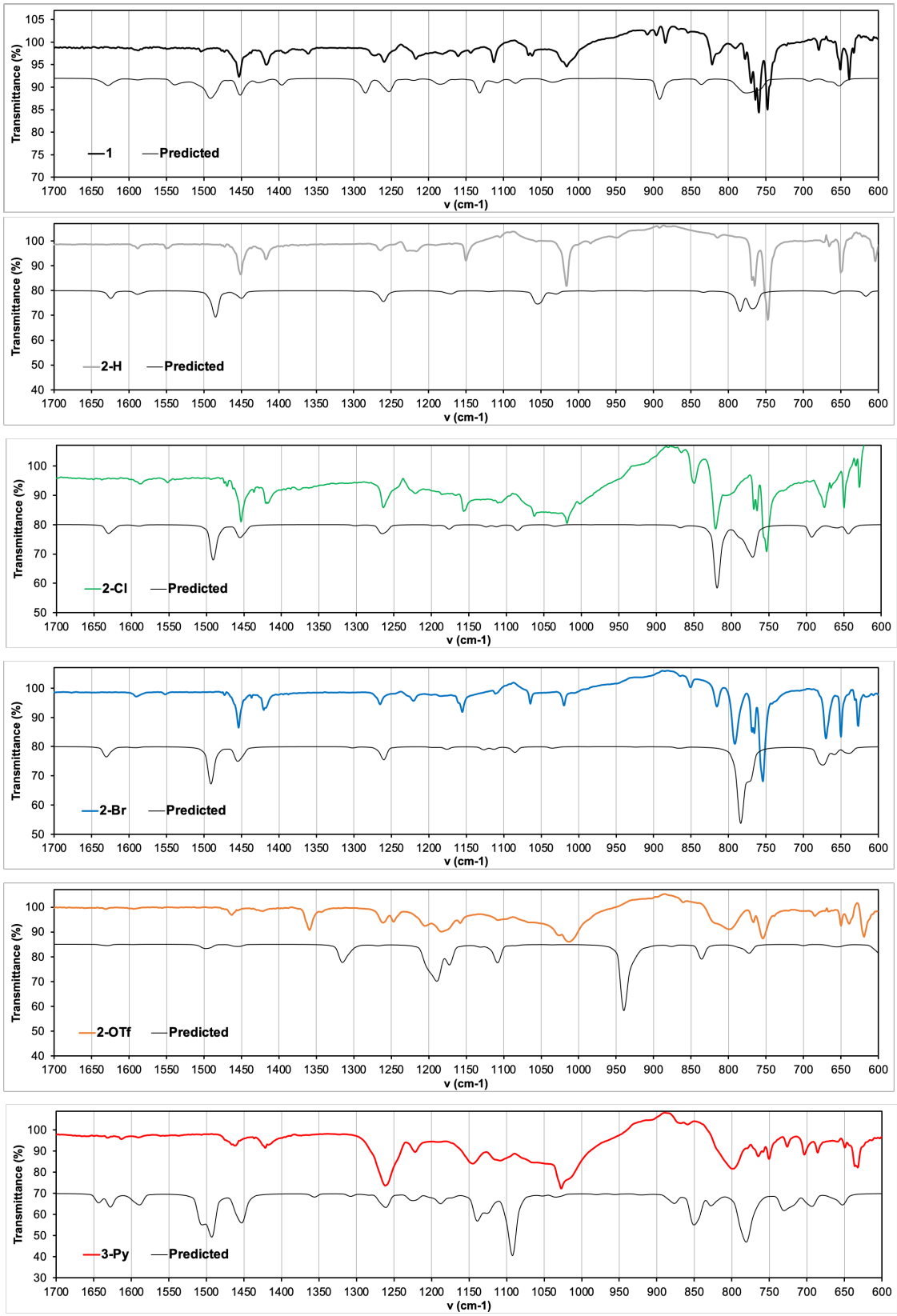

Figure S38b. Comparison of computed ATR-IR spectra with experimental data, expansions

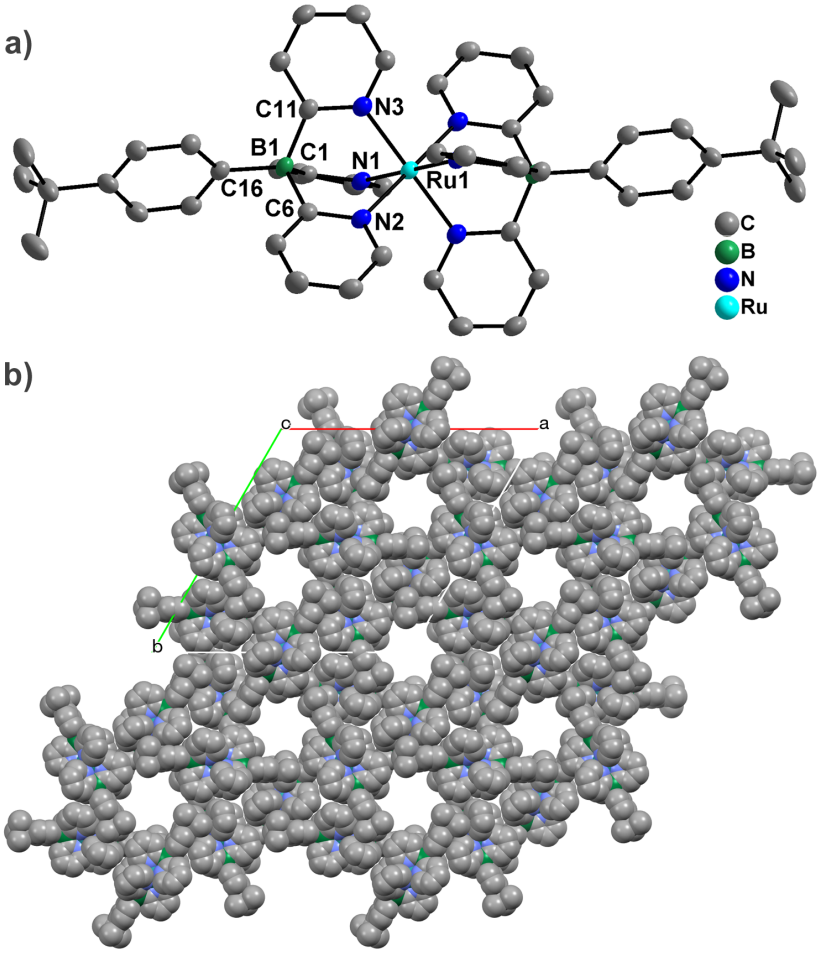

Figure S39. a) Plot of the X-ray structure of compound **1** (thermal ellipsoids at 50%, hydrogen atoms are omitted). Selected interatomic distances (Å) and angles (º): Ru1-N1 2.075(2), Ru1-N2 2.049(2), Ru1-N3 2.080(2), B1-C1 1.632(4), B1-C6 1.643(4), B1-C11 1.628(4), B1-C16 1.634(4), N1-Ru1-N2 89.46(9), N1-Ru1-N3 88.19(9), N2-Ru1-N3 89.29(9), N1-Ru1-N2A 90.53(9), N1-Ru1-N3A 91.81(9), N2-Ru1-N3A 90.71(9), N1-Ru1-N1A 180.0, N2-Ru1-N2A 180.0, N3-Ru1-N3A 180.0, C1-B1-C6 111.3(2), C1-B1-C11 101.1(2), C1-B1-C16 113.6(2), C6-B1-C11 110.1(2), C6-B1-C16 106.4(2), C11-B1-C16 114.5(2); b) Extended structure illustrating the pores along the *c*-axis (disordered solvent molecules present in the channels were removed using the SQUEEZE routine in Platon).

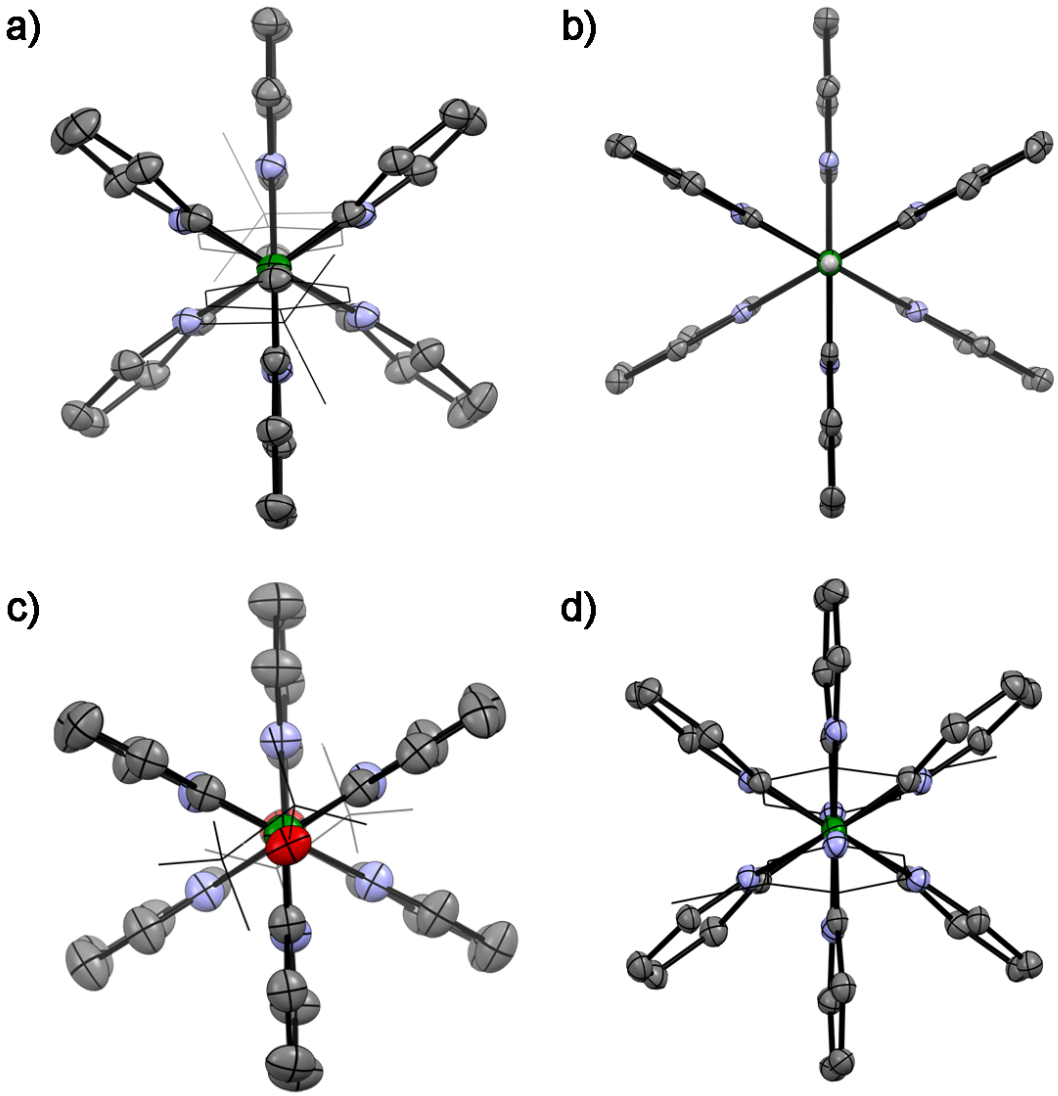

Figure S40. X-ray structure plots of a) **1**, b) **2-H**, c) **2-OTf**, d) **3-Py** (thermal ellipsoids at 50%, hydrogens omitted except for B-H) viewed along the B···B vector. C (grey), H (white), B (dark green), N (blue), O (red), Ru (turquoise). The *tert*-butylphenyl, triflate and pyridyl groups are indicated as wireframe except for the atom directly attached to boron for better visualization of the complex structure.

Table S2. Selected bond lengths (Å) and angles (º) for complexes **1**, **2-H**, **2-OTf** and **3-Py**

	1	**2-H**	**2-OTf**	**3-Py**
Ru(1)-N(1)	2.075(2)	2.075(2)	2.080(2)	2.077(3)
Ru(1)-N(2)	**2.049(2)**	2.077(2)	2.080(2)	**2.057(3)**
Ru(1)-N(3)	2.080(2)	2.078(2)	2.080(2)	2.090(3)
B(1)-X [a]	1.634(4)	1.10(2)	1.579(8)	1.608(6)
B(1)-C(1)	1.632(4)	1.614(3)	1.613(3)	1.632(6)
B(1)-C(6)	1.643(4)	1.618(3)	1.613(3)	1.632(6)
B(1)-C(11)	1.628(4)	1.615(3)	1.613(3)	1.613(3)
N(1)-Ru(1)-N(1)#1	180.0	180.0	180.0	180.0
N(2)-Ru(1)-N(2)#1	180.0	180.0	180.0	180.0
N(3)-Ru(1)-N(3)#1	180.0	180.0	180.0	180.0
N(1)-Ru(1)-N(2)	89.46(9)	88.69(6)	88.64(9)	89.33(13)
N(1)#1-Ru(1)-N(2)	90.53(9)	91.31(6)	91.36(9)	90.67(13)
N(1)-Ru(1)-N(3)	88.19(9)	89.22(6)	88.64(9)	88.43(13)
N(1)-Ru(1)-N(3)#1	91.81(9)	90.78(6)	91.36(9)	91.57(13)
N(2)-Ru(1)-N(3)	89.29(9)	89.02(6)	88.64(9)	89.99(14)
N(2)#1-Ru(1)-N(3)	90.71(9)	90.98(6)	91.36(9)	90.01(14)
C(1)-B(1)-C(6)	111.3(2)	108.52(16)	110.24(18)	113.5(3)
C(1)-B(1)-C(11)	**101.1(2)**	108.79(16)	110.24(18)	**103.0(3)**
C(6)-B(1)-C(11)	110.1(2)	108.13(16)	110.24(18)	112.0(3)
C(1)-B(1)-X [a]	113.6(2)	110.3(12)	101(4)	112.8(3)
C(6)-B(1)-X [a]	**106.4(2)**	110.3(11)	110(9)	**103.3(3)**
C(11)-B(1)-X [a]	114.5(2)	110.7(11)	115(5)	112.6(3)

[a] X = C (**1**), H (**2-H**), O (**2-OTf**), N (**3-Py**).

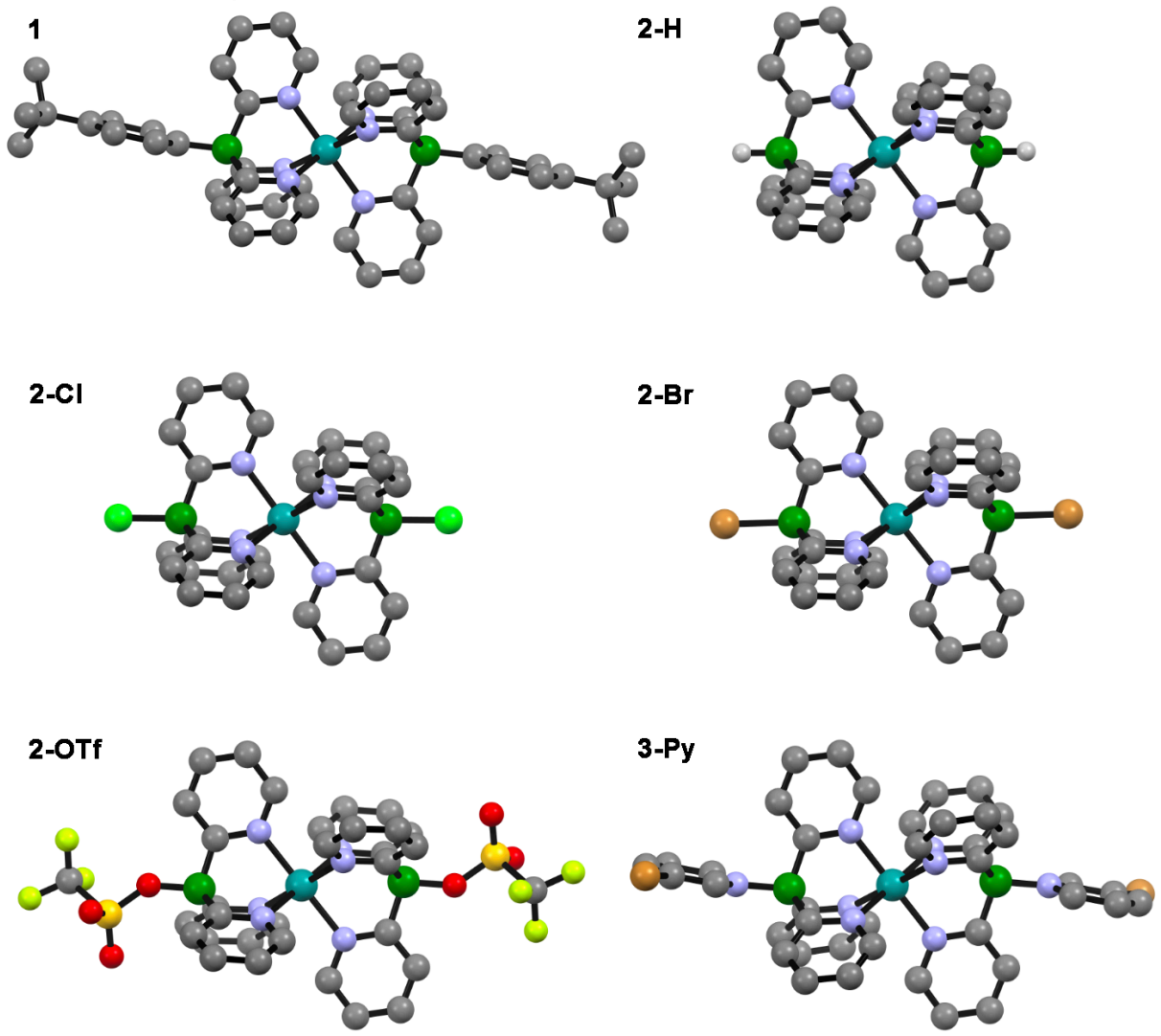

Figure S41. Optimized structures of complexes **1**, **2-H**, **2-Cl, 2-Br, 2-OTf** and **3-Py** (DFT, B3LYP/LanL2DZ [Ru, Br] + 6-311G++(d,p) [C, H, N, B, O, S, F, Cl]); C (grey), H (white), B (dark green), N (blue), F (yellow), Cl (light green), Br (brown), O (red), S (orange), Ru (turquoise); H atoms are omitted except for the boron-bound hydrogens of **2-H**.

Table S3. Computed bond lengths (Å) and angles (º) for **1**, **2-H**, **2-Cl, 2-Br**, **2-OTf** and **3-Py** (DFT, B3LYP/LanL2DZ [Ru, Br] + 6-311G++(d,p) [C, H, N, B, O, S, F, Cl]); X-ray data provided in brackets for comparison where available.

	1	**2-H**	**2-Cl**	**2-Br**	**2-OTf**	**3-Py**
Ru(1)-N(1)	2.126 *[2.075]*	2.127 *[2.075]*	2.122	2.121	2.124 *[2.080]*	2.135 *[2.077]*
Ru(1)-N(2)	2.103 *[2.049]*	2.127 *[2.077]*	2.122	2.121	2.120 *[2.080]*	2.106 [2.057]
Ru(1)-N(3)	2.126 *[2.080]*	2.127 *[2.078]*	2.122	2.121	2.124 *[2.080]*	2.135 *[2.090]*
B(1)-X [a]	1.643 *[1.634]*	1.213 *[1.10]*	1.923	2.141	1.563 *[1.579]*	1.637 *[1.608]*
B(1)-C(1)	1.651 *[1.632]*	1.621 *[1.614]*	1.631	1.631	1.628 *[1.613]*	1.638 *[1.632]*
B(1)-C(6)	1.660 *[1.643]*	1.620 *[1.618]*	1.631	1.632	1.628 [1.613]	1.646 *[1.632]*
B(1)-C(11)	1.651 *[1.628]*	1.621 *[1.615]*	1.631	1.631	1.628 *[1.613]*	1.638 *[1.613]*
C(1)-B(1)-C(6)	109.8 *[111.3]*	108.8 *[108.5]*	109.5	110.0	108.8 *[110.2]*	112.9 *[113.5]*
C(1)-B(1)-C(11)	101.5 *[101.1]*	108.8 *[108.8]*	109.5	110.0	111.4 *[110.2]*	103.1 *[103.0]*
C(6)-B(1)-C(11)	109.8 *[110.1]*	108.8 *[108.1]*	109.5	110.0	109.6 *[110.2]*	112.8 *[112.0]*
C(1)-B(1)-X [a]	114.5 *[113.6]*	110.1 *[110.3]*	109.4	108.9	110.4 *[110]*	112.3 *[112.8]*
C(6)-B(1)-X [a]	106.6 *[106.4]*	110.2 *[110.3]*	109.4	109.0	103.5 *[101]*	103.9 *[103.3]*
C(11)-B(1)-X [a]	114.6 *[114.5]*	110.1 *[110.7]*	109.4	108.9	112.9 *[116]*	112.2 *[112.6]*

[a] X = C (**1**), H (**2-H**), Cl (**2-Cl**), Br (**2-Br**), O (**2-OTf**), N (**3-Py**).

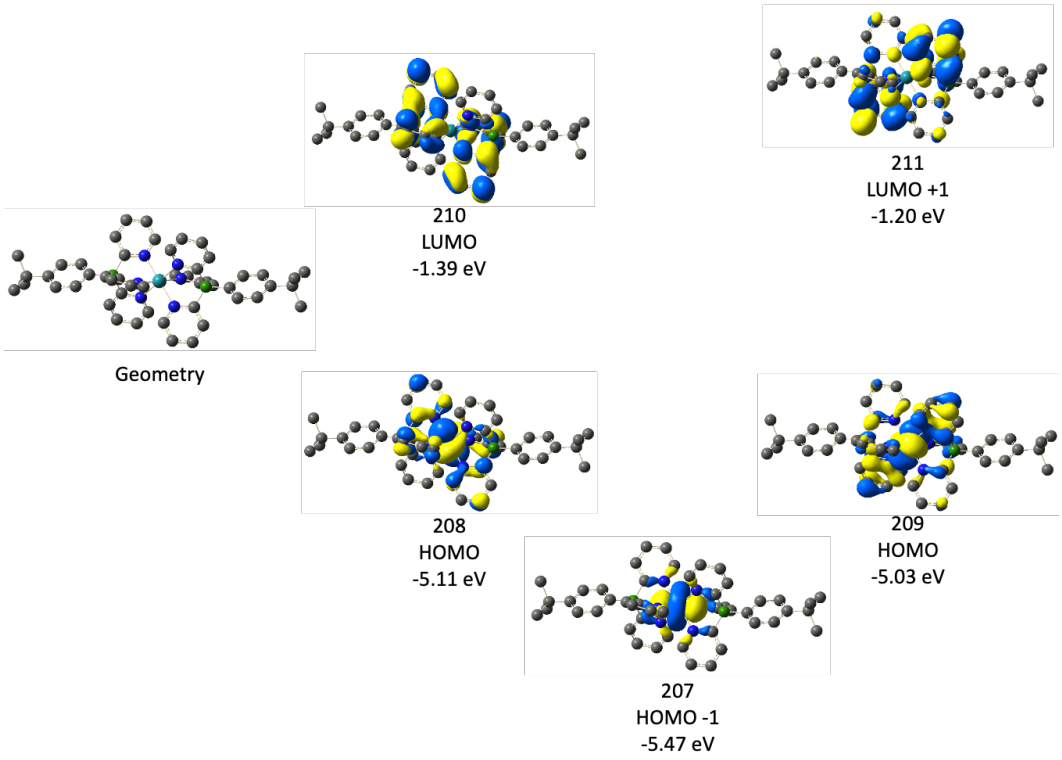

E(RB3LYP) = -2408.31298433; Total Energy, E(TD-HF/TD-DFT) = -2408.20806629

$S_0 \rightarrow S_1$ 2.8550 eV 434.3 nm f=0.0113
209 -> 210 0.70212
$S_0 \rightarrow S_2$ 3.0107 eV 411.8 nm f=0.0803
208 -> 210 0.64324
209 -> 211 -0.22003
209 -> 212 -0.17659
$S_0 \rightarrow S_5$ 3.1878 eV 388.9 nm f=0.2431
207 -> 210 0.17512
208 -> 210 0.25131
209 -> 211 0.62801
$S_0 \rightarrow S_6$ 3.2162 eV 3856 nm f=0.0163
207 -> 210 0.68043
209 -> 211 -0.18754
$S_0 \rightarrow S_9$ 3.2621 eV 380.1 nm f=0.0854
208 -> 210 0.13412
209 -> 211 -0.12769
209 -> 212 0.67644
$S_0 \rightarrow S_{10}$ 3.3511 eV 370.0 nm f=0.0797
208 -> 210 0.69168

Figure S42. Orbital plots, orbital energies, and computed electronic transitions for **1**

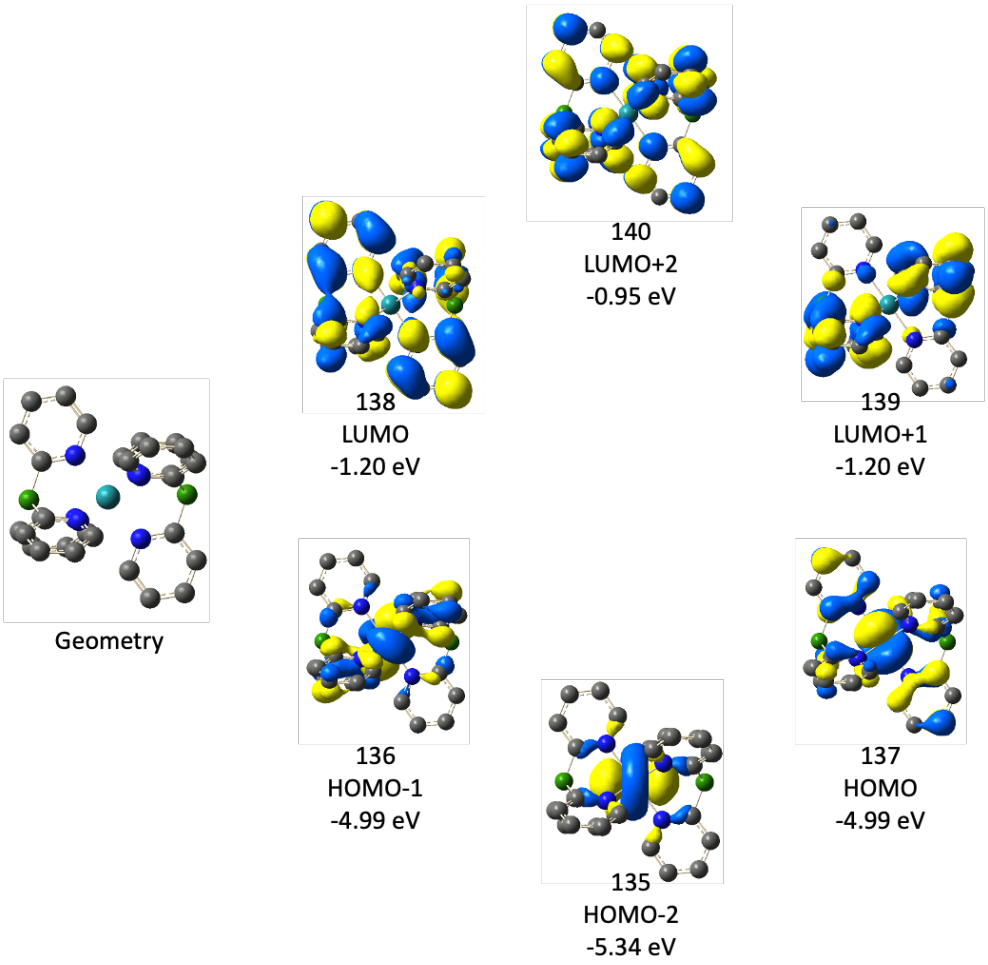

E(RB3LYP) = -1631.52358423; Total Energy, E(TD-HF/TD-DFT) = -1631.41386543

$S_0 \rightarrow S_1$ 2.9856 eV 415.3 nm f=0.0000

136 -> 138	0.49989
137 -> 139	0.49685

$S_0 \rightarrow S_2$ 3.0348 eV 408.5 nm f=0.0374

136 -> 138	0.29604
136 -> 139	0.38455
137 -> 138	0.38657
137 -> 139	-0.29757
137 -> 140	0.14758

$S_0 \rightarrow S_3$ 3.0350 eV 408.5 nm f=0.0376

136 -> 138	-0.38415
136 -> 139	0.29616
136 -> 140	0.14779
137 -> 138	0.29742
137 -> 139	0.38691

$S_0 \rightarrow S_5$ 3.1764 eV 390.3 nm f=0.2233

136 -> 139	0.49791
137 -> 138	-0.49557

Figure S43. Orbital plots, orbital energies, and computed electronic transitions for **2-H**

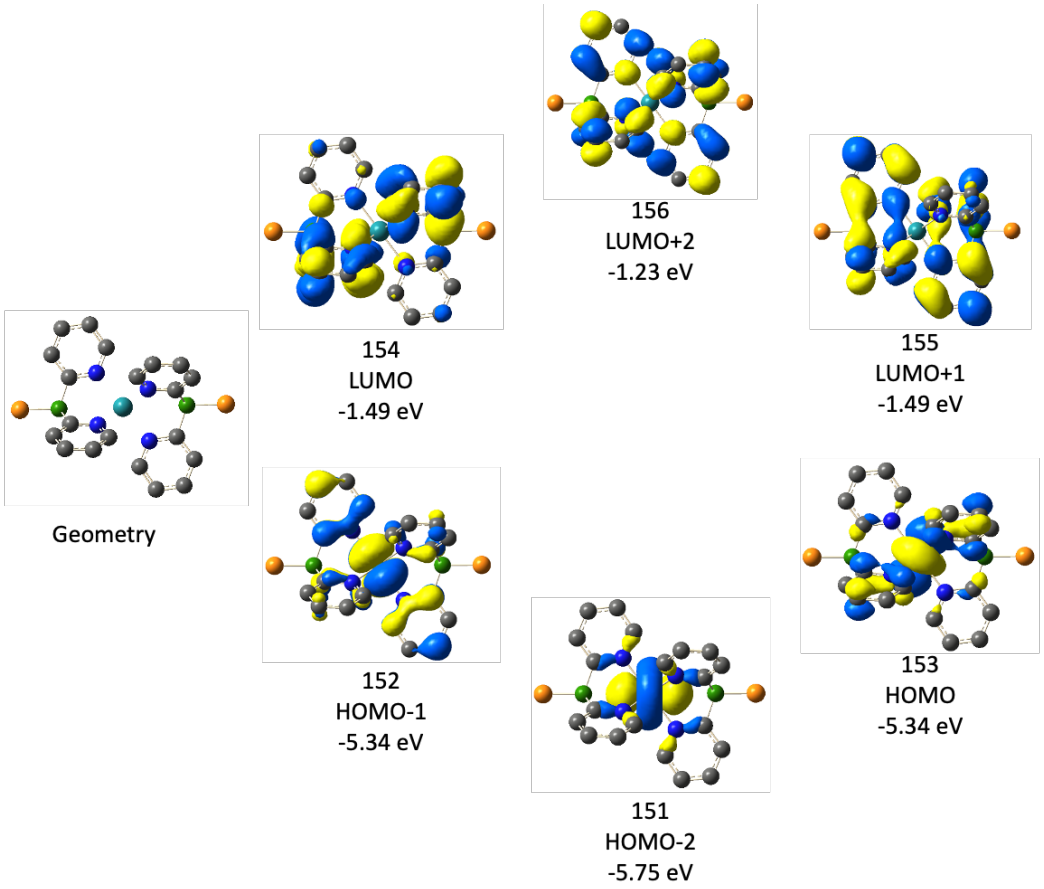

E(RB3LYP) = -2550.87804357; Total Energy, E(TD-HF/TD-DFT) = -2550.76607614

$S_0 \rightarrow S_1$ 3.0468 eV 406.9 nm f=0.0000

152 -> 154	0.47132
152 -> 155	-0.16626
153 -> 154	0.16695
153 -> 155	0.46969

$S_0 \rightarrow S_2$ 3.0974 eV 400.3 nm f=0.0384

152 -> 154	-0.43960
152 -> 155	0.20903
153 -> 154	0.20998
153 -> 155	0.44054
153 -> 156	-0.13609

$S_0 \rightarrow S_3$ 3.0974 eV 400.3 nm f=0.0385

152 -> 154	0.20876
152 -> 155	0.44001
152 -> 156	0.13616
153 -> 154	0.44011
153 -> 155	-0.21023

$S_0 \rightarrow S_5$ 3.2339 eV 383.4 nm f=0.2263

152 -> 154	0.16585
152 -> 155	0.46914
153 -> 154	-0.46839
153 -> 155	0.1661

Figure S44. Orbital plots, orbital energies, and computed electronic transitions for **2-Cl**

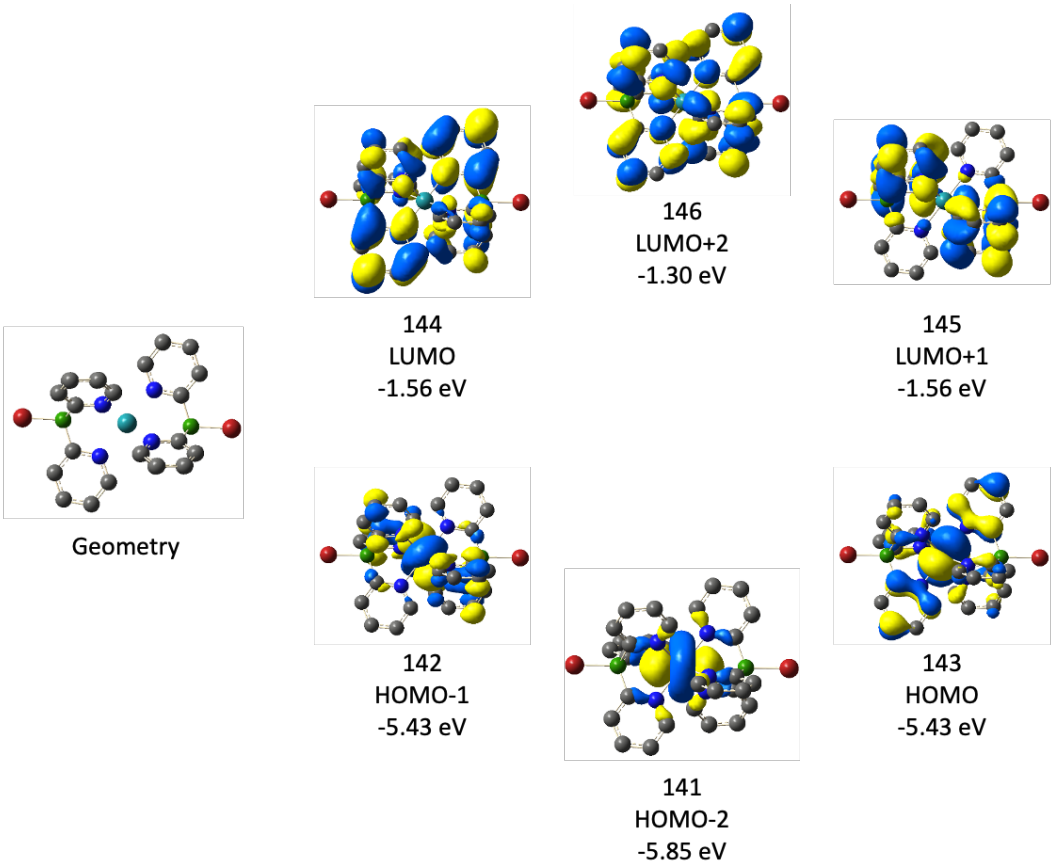

E(RB3LYP) = -1656.74757224; Total Energy, E(TD-HF/TD-DFT) = -1656.63530124

$S_0 \rightarrow S_1$ 3.0550 eV 405.8 nm f=0.0000
142 -> 144 0.50116
143 -> 145 0.49544

$S_0 \rightarrow S_2$ 3.1056 eV 399.2 nm f=0.0380
142 -> 145 0.48147
143 -> 144 0.48604
143 -> 146 0.14032

$S_0 \rightarrow S_3$ 3.1059 eV 399.2 nm f=0.0384
142 -> 144 -0.48084
142 -> 146 0.14073
143 -> 145 0.48652

$S_0 \rightarrow S_5$ 3.2405 eV 382.6 nm f=0.2301
142 -> 145 0.49875
143 -> 144 -0.49408

Figure S45. Orbital plots, orbital energies, and computed electronic transitions for **2-Br**

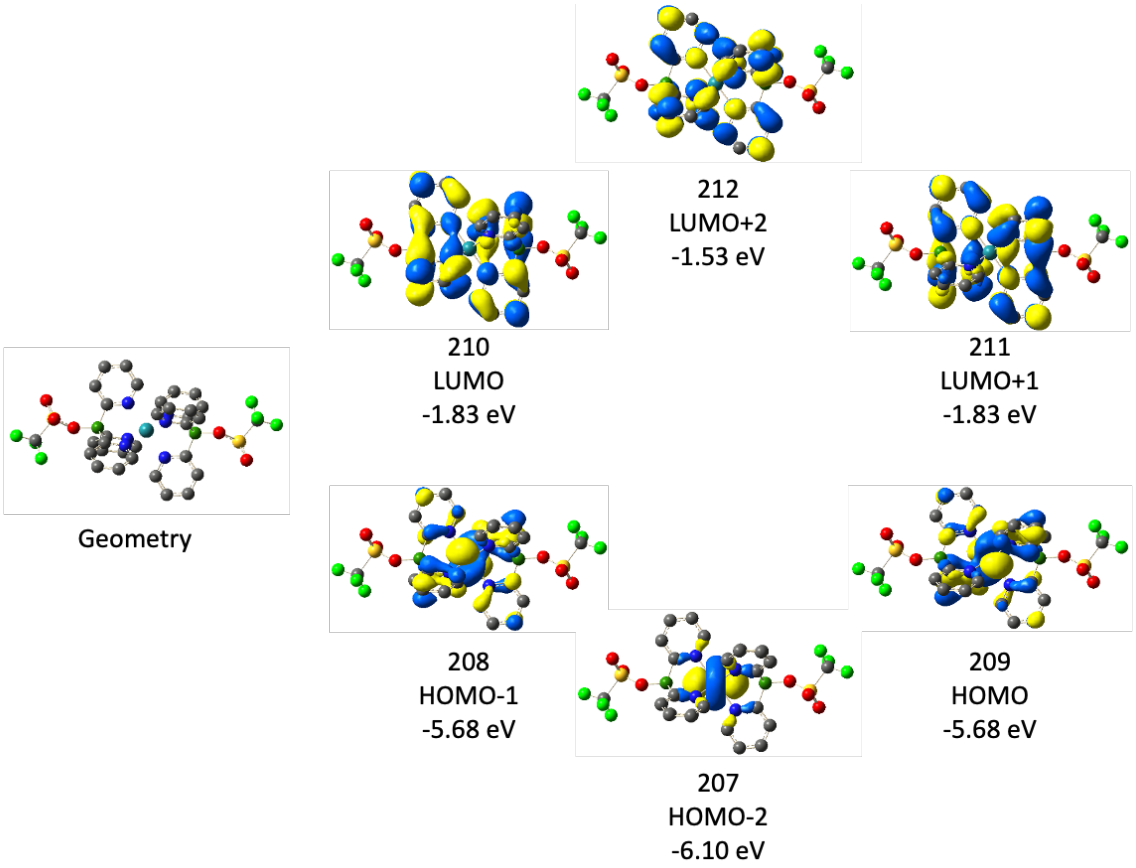

E(RB3LYP) = -3553.65608302; Total Energy, E(TD-HF/TD-DFT) = -3553.54428436

$S_0 \rightarrow S_1$ 3.0422 eV 407.6 nm f=0.0096
208 -> 211 -0.19488
209 -> 210 0.67625

$S_0 \rightarrow S_2$ 3.1119 eV 398.4 nm f=0.0408
208 -> 210 0.55758
209 -> 211 -0.40889

$S_0 \rightarrow S_3$ 3.1443 eV 394.3 nm f=0.0297
208 -> 211 0.66616
208 -> 212 -0.10141
209 -> 210 0.18039

$S_0 \rightarrow S_5$ 3.2549 eV 380.9 nm f=0.2361
208 -> 210 0.42079
209 -> 211 0.56187

Figure S46. Orbital plots, orbital energies, and computed electronic transitions for **2-OTf**

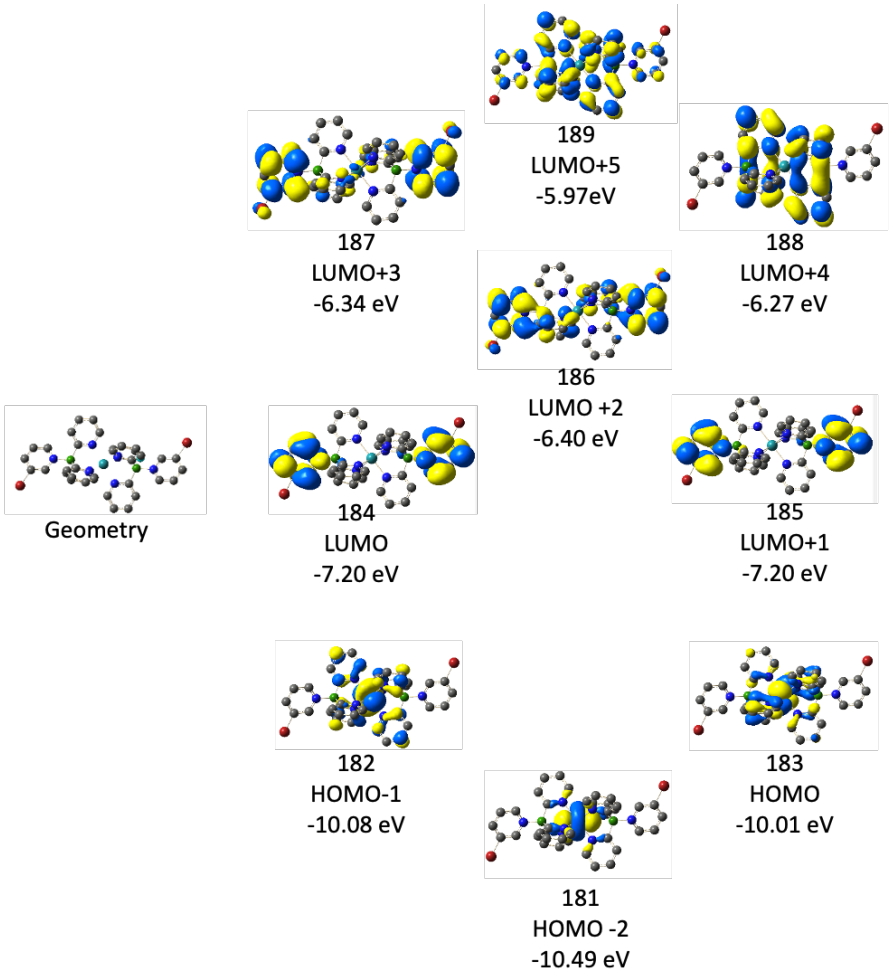

E(RB3LYP) = -2151.71226381; Total Energy, E(TD-HF/TD-DFT) = -2151.62724207)

$S_0 \rightarrow S_1$ 2.3136 eV 535.9 nm f=0.0000
183 -> 184 0.70652

$S_0 \rightarrow S_2$ 2.3203 eV 534.4 nm f=0.0001
183 -> 185 0.70663

$S_0 \rightarrow S_4$ 2.3987 eV 516.9 nm f=0.0028
182 -> 185 0.70679

$S_0 \rightarrow S_7$ 2.9451 eV 421.0 nm f=0.0115
183 -> 188 0.70274

$S_0 \rightarrow S_8$ 3.0673 eV 404.2 nm f=0.0710
182 -> 188 -0.25960
183 -> 186 0.62858
183 -> 189 0.15191

$S_0 \rightarrow S_{10}$ 3.1085 eV 398.9 nm f=0.1181
182 -> 188 0.62118
183 -> 186 0.27759
183 -> 189 -0.12927
183 -> 191 -0.12252

$S_0 \rightarrow S_{16}$ 3.3419 eV 371.0 nm f=0.1108
181 -> 188 0.35864
182 -> 188 0.19243
183 -> 189 0.53796
183 -> 191 0.19716

Figure S47. Orbital plots, orbital energies, and computed electronic transitions for **3-Py**

Table S4. Comparison of Computational Data with Experimental Results

Compound	**CV Data** [a]	**DFT Data** [b]			**UV-Vis**	**TD-DFT**
	$E_{1/2}$ / E_{HOMO} (mV / eV)	E_{HOMO} (eV)	E_{LUMO} (eV)	$\Delta E_{g,\,DFT}$ (eV)	λ_{max}, $\Delta E_{g,\,opt}$ [c] (eV / nm)	[d] (eV / nm)
1	–128 / -4.67	-5.03	-1.39	3.64	2.81 / 441	2.855 / 434.3 ($S_0 \rightarrow S_1$)
2-H	–138 / -4.66	-4.99	-1.20	3.79	2.90 / 428	3.035 / 408.5 ($S_0 \rightarrow S_2$)
2-Cl	+110 / -4.91	-5.34	-1.49	3.85	2.91 / 424	3.047 / 406.9 ($S_0 \rightarrow S_2$)
2-Br	+149 / -4.95	-5.43	-1.56	3.87	2.92 / 424	3.106 / 399.2 ($S_0 \rightarrow S_2$)
2-OTf	+292 / -5.09	-5.68	-1.83	3.85	2.96 / 419	3.112 / 398.4 ($S_0 \rightarrow S_2$)
3-Py	+396 / -5.20	-7.20	-10.0	2.80	2.90 / 428	3.067 / 404.2 ($S_0 \rightarrow S_8$)

[a] From cyclic voltammetry data in CH_2Cl_2 containing 0.1 M $Bu_4N[PF_6]$ at 100 mV s^{-1}, E_{HOMO} estimated as $E_{HOMO} = -(4.8+E_{1/2})$; [b] computed at the B3LYP/LanL2DZ [Ru, Br] + 6-311G++(d,p) [C, H, N, B, O, S, F, Cl] level; [c] optical gap estimated from longest wavelength absorption maxima; [d] lowest energy transition with oscillator strength >0.01.

1, Charge = 0, E= –2408.312984 Hartree, B3LYP/LanL2DZ [Ru] + 6-311G++(d,p) [C, H, N, B] level

Center Number	Atomic Number	Atomic Type	Coordinates (Angstroms) X	Y	Z
1	44	0	-0.000003	0.000023	0.000016
2	7	0	-1.197703	0.963740	1.468514
3	7	0	-1.181971	0.981391	-1.469900
4	7	0	-1.400035	-1.569966	-0.017256
5	5	0	-3.213655	0.319340	-0.016015
6	6	0	-2.540794	1.103600	1.271305
7	6	0	-3.243819	1.985062	2.110759
8	1	0	-4.291015	2.164957	1.914361
9	6	0	-2.624554	2.630513	3.172161
10	1	0	-3.186226	3.304959	3.809827
11	6	0	-1.271937	2.392952	3.402179
12	1	0	-0.738731	2.851885	4.225609
13	6	0	-0.599468	1.568244	2.518133
14	1	0	0.462247	1.388551	2.622347
15	6	0	-2.527145	1.119986	-1.285829
16	6	0	-3.219903	2.012884	-2.121690
17	1	0	-4.268788	2.191967	-1.934172
18	6	0	-2.588383	2.670794	-3.168129
19	1	0	-3.142364	3.353879	-3.803326
20	6	0	-1.233607	2.434581	-3.386374
21	1	0	-0.690962	2.903112	-4.198148
22	6	0	-0.571683	1.598304	-2.505249
23	1	0	0.490999	1.419040	-2.599853
24	6	0	-2.727714	-1.267784	-0.024443
25	6	0	-3.644738	-2.335143	-0.039442
26	1	0	-4.701545	-2.112762	-0.046139
27	6	0	-3.226277	-3.658719	-0.045840
28	1	0	-3.952949	-4.464147	-0.057243
29	6	0	-1.861447	-3.929971	-0.037253
30	1	0	-1.474328	-4.941554	-0.041444
31	6	0	-0.989156	-2.857004	-0.023304
32	1	0	0.081280	-3.012348	-0.016686
33	7	0	1.197699	-0.963704	-1.468485
34	7	0	1.181958	-0.981329	1.469927
35	7	0	1.400028	1.570013	0.017278
36	5	0	3.213650	-0.319286	0.016021
37	6	0	2.540788	-1.103585	-1.271268
38	6	0	3.243798	-1.985075	-2.110704
39	1	0	4.290995	-2.164975	-1.914309
40	6	0	2.624521	-2.630544	-3.172088
41	1	0	3.186181	-3.305020	-3.809733
42	6	0	1.271910	-2.392960	-3.402118
43	1	0	0.738701	-2.851896	-4.225544
44	6	0	0.599456	-1.568212	-2.518097
45	1	0	-0.462252	-1.388484	-2.622328
46	6	0	2.527140	-1.119890	1.285868
47	6	0	3.219925	-2.012724	2.121776
48	1	0	4.268818	-2.191771	1.934272
49	6	0	2.588424	-2.670615	3.168237
50	1	0	3.142425	-3.353649	3.803472
51	6	0	1.233636	-2.434449	3.386454

52	1	0	0.690998	-2.902971	4.198238
53	6	0	0.571688	-1.598232	2.505292
54	1	0	-0.491002	-1.419008	2.599880
55	6	0	2.727709	1.267839	0.024414
56	6	0	3.644728	2.335203	0.039349
57	1	0	4.701537	2.112831	0.045990
58	6	0	3.226258	3.658777	0.045757
59	1	0	3.952926	4.464209	0.057114
60	6	0	1.861426	3.930021	0.037244
61	1	0	1.474302	4.941602	0.041451
62	6	0	0.989141	2.857049	0.023340
63	1	0	-0.081297	3.012386	0.016765
64	6	0	-4.856650	0.306631	-0.022057
65	6	0	-5.614860	0.176158	1.158340
66	6	0	-5.610446	0.205733	-1.202960
67	6	0	-6.998463	0.017256	1.159419
68	1	0	-5.113271	0.165286	2.119970
69	6	0	-6.999342	0.047383	-1.215039
70	1	0	-5.107643	0.217415	-2.163916
71	6	0	-7.736537	-0.037320	-0.031109
72	1	0	-7.505315	-0.074321	2.114848
73	1	0	-7.497509	-0.018324	-2.174702
74	6	0	4.856647	-0.306571	0.022045
75	6	0	5.610448	-0.205608	1.202928
76	6	0	5.614849	-0.176184	-1.158378
77	6	0	6.999355	-0.047280	1.214982
78	1	0	5.107654	-0.217212	2.163890
79	6	0	6.998445	-0.017312	-1.159483
80	1	0	5.113236	-0.165359	-2.119996
81	6	0	7.736537	0.037306	0.031046
82	1	0	7.497522	0.018534	2.174636
83	1	0	7.505304	0.074208	-2.114913
84	6	0	-9.266180	-0.197148	0.005787
85	6	0	9.266202	0.196945	-0.005858
86	6	0	9.634966	1.509634	-0.735828
87	1	0	10.722252	1.632404	-0.774832
88	1	0	9.260899	1.521410	-1.762137
89	1	0	9.213387	2.374982	-0.216637
90	6	0	9.883547	0.244394	1.403819
91	1	0	9.682576	-0.671588	1.966181
92	1	0	10.969099	0.353614	1.326684
93	1	0	9.507100	1.091155	1.984374
94	6	0	9.889693	-0.998599	-0.763622
95	1	0	10.979421	-0.899822	-0.803725
96	1	0	9.651445	-1.942162	-0.264669
97	1	0	9.521415	-1.062241	-1.790218
98	6	0	-9.889872	0.997971	0.764026
99	1	0	-9.651818	1.941781	0.265446
100	1	0	-10.979580	0.898971	0.804105
101	1	0	-9.521620	1.061305	1.790652
102	6	0	-9.883576	-0.244129	-1.403886
103	1	0	-10.969123	-0.353380	-1.326734
104	1	0	-9.682610	0.672050	-1.965931
105	1	0	-9.507167	-1.090695	-1.984743
106	6	0	-9.634669	-1.510214	0.735255
107	1	0	-9.212826	-2.375251	0.215765

108	1	0	-9.260637	-1.522255	1.761572
109	1	0	-10.721927	-1.633290	0.774149

2-H, Charge = 0, E= –1631.523584 Hartree, B3LYP/LanL2DZ [Ru] + 6-311G++(d,p) [C, H, N, B] level

---

Center Number	Atomic Number	Atomic Type	Coordinates (Angstroms) X	Y	Z
1	44	0	0.000000	-0.000000	0.000003
2	7	0	1.262428	0.255733	-1.693022
3	7	0	1.261819	1.338445	1.068510
4	7	0	1.261430	-1.594678	0.625285
5	5	0	3.168492	-0.000550	0.000886
6	1	0	4.381179	-0.000788	0.001276
7	6	0	2.610923	0.226888	-1.503833
8	6	0	3.458221	0.393972	-2.610113
9	1	0	4.528145	0.368665	-2.442777
10	6	0	2.944840	0.586703	-3.885570
11	1	0	3.605531	0.715190	-4.736489
12	6	0	1.560701	0.611954	-4.050597
13	1	0	1.103750	0.758710	-5.021604
14	6	0	0.761107	0.443213	-2.932426
15	1	0	-0.318296	0.455624	-3.011088
16	6	0	2.610380	1.188903	0.950052
17	6	0	3.457172	2.063575	1.648300
18	1	0	4.527178	1.931247	1.543549
19	6	0	2.943225	3.072178	2.452092
20	1	0	3.603536	3.745085	2.989002
21	6	0	1.558995	3.202837	2.555037
22	1	0	1.101600	3.970781	3.166799
23	6	0	0.759900	2.318655	1.849483
24	1	0	-0.319548	2.380980	1.898144
25	6	0	2.610031	-1.417201	0.556231
26	6	0	3.456545	-2.459265	0.965060
27	1	0	4.526600	-2.302253	0.903931
28	6	0	2.942277	-3.660036	1.435363
29	1	0	3.602378	-4.461593	1.749780
30	6	0	1.558013	-3.814845	1.495307
31	1	0	1.100401	-4.729004	1.853224
32	6	0	0.759190	-2.761572	1.082216
33	1	0	-0.320281	-2.835158	1.110398
34	7	0	-1.262427	-0.255757	1.693023
35	7	0	-1.261820	-1.338429	-1.068526
36	7	0	-1.261432	1.594685	-0.625259
37	5	0	-3.168492	0.000549	-0.000880
38	1	0	-4.381179	0.000782	-0.001266
39	6	0	-2.610923	-0.226911	1.503837
40	6	0	-3.458219	-0.394008	2.610113
41	1	0	-4.528143	-0.368695	2.442786
42	6	0	-2.944834	-0.586766	3.885567
43	1	0	-3.605526	-0.715267	4.736485
44	6	0	-1.560697	-0.612032	4.050590
45	1	0	-1.103748	-0.758811	5.021594
46	6	0	-0.761104	-0.443275	2.932419
47	1	0	0.318300	-0.455705	3.011077

48	6	0	-2.610380	-1.188890	-0.950066
49	6	0	-3.457172	-2.063543	-1.648337
50	1	0	-4.527179	-1.931218	-1.543580
51	6	0	-2.943225	-3.072122	-2.452159
52	1	0	-3.603535	-3.745010	-2.989095
53	6	0	-1.558995	-3.202778	-2.555107
54	1	0	-1.101599	-3.970709	-3.166885
55	6	0	-0.759900	-2.318612	-1.849532
56	1	0	0.319549	-2.380929	-1.898204
57	6	0	-2.610031	1.417203	-0.556209
58	6	0	-3.456547	2.459270	-0.965035
59	1	0	-4.526602	2.302251	-0.903913
60	6	0	-2.942282	3.660047	-1.435318
61	1	0	-3.602381	4.461608	-1.749729
62	6	0	-1.558016	3.814868	-1.495242
63	1	0	-1.100409	4.729038	-1.853136
64	6	0	-0.759192	2.761594	-1.082159
65	1	0	0.320278	2.835188	-1.110316

2-Cl, Charge = 0, E= –2550.878044 Hartree, B3LYP/LanL2DZ [Ru] + 6-311G++(d,p) [C, H, N, B, Cl] level

Center Number	Atomic Number	Atomic Type	Coordinates (Angstroms) X	Y	Z
1	44	0	0.000000	-0.000000	0.000000
2	7	0	-1.261443	-0.244856	-1.689358
3	7	0	-1.261338	-1.340840	1.056554
4	7	0	-1.261364	1.585403	0.632768
5	5	0	-3.153872	0.000003	0.000155
6	6	0	-2.611946	-0.220466	-1.522202
7	6	0	-3.441859	-0.382264	-2.640645
8	1	0	-4.512718	-0.360764	-2.493500
9	6	0	-2.905204	-0.565793	-3.907772
10	1	0	-3.554504	-0.690159	-4.767644
11	6	0	-1.520242	-0.587149	-4.053519
12	1	0	-1.047516	-0.726872	-5.017891
13	6	0	-0.740056	-0.423478	-2.922291
14	1	0	0.340020	-0.432426	-2.983191
15	6	0	-2.611851	-1.208179	0.952209
16	6	0	-3.441637	-2.095892	1.651687
17	1	0	-4.512518	-1.979174	1.559762
18	6	0	-2.904833	-3.101590	2.443969
19	1	0	-3.554029	-3.784073	2.981743
20	6	0	-1.519846	-3.217292	2.534892
21	1	0	-1.047023	-3.982765	3.137798
22	6	0	-0.739792	-2.319447	1.827392
23	1	0	0.340295	-2.367753	1.865221
24	6	0	-2.611868	1.428587	0.570370
25	6	0	-3.441652	2.478215	0.989419
26	1	0	-4.512521	2.340160	0.934438
27	6	0	-2.904853	3.667320	1.463921
28	1	0	-3.554046	4.474281	1.786100
29	6	0	-1.519872	3.804049	1.518305
30	1	0	-1.047042	4.709047	1.879438
31	6	0	-0.739823	2.742424	1.094494

32	1	0	0.340258	2.799518	1.117031
33	7	0	1.261443	0.244850	1.689359
34	7	0	1.261338	1.340844	-1.056549
35	7	0	1.261364	-1.585400	-0.632773
36	5	0	3.153872	-0.000003	-0.000155
37	6	0	2.611946	0.220461	1.522202
38	6	0	3.441859	0.382253	2.640646
39	1	0	4.512718	0.360753	2.493502
40	6	0	2.905205	0.565774	3.907775
41	1	0	3.554505	0.690134	4.767647
42	6	0	1.520242	0.587126	4.053522
43	1	0	1.047517	0.726839	5.017897
44	6	0	0.740057	0.423461	2.922295
45	1	0	-0.340019	0.432405	2.983195
46	6	0	2.611851	1.208181	-0.952205
47	6	0	3.441637	2.095899	-1.651679
48	1	0	4.512518	1.979180	-1.559755
49	6	0	2.904833	3.101602	-2.443955
50	1	0	3.554029	3.784087	-2.981723
51	6	0	1.519846	3.217306	-2.534874
52	1	0	1.047023	3.982784	-3.137774
53	6	0	0.739792	2.319458	-1.827378
54	1	0	-0.340295	2.367767	-1.865204
55	6	0	2.611868	-1.428585	-0.570375
56	6	0	3.441651	-2.478211	-0.989430
57	1	0	4.512520	-2.340156	-0.934447
58	6	0	2.904852	-3.667313	-1.463938
59	1	0	3.554046	-4.474272	-1.786122
60	6	0	1.519872	-3.804040	-1.518326
61	1	0	1.047041	-4.709035	-1.879466
62	6	0	0.739823	-2.742417	-1.094510
63	1	0	-0.340258	-2.799509	-1.117050
64	17	0	5.077259	-0.000126	-0.000178
65	17	0	-5.077259	0.000126	0.000177

2-Br, Charge = 0, E= –1656.747572 Hartree, B3LYP/LanL2DZ [Ru and Br] + 6-311G++(d,p) [C, H, N, B] level

---

Center Number	Atomic Number	Atomic Type	Coordinates (Angstroms) X	Y	Z
1	44	0	0.000000	0.000000	0.000000
2	7	0	-1.260973	1.522987	0.768238
3	7	0	-1.261417	-0.095944	-1.702842
4	7	0	-1.261020	-1.427093	0.934379
5	5	0	-3.143113	0.000069	0.000437
6	6	0	-2.613305	1.377807	0.695490
7	6	0	-3.432990	2.393920	1.207950
8	1	0	-4.505008	2.272919	1.147356
9	6	0	-2.886968	3.533881	1.782126
10	1	0	-3.531680	4.312650	2.174725
11	6	0	-1.501713	3.658196	1.843892
12	1	0	-1.022025	4.525524	2.280434
13	6	0	-0.730744	2.632460	1.326687
14	1	0	0.349647	2.680095	1.349864
15	6	0	-2.613720	-0.086760	-1.540372

16	6	0	-3.433724	-0.150862	-2.676358
17	1	0	-4.505698	-0.143203	-2.540930
18	6	0	-2.888051	-0.222860	-3.950876
19	1	0	-3.532999	-0.272020	-4.821444
20	6	0	-1.502836	-0.230726	-4.089838
21	1	0	-1.023416	-0.285503	-5.059417
22	6	0	-0.731552	-0.165974	-2.943130
23	1	0	0.348811	-0.169009	-2.996379
24	6	0	-2.613352	-1.290908	0.845862
25	6	0	-3.433073	-2.242956	1.469267
26	1	0	-4.505085	-2.129438	1.395500
27	6	0	-2.887090	-3.311290	2.167770
28	1	0	-3.531825	-4.040984	2.645400
29	6	0	-1.501837	-3.428020	2.242969
30	1	0	-1.022169	-4.240884	2.774099
31	6	0	-0.730837	-2.466922	1.613787
32	1	0	0.349555	-2.511807	1.641989
33	7	0	1.260973	-1.522986	-0.768242
34	7	0	1.261417	0.095939	1.702842
35	7	0	1.261020	1.427095	-0.934376
36	5	0	3.143113	-0.000069	-0.000437
37	6	0	2.613305	-1.377805	-0.695494
38	6	0	3.432989	-2.393916	-1.207959
39	1	0	4.505008	-2.272915	-1.147365
40	6	0	2.886968	-3.533875	-1.782139
41	1	0	3.531680	-4.312641	-2.174742
42	6	0	1.501713	-3.658189	-1.843907
43	1	0	1.022025	-4.525515	-2.280454
44	6	0	0.730743	-2.632455	-1.326697
45	1	0	-0.349647	-2.680089	-1.349876
46	6	0	2.613720	0.086755	1.540372
47	6	0	3.433724	0.150853	2.676358
48	1	0	4.505698	0.143194	2.540930
49	6	0	2.888051	0.222846	3.950876
50	1	0	3.532999	0.272002	4.821445
51	6	0	1.502836	0.230710	4.089839
52	1	0	1.023416	0.285483	5.059418
53	6	0	0.731552	0.165963	2.943130
54	1	0	-0.348811	0.168995	2.996380
55	6	0	2.613352	1.290910	-0.845858
56	6	0	3.433073	2.242962	-1.469259
57	1	0	4.505085	2.129443	-1.395492
58	6	0	2.887091	3.311299	-2.167757
59	1	0	3.531825	4.040995	-2.645383
60	6	0	1.501838	3.428029	-2.242955
61	1	0	1.022170	4.240896	-2.774080
62	6	0	0.730837	2.466928	-1.613777
63	1	0	-0.349555	2.511814	-1.641977
64	35	0	5.284436	-0.000125	-0.000630
65	35	0	-5.284436	0.000125	0.000629

2-TfO, Charge = 0, E= –3553.656083 Hartree, B3LYP/LanL2DZ [Ru] + 6-311G++(d,p) [C, H, N, B, O, S, F] level

---

Center Number	Atomic Number	Atomic Type	Coordinates (Angstroms) X	Y	Z

1	44	0	0.000017	0.000028	0.000092
2	7	0	1.181569	1.753379	-0.206153
3	7	0	1.227313	-0.559574	1.641211
4	7	0	1.365015	-0.991546	-1.282550
5	5	0	3.132782	0.173456	0.125441
6	6	0	2.535590	1.673062	-0.083391
7	6	0	3.293602	2.850822	-0.113976
8	1	0	4.363066	2.812219	0.031448
9	6	0	2.687187	4.085613	-0.309099
10	1	0	3.285438	4.989471	-0.334739
11	6	0	1.306170	4.138742	-0.467428
12	1	0	0.782604	5.073045	-0.627559
13	6	0	0.595026	2.953124	-0.400437
14	1	0	-0.482373	2.943383	-0.495694
15	6	0	2.574381	-0.421592	1.532677
16	6	0	3.397289	-0.777873	2.608440
17	1	0	4.466427	-0.656283	2.506246
18	6	0	2.849872	-1.273512	3.784517
19	1	0	3.488710	-1.548171	4.616629
20	6	0	1.466570	-1.409770	3.874916
21	1	0	0.987003	-1.790787	4.767979
22	6	0	0.696062	-1.041876	2.785096
23	1	0	-0.382120	-1.127624	2.808375
24	6	0	2.700518	-0.814524	-1.094688
25	6	0	3.602221	-1.495110	-1.922391
26	1	0	4.662084	-1.354590	-1.785191
27	6	0	3.150515	-2.333034	-2.933424
28	1	0	3.857396	-2.850692	-3.572163
29	6	0	1.779409	-2.490467	-3.113110
30	1	0	1.372354	-3.128917	-3.887344
31	6	0	0.925987	-1.803920	-2.267280
32	1	0	-0.147584	-1.895370	-2.363246
33	7	0	-1.181549	-1.753331	0.206330
34	7	0	-1.227254	0.559619	-1.641007
35	7	0	-1.364966	0.991567	1.282754
36	5	0	-3.132737	-0.173451	-0.125267
37	6	0	-2.535581	-1.673050	0.083593
38	6	0	-3.293571	-2.850820	0.114265
39	1	0	-4.363042	-2.812227	-0.031096
40	6	0	-2.687126	-4.085596	0.309388
41	1	0	-3.285360	-4.989466	0.335075
42	6	0	-1.306101	-4.138696	0.467647
43	1	0	-0.782509	-5.072986	0.627765
44	6	0	-0.594982	-2.953064	0.400612
45	1	0	0.482416	-2.943304	0.495844
46	6	0	-2.574319	0.421584	-1.532512
47	6	0	-3.397208	0.777796	-2.608310
48	1	0	-4.466343	0.656169	-2.506144
49	6	0	-2.849780	1.273438	-3.784381
50	1	0	-3.488605	1.548039	-4.616522
51	6	0	-1.466483	1.409783	-3.874730
52	1	0	-0.986907	1.790827	-4.767776
53	6	0	-0.695991	1.041951	-2.784881
54	1	0	0.382185	1.127768	-2.808121
55	6	0	-2.700457	0.814486	1.094896

56	6	0	-3.602205	1.494929	1.922669
57	1	0	-4.662059	1.354288	1.785490
58	6	0	-3.150537	2.332830	2.933739
59	1	0	-3.857440	2.850398	3.572527
60	6	0	-1.779437	2.490357	3.113400
61	1	0	-1.372413	3.128790	3.887663
62	6	0	-0.925976	1.803904	2.267531
63	1	0	0.147590	1.895390	2.363514
64	8	0	4.684291	0.157848	0.313881
65	8	0	-4.684257	-0.157548	-0.313536
66	16	0	5.971183	0.733839	-0.329684
67	16	0	-5.971306	-0.733755	0.329490
68	8	0	-6.441113	-1.917363	-0.373286
69	8	0	-5.935094	-0.724272	1.784079
70	8	0	5.934392	0.724431	-1.784257
71	8	0	6.441424	1.917340	0.372981
72	6	0	7.138587	-0.652295	0.191327
73	6	0	-7.138639	0.652230	-0.192054
74	9	0	7.138422	-0.796676	1.518967
75	9	0	8.372420	-0.349942	-0.212661
76	9	0	6.772362	-1.811373	-0.368520
77	9	0	-7.138122	0.796381	-1.519729
78	9	0	-6.772629	1.811406	0.367702
79	9	0	-8.372574	0.349873	0.211634

3-Py, Charge = +2, E= –2151.712264 Hartree, B3LYP/LanL2DZ [Ru and Br] + 6-311G++(d,p) [C, H, N, B] level

Center Number	Atomic Number	Atomic Type	Coordinates (Angstroms) X	Y	Z
1	44	0	0.000018	0.000021	-0.000004
2	7	0	1.357638	-0.476087	1.538410
3	7	0	1.478356	-0.618452	-1.411639
4	7	0	0.868643	1.949254	-0.078315
5	5	0	3.075720	0.712731	0.034557
6	6	0	2.656956	-0.098671	1.403977
7	6	0	3.554757	-0.421633	2.432763
8	1	0	4.595268	-0.139275	2.361126
9	6	0	3.144019	-1.108952	3.569721
10	1	0	3.853351	-1.348761	4.353226
11	6	0	1.809943	-1.479777	3.677602
12	1	0	1.432368	-2.016084	4.538769
13	6	0	0.956533	-1.143563	2.640990
14	1	0	-0.090578	-1.410829	2.678435
15	6	0	2.749928	-0.133642	-1.329328
16	6	0	3.600309	-0.286162	-2.433422
17	1	0	4.577995	0.177404	-2.434308
18	6	0	3.208824	-1.008782	-3.555000
19	1	0	3.879375	-1.120918	-4.399015
20	6	0	1.942712	-1.582467	-3.567843
21	1	0	1.592256	-2.175180	-4.403055
22	6	0	1.108802	-1.344181	-2.488535
23	1	0	0.095592	-1.722138	-2.476798
24	6	0	2.220960	2.093767	-0.173885
25	6	0	2.738133	3.339583	-0.555947

26	1	0	3.797858	3.452973	-0.741958
27	6	0	1.911978	4.444323	-0.730378
28	1	0	2.327258	5.401534	-1.023545
29	6	0	0.546026	4.293152	-0.521180
30	1	0	-0.142594	5.122562	-0.619109
31	6	0	0.069822	3.028686	-0.218915
32	1	0	-0.990238	2.848619	-0.103029
33	7	0	-1.357600	0.476165	-1.538410
34	7	0	-1.478327	0.618514	1.411648
35	7	0	-0.868618	-1.949184	0.078318
36	5	0	-3.075694	-0.712643	-0.034570
37	6	0	-2.656941	0.098846	-1.403938
38	6	0	-3.554780	0.422004	-2.432630
39	1	0	-4.595318	0.139757	-2.360947
40	6	0	-3.144046	1.109383	-3.569552
41	1	0	-3.853410	1.349364	-4.352976
42	6	0	-1.809932	1.480052	-3.677502
43	1	0	-1.432353	2.016373	-4.538660
44	6	0	-0.956491	1.143666	-2.640974
45	1	0	0.090649	1.410816	-2.678469
46	6	0	-2.749889	0.133668	1.329361
47	6	0	-3.600236	0.286122	2.433492
48	1	0	-4.577898	-0.177498	2.434403
49	6	0	-3.208740	1.008730	3.555075
50	1	0	-3.879262	1.120820	4.399118
51	6	0	-1.942655	1.582474	3.567880
52	1	0	-1.592196	2.175186	4.403091
53	6	0	-1.108770	1.344237	2.488542
54	1	0	-0.095573	1.722232	2.476786
55	6	0	-2.220941	-2.093681	0.173836
56	6	0	-2.738150	-3.339494	0.555856
57	1	0	-3.797889	-3.452873	0.741795
58	6	0	-1.912018	-4.444245	0.730325
59	1	0	-2.327325	-5.401450	1.023471
60	6	0	-0.546052	-4.293089	0.521200
61	1	0	0.142551	-5.122509	0.619160
62	6	0	-0.069818	-3.028631	0.218948
63	1	0	0.990248	-2.848581	0.103095
64	6	0	-5.118439	-2.069471	-0.912895
65	6	0	-5.573653	-0.041509	0.121173
66	6	0	-6.458717	-2.256496	-1.209070
67	1	0	-4.368706	-2.770373	-1.243669
68	6	0	-6.927445	-0.174917	-0.147812
69	1	0	-5.186421	0.844967	0.597080
70	6	0	-7.393080	-1.306881	-0.809688
71	1	0	-6.763699	-3.138533	-1.757361
72	1	0	-8.447054	-1.431721	-1.024539
73	6	0	5.573597	0.041405	-0.121144
74	6	0	5.118605	2.069531	0.912696
75	6	0	6.927410	0.174727	0.147761
76	1	0	5.186259	-0.845104	-0.596910
77	6	0	6.458914	2.256473	1.208792
78	1	0	4.368950	2.770529	1.243442
79	6	0	7.393176	1.306732	0.809479
80	1	0	6.763991	3.138545	1.756975
81	1	0	8.447173	1.431508	1.024258

82	7	0	4.678471	0.994642	0.220575
83	7	0	-4.678428	-0.994620	-0.220631
84	35	0	8.128714	-1.227750	-0.388200
85	35	0	-8.128890	1.227400	0.388249

References

1. I. P. Evans, A. Spencer and G. Wilkinson, *J. Chem. Soc., Dalton Trans.*, 1973, 204-209.
2. a) C. Cui, R. A. Lalancette and F. Jäkle, *Chem. Commun.*, 2012, **48**, 6930–6932; b) C. Cui, P. R. Shipman, R. A. Lalancette and F. Jäkle, *Inorg. Chem.*, 2013, **52**, 9440-9448.
3. G. R. Fulmer, A. J. M. Miller, N. H. Sherden, H. E. Gottlieb, A. Nudelman, B. M. Stoltz, J. E. Bercaw and K. I. Goldberg, *Organometallics*, 2010, **29**, 2176-2179.
4. a) Bruker, SAINT Version 7.23a, Bruker AXS Inc., Madison, Wisconsin, USA, (2005). b) Bruker, APEX 2 Version 2.0-2, Bruker AXS Inc., Madison, Wisconsin, USA, (2005). c) Sheldrick, G. M., SADABS, University of Göttingen, Germany, (2005).
5. G. M. Sheldrick, *Acta Crystallogr.*, 2008, **A64**, 112–122.
6. a) G. M. Sheldrick, *Acta Crystallogr.,* 2015, **C71**, 3-8. b) O. V. Dolomanov, L. J. Bourhis, R. J. Gildea, J. A. K. Howard and H. Puschmann, *J. Appl. Cryst*, 2009, **42**, 339-341; b) G. Sheldrick, *Acta Crystallogr.* 2015, **A71**, 3-8.
7. Rigaku Oxford Diffraction, (2021), CrysAlisPro Software system, version 41.110a 64-bit, Rigaku Corporation, Oxford, UK.
8. *SCALE3 ABSPACK*; A Rigaku Oxford Diffraction program (1.0.11,gui:1.0.7) (c) 2005-2021 Rigaku Oxford Diffraction.
9. Gaussian 16, Revision A.03, M. J. Frisch, G. W. Trucks, H. B. Schlegel, G. E. Scuseria, M. A. Robb, J. R. Cheeseman, G. Scalmani, V. Barone, B. Mennucci, G. A. Petersson, H. Nakatsuji, M. Caricato, X. Li, H. P. Hratchian, A. F. Izmaylov, J. Bloino, G. Zheng, J. L. Sonnenberg, M. Hada, M. Ehara, K. Toyota, R. Fukuda, J. Hasegawa, M. Ishida, T. Nakajima, Y. Honda, O. Kitao, H. Nakai, T. Vreven, J. A. Montgomery, Jr., J. E. Peralta, F. Ogliaro, M. Bearpark, J. J. Heyd, E. Brothers, K. N. Kudin, V. N. Staroverov, T. Keith, R. Kobayashi, J. Normand, K. Raghavachari, A. Rendell, J. C. Burant, S. S. Iyengar, J. Tomasi, M. Cossi, N. Rega, J. M. Millam, M. Klene, J. E. Knox, J. B. Cross, V. Bakken, C. Adamo, J. Jaramillo, R. Gomperts, R. E. Stratmann, O. Yazyev, A. J. Austin, R. Cammi, C. Pomelli, J. W. Ochterski, R. L. Martin, K. Morokuma, V. G. Zakrzewski, G. A. Voth, P. Salvador, J. J. Dannenberg, S. Dapprich, A. D. Daniels, O. Farkas, J. B. Foresman, J. V. Ortiz, J. Cioslowski, and D. J. Fox, Gaussian, Inc., Wallingford CT, 2016.